



Salmon Sub-program:
Marine currents, nutrients and
plankton in the coastal waters of
south eastern Tasmania and
responses to changing weather
patterns

Kerrie M. Swadling
Ruth S. Eriksen
Jason M. Beard
Christine M. Crawford

June 2017

FRDC Project No **2014/031**

© 2017 Fisheries Research and Development Corporation.
All rights reserved.

ISBN Print: 978-1-86295-890-6

ISBN Electronic: 978-1-86295-891-3

Salmon Sub-program: Marine currents, nutrients and plankton in the coastal waters of south eastern Tasmania and responses to changing weather patterns

2014/031

2017

Ownership of Intellectual property rights

Unless otherwise noted, copyright (and any other intellectual property rights, if any) in this publication is owned by the Fisheries Research and Development Corporation [and if applicable insert research provider organisation/s e.g. CSIRO Marine Research]

This publication (and any information sourced from it) should be attributed to [Swadling, K.M., Eriksen, R.S., Beard, J.M. and Crawford, C.M. Institute for Marine and Antarctic Studies, 2017, *Salmon Sub-program: Marine currents, nutrients and plankton in the coastal waters of south eastern Tasmania and responses to changing weather patterns*, Hobart, Tasmania, June. CC BY 3.0]

Creative Commons licence

All material in this publication is licensed under a Creative Commons Attribution 3.0 Australia Licence, save for content supplied by third parties, logos and the Commonwealth Coat of Arms.



Creative Commons Attribution 3.0 Australia Licence is a standard form licence agreement that allows you to copy, distribute, transmit and adapt this publication provided you attribute the work. A summary of the licence terms is available from creativecommons.org/licenses/by/3.0/au/deed.en. The full licence terms are available from creativecommons.org/licenses/by/3.0/au/legalcode.

Inquiries regarding the licence and any use of this document should be sent to: frdc@frdc.com.au

Disclaimer

The authors do not warrant that the information in this document is free from errors or omissions. The authors do not accept any form of liability, be it contractual, tortious, or otherwise, for the contents of this document or for any consequences arising from its use or any reliance placed upon it. The information, opinions and advice contained in this document may not relate, or be relevant, to a readers particular circumstances. Opinions expressed by the authors are the individual opinions expressed by those persons and are not necessarily those of the publisher, research provider or the FRDC.

The Fisheries Research and Development Corporation plans, invests in and manages fisheries research and development throughout Australia. It is a statutory authority within the portfolio of the federal Minister for Agriculture, Fisheries and Forestry, jointly funded by the Australian Government and the fishing industry.

Researcher Contact Details

Name:
Address:

Phone:
Fax:
Email:

FRDC Contact Details

Address: 25 Geils Court
Deakin ACT 2600
Phone: 02 6285 0400
Fax: 02 6285 0499
Email: frdc@frdc.com.au
Web: www.frdc.com.au

In submitting this report, the researcher has agreed to FRDC publishing this material in its edited form.

Contents

Tables	iv
Figures	iv
Acknowledgments	ix
Abbreviations	x
Executive Summary	xi
1. Introduction	1
2. Methods	4
2.1 Characteristics of water masses influencing Tasmania.....	4
2.2 Sampling sites in Storm Bay	7
2.3 Baseline water quality data	9
2.4 Plankton sampling.....	9
2.5 Data analysis	10
3. Results	11
3.1 Storm Bay – general overview of conditions	11
3.2 Sites in Storm Bay	26
3.3 Phytoplankton and Zooplankton	38
3.4 Detection of <i>Neoparamoeba perurans</i> in Storm Bay	52
3.5 Primary Production in Storm Bay	54
3.6 Historical Comparison	59
4. Discussion	63
4.1 Physical and chemical water quality in Storm Bay	63
4.2 Historical comparison	65
4.3 Phytoplankton and Zooplankton in Storm Bay	67
4.4 Detection of <i>Neoparamoeba perurans</i> in Storm Bay	70
4.5 Assessment of the FRRF in Storm Bay	70
5. Conclusion	71
Implications	72
Further development	73
Extension and Adoption	74
Glossary	75
Project materials developed	76
Presentations	76

Student projects.....	76
Scientific papers.....	76
Industry update.....	77
Appendices	78
Appendix 1: List of researchers and project staff (boat skippers, technicians, consultants).....	78
Appendix 2: Intellectual Property	78
Appendix 3: References	79
Appendix 4.....	85

Tables

Table 2.1 Longitude and latitude of sites sampled in Storm Bay, with maximum depth sampled (approximately 5 m from the bottom) at each site.....	8
Table 3.1 <i>Neoparamoeba perurans</i> detected in Storm Bay during 2014 and 2015. Temperature and salinity at the time and depth of sampling are also shown.	53
Table 3.2. Light (PAR, $\mu\text{mol photons m}^{-2} \text{ s}^{-1}$), Chlorophyll (Chl, $\text{mg chl} \text{ a m}^{-3}$) and Fv/Fm (dimensionless) at sites 1, 2, 3, 5, 6 and 9, depths of 10 m and 20 m (or the greatest depth if less than 20 m) on the 15 th January, 10 th March and 22 nd April 2015.....	56

Figures

Figure 2.1 Major currents and water masses influencing the east coast of Tasmania, including Storm Bay; ZC = Zeehan Current, EAC = East Australian Current, SC = Subantarctic Current (from Cresswell 2000).	4
Figure 2.2 Sea surface temperature plot (10 March, 2015) showing flow down the east coast of Tasmania (black arrows), including eddy fields to the east and southwest of the island (http://oceancurrent.imos.org.au/sst.php . Accessed 20 October 2016).	5
Figure 2.3 Sea surface temperature plot (4 July, 2014) showing flow across from the Great Australian Bight, along the west coast of Tasmania, around the southern tip and up the east coast (black arrows) (http://oceancurrent.imos.org.au/sst.php . Accessed 20 October 2016).	6
Figure 2.4 Connie 2 model results displaying the likely origins of water over a 30-day dispersal period flowing into a sink representing the study site in southern Tasmania. Dispersal of water at 5, 15 and 55 m depths were applied to winter (01/06 – 31/08), spring (01/09 – 30/11), summer (01/12 – 28/02) and autumn (01/03 – 31/05) oceanographic conditions averaged over a seven-year period (2001 – 2007). <i>Colourbar</i> represents the proportional likelihood of water from a region flowing into the study site.....	7
Figure 2.5 Map of Storm Bay showing site locations, and bathymetry (m).....	8
Figure 3.1 Top panel: Southern Ocean Index (SOI), 2010 – 2015 (Data from Bureau of Meteorology), dashed lines show +7 and -7; Bottom panel: Average rainfall (black line) measured at the Ellerslie Road BoM site, 2010-2015. Long-term average monthly rainfall (1885-2009) shown in red (repeated for each year of sampling).....	11

Figure 3.2 Average annual long-term wind strength and direction (1958 – 2004). Data sourced from Bureau of Meteorology weather station at Ellerslie Road, Hobart and Hobart Airport. Wind roses for all seasons at A) 9 am and B) 3 pm.	12
Figure 3.3 Water temperature (°C) across all sites (a) and months (b) in Storm Bay, 2009 – 2015. Box plots show the median temperature (50 th percentile, black line), the 25 th and 75 th percentiles (horizontal edges of boxes), the 10 th and 90 th percentiles (capped bars), and outliers (open circles).	13
Figure 3.4. Map of Storm Bay, showing glider tracks. Slocum Gliders have been deployed by the ANFOG (Australian National Facility for Ocean Gliders) for IMOS, from the mouth of the Derwent Estuary to the continental shelf, passing close to sites 1, 2 and 3 in the present study.	14
Figure 3.5 Glider transects of temperature with starting dates: 8 February 2013 (summer), 26 March 2014 (autumn), 8 June 2012 (winter) and 3 September 2014 (spring). <i>Colourbars</i> range from 9.7 °C to 19.2 °C.	15
Figure 3.6 Salinity across all sites (a) and months (b) in Storm Bay, 2009 – 2015. Box plots show the median salinity (black line), the 25 th and 75 th percentiles (horizontal edges of boxes), the 10 th and 90 th percentiles (capped bars), and outliers (open circles).	16
Figure 3.7 Glider transects of salinity with starting dates: 8 February 2013 (summer), 26 March 2014 (autumn), 8 June 2012 (winter) and 3 September 2014 (spring). <i>Colourbars</i> range from 32.12 to 35.40. .	17
Figure 3.8 Temperature-salinity plots. Points show data from each CTD deployment on every sampling date for each site. <i>Colourbar</i> is seawater density, with less dense water layers showing to the left of each plot.	17
Figure 3.9 Dissolved oxygen across all sites (a) and months (b) in Storm Bay, 2010 – 2015. Box plots show the median DO (black line), the 25 th and 75 th percentiles (horizontal edges of boxes), the 10 th and 90 th percentiles (capped bars), and outliers (open circles). Note that trips 11 – 54 only were plotted due to instrument unreliability during the first 10 sampling trips.	18
Figure 3.10 Glider transects of dissolved oxygen with starting dates: 8 February 2013 (summer), 26 March 2014 (autumn), 8 June 2012 (winter) and 3 September 2014 (spring). <i>Colourbars</i> range from 171 to 283 $\mu\text{mol kg}^{-1}$	19
Figure 3.11 Concentration of chlorophyll <i>a</i> across all sites (a) and months (b) in Storm Bay, 2009 – 2015. Box plots show the median chlorophyll (black line), the 25 th and 75 th percentiles (horizontal edges of boxes), the 10 th and 90 th percentiles (capped bars), and outliers (open circles).	20
Figure 3.12 Concentration of chlorophyll <i>a</i> (\log_{10}) versus Secchi depth across all sites for each season...	21
Figure 3.13 Glider transects of dissolved oxygen with starting dates: 8 February 2013 (summer), 26 March 2014 (autumn), 8 June 2012 (winter) and 3 September 2014 (spring). <i>Colourbars</i> range from 0.0 to 4.0 mg m^{-3}	21
Figure 3.14 Concentration of nitrate + nitrite across all depths for sites (a) and months (b) in Storm Bay, 2009 – 2015. Box plots show the median NO _x (black line), the 25 th and 75 th percentiles (horizontal edges of boxes), the 10 th and 90 th percentiles (capped bars), and outliers (open circles).	22
Figure 3.15 Concentration of phosphate across all depths for all sites (a) and months (b) in Storm Bay, 2009 – 2015. Box plots show the median phosphate (black line), the 25 th and 75 th percentiles (horizontal edges of boxes), the 10 th and 90 th percentiles (capped bars), and outliers (open circles).	23
Figure 3.16 Concentration of ammonium across depths and all sites (a) and months (b) in Storm Bay, 2009 – 2015. Box plots show the median ammonium (black line), the 25 th and 75 th percentiles (horizontal edges of boxes), the 10 th and 90 th percentiles (capped bars), and outliers (open circles).	24

Figure 3.17 Concentration of silicate across all depths and sites (a) and months (b) in Storm Bay, 2009 – 2015. Box plots show the median silicate (black line), the 25 th and 75 th percentiles (horizontal edges of boxes), the 10 th and 90 th percentiles (capped bars), and outliers (open circles).....	25
Figure 3.18 Principal Components Analysis of the six physical and chemical factors measured at the six sites between November 2009 and April 2015. PC1 accounted for 42% of the variation in the data, and PC2 accounted for 22%.....	26
Figure 3.19 Temperature, salinity, dissolved oxygen and chlorophyll <i>a</i> concentration at site 1, 2009 – 2015. Surface measurements (black circle and line) were at 0.5 m and bottom measurements (red circle and line) at 15 m. The first 10 months of oxygen measurements were omitted due to technical errors with the instrument.....	27
Figure 3.20 Concentration of nutrients at site 1, 2009 – 2015. Surface measurements (black circle and line) were at 0.5 m and bottom measurements (red circle and line) at 15 m.....	28
Figure 3.21 Temperature, salinity, dissolved oxygen and chlorophyll <i>a</i> concentration at site 2, 2009 – 2015. Surface measurements (black circle and line) were at 0.5 m and bottom measurements (red circle and line) at 20 m. The first 10 oxygen measurements were omitted due to technical errors with the instrument.....	29
Figure 3.22 Concentration of nutrients at site 2, 2009 – 2015. Surface measurements (black circle and line) were at 0.5 m and bottom measurements (red circle and line) at 20 m.....	30
Figure 3.23 Temperature, salinity, dissolved oxygen and chlorophyll <i>a</i> concentration at site 3, 2009 – 2015. Measurements were at 0.5 m (black circle and line), 50 m (green circle and line) and 90 m (red circle and line). The first 10 oxygen measurements were omitted due to technical errors with the instrument.....	31
Figure 3.24 Concentration of nutrients at site 3, 2009 – 2015. Measurements were at 0.5 m (black circle and line), 50 m (green circle and line) and 90 m (red circle and line).....	32
Figure 3.25 Temperature, salinity, dissolved oxygen and chlorophyll <i>a</i> concentration at site 5, 2009 – 2015. Surface measurements (black circle and line) were at 0.5 m and bottom measurements (red circle and line) at 30 m. The first 10 oxygen measurements were omitted due to technical errors with the instrument.....	33
Figure 3.26 Concentration of nutrients at site 5, 2009 – 2015. Surface measurements (black circle and line) were at 0.5 m and bottom measurements (red circle and line) at 30 m.....	34
Figure 3.27 Temperature, salinity, dissolved oxygen and chlorophyll <i>a</i> concentration at site 6, 2009 – 2015. Surface measurements (black circle and line) were at 0.5 m and bottom measurements (red circle and line) at 30 m. The first 10 oxygen measurements were omitted due to technical errors with the instrument.....	35
Figure 3.28 Concentration of nutrients at site 6, 2009 – 2015. Surface measurements (black circle and line) were at 0.5 m and bottom measurements (red circle and line) at 30 m.....	36
Figure 3.29 Temperature, salinity, dissolved oxygen and chlorophyll <i>a</i> concentration at site 9, 2011 – 2015. Surface measurements (black circle and line) were at 0.5 m and bottom measurements (red circle and line) at 20 m.....	37
Figure 3.30 Concentration of nutrients at site 9, 2011 – 2015. Surface measurements (black circle and line) were at 0.5 m and bottom measurements (red circle and line) at 20 m.....	38
Figure 3.31 Chlorophyll <i>a</i> concentration for each site from January 2010- April 2015. Data from integrated ‘snake’ tube, 0 – 10 m.....	39

Figure 3.32 Surface and depth-integrated chlorophyll <i>a</i> time series for Sites 1-6, January 2010 to December 2015. Red line and circles are surface samples; black line and circles are integrated snake samples.	40
Figure 3.33 Total phytoplankton abundance (cells L ⁻¹) at Sites 1-6 in Storm Bay (integrated snake sample) from November 2009 to April 2015.	42
Figure 3.34 Total diatoms (cells L ⁻¹) at sites 1-6 in Storm Bay (integrated snake sample).	42
Figure 3.35 Total dinoflagellates (cells L ⁻¹) at sites 1-6 in Storm Bay (integrated snake sample).	42
Figure 3.36 Canonical analysis of principle components of all phytoplankton species from sites 1,2,3, 5 and 6.	43
Figure 3.37 Time series for <i>Pseudo-nitzschia</i> spp. at Sites 1,2,3,5 and 6 from depth-integrated snake samples.	44
Figure 3.38 Time series for <i>Dinophysis</i> spp. at Sites 1,2,3,5 and 6 from the depth-integrated snake sample.	45
Figure 3.39 Time series for <i>Cerataulina</i> at Sites 1,2,3,5 and 6 from the depth-integrated snake sample. ...	45
Figure 3.40 Time series for <i>Noctiluca scintillans</i> at Sites 1,2,3,5 and 6 from the depth-integrated snake sample.	46
Figure 3.41 Time series for the genus <i>Karenia</i> at Sites 1,2,3,5 and 6 from the depth-integrated snake sample.	46
Figure 3.42 Time series for <i>Gymnodinium catenatum</i> at Sites 1,2,3,5 and 6, from the depth integrated snake sample.	47
Figure 3.43 Time series for the genus <i>Chaetoceros</i> at Sites 1,2,3,5 and 6 from the depth-integrated snake sample.	47
Figure 3.44 Plot showing canonical analysis of principal coordinates for zooplankton-sample relationships for sites 2, 5 and 6 for 2009-2015.	48
Figure 3.45 Total zooplankton abundance at three sites in Storm Bay, for the period November 2009 to April 2015.	49
Figure 3.46 Total copepod abundance at three sites in Storm Bay, for the period November 2009 to April 2015.	49
Figure 3.47 Total euphausiid abundance at three sites in Storm Bay, for the period November 2009 to April 2015.	50
Figure 3.48 Total cladoceran abundance at three sites in Storm Bay, for the period November 2009 to April 2015. Black lines and dots are <i>Evadne</i> sp., red are <i>Penilia</i> sp. and green <i>Podon</i> sp. (a) site 2, (b) site 5 and (c) site 6.	50
Figure 3.49 Total gelatinous groups at three sites in Storm Bay, for the period November 2009 to April 2015. Black lines and dots are hydrozoans and red are Thaliaceans (a) site 2, (b) site 5 and (c) site 6.	51
Figure 3.50 Light ($\mu\text{mol photons m}^{-2} \text{ s}^{-1}$), biomass ($\text{mg Chl}a \text{ m}^{-3}$) and gross primary productivity ($\mu\text{g C m}^{-3} \text{ s}^{-1}$) at sites 1, 2, 3, 5, 6 and 9 in Storm Bay on January 27 th 2015. Note that axes are not uniform in scale.	55
Figure 3.51. Light ($\mu\text{mol photons m}^{-2} \text{ s}^{-1}$), biomass ($\text{mg Chl}a \text{ m}^{-3}$) and gross primary productivity ($\mu\text{g C m}^{-3} \text{ s}^{-1}$) at sites 1, 2, 3, 5 and 6 in Storm Bay on March 10 th 2015. Note that axes are not uniform in scale. ...	57

Figure 3.52. Light ($\mu\text{mol photons m}^{-2} \text{ s}^{-1}$), biomass ($\text{mg Chl}a \text{ m}^{-3}$) and gross primary productivity ($\mu\text{g C m}^{-3} \text{ s}^{-1}$) at sites 1, 2, 3, 5, 6 and 9 in Storm Bay on April 22nd 2015. Note that axes are not uniform in scale. 58

Figure 3.53 Comparison of temperature (top panel), salinity (middle panel) and chlorophyll *a* concentration (bottom panel) at site 2, 10 m depth between the original CSIRO sampling period and the new study..... 60

Figure 3.54 Comparison of nitrate + nitrite (top panel), phosphate (middle panel) and dissolved oxygen (bottom panel) at site 2, 10 m depth between the original CSIRO sampling period and the new study. 61

Figure 3.55 Plot showing principal components analysis for environmental data for the two periods of Storm Bay sampling, 1985 – 1989 and 2009 – 2015..... 62

Acknowledgments

We are particularly grateful to Lisette Robertson and Andrew Pender from TAFI/IMAS who have made major contributions to the 'Storm Bay' project over the five-year period, especially with management of field trips, laboratory analyses and data collation. We are also very appreciative of the efforts of numerous students, volunteers and casual staff who helped with field sampling, including Jake Wallis, Andreas Seger and Shihong Lee. Additionally, many thanks to Pieter van der Woude, skipper of *Odalisque* and his first mate, Dave Denison, and to fill-in skippers Phil Pyke and Scott Palmer on *ICON*, who made our field trips run smoothly, with lots of interesting conversations.

We also wish to thank Prof. Andrew McMinn and Shihong Lee from IMAS for their informative work on primary production using their Fast Repetition Rate Fluorometry equipment, and to Prof. Barbara Nowak, also from IMAS, for advice and analysis of amoebic gill disease in water samples. Dr Daniel Ray helped with data mining and manipulation. The contribution of Peter Walsh (IMAS), and Oliver George and Mark Hepburn (Condense Pty Ltd) towards developing the database is also gratefully acknowledged.

The data proved by the Integrated Marine Observing System (IMOS), a national collaborative research infrastructure supported by the Australian Government, has enhanced the interpretation of the Storm Bay data. Our colleagues at CSIRO, Pru Bonham, Dr Peter Thompson and Lesley Clementson, are thanked for their interest and contributions to this project during the first two years. We also thank Dr Benedicte Pasquer (IMOS) for her help with presentation of the glider data, Dr Michael Sumner (Australian Antarctic Division) for his help with presenting the oceanographic plots and Justin Hulls (IMAS) for producing maps.

Finally, we greatly appreciate the support provided by Prof. Colin Buxton and TAFI/IMAS, which funded the costs of vessel charter.

Abbreviations

AGD Amoebic gill disease
EAC East Australian Current
FRRF Fast repetition rate fluorometer
HAB Harmful algal blooms
HAC Huon Aquaculture Company
IMAS Institute of Marine and Antarctic Studies
IMOS Integrated Marine Observing System
LC (ZC) Leeuwin Current (Zeehan Current)
NH₄ Ammonium
NO_x Nitrate (NO₃) + nitrite (NO₂)
PO₄ Phosphate
NRS National Reference Station (IMOS)
SC Subantarctic Current
SOI Southern Oscillation Index
SO₄ Silicate
SSS Sea surface salinity
SST Sea surface temperature
TAFI Tasmanian Aquaculture and Fisheries Institute

Executive Summary

This report is an evaluation of one of the largest longer term data sets of water quality collected in a major waterway in Australia in recent years. Storm Bay at the mouth of the River Derwent, Tasmania, was sampled monthly for five years 2009-2015 for water quality – physical characteristics, nutrients, and phyto- and zoo-plankton - by the Institute for Marine and Antarctic Studies at the University of Tasmania. The project was conducted primarily for the Tasmanian salmon aquaculture industry and is the first major baseline assessment of water quality before salmon farming commences in a new region. The report is also of importance to other users of coastal waters in southeastern Tasmania, including commercial and recreational fishers, because it describes the major oceanic currents and weather patterns that influence water quality and productivity in the region. It also examines changes that have occurred over the previous three decades.

The research was initiated to provide baseline water quality data and a better understanding of water movements and productivity in Storm Bay for the Tasmanian salmon aquaculture industry because they were considering expansion of Atlantic salmon, *Salmo salar*, farming into Storm Bay. Culture of Atlantic salmon has been very successful in Tasmania and current production is almost 55,000 tonnes per annum. The industry wishes to expand to meet demand from the Australian domestic market; however, they have reached capacity in their current growing areas. Storm Bay, a large deep bay at the entrance to the River Derwent and downstream of the Tasmanian capital city of Hobart, is recognised as a suitable site for expansion of the industry because it has deep, well-flushed waters, is in close proximity to salmon farm infrastructure and has ready access to mainland and overseas markets, as well as a skilled workforce.

The objectives of this project were:

1. Build on available data and establish baseline environmental conditions in south-eastern Tasmanian coastal waters to support informed expansion of finfish farming in this region.
2. Enhance risk assessments underpinning Decision Support Systems for effects of changing weather patterns on water temperature, nutrients and plankton, especially in relation to HABs and gelatinous zooplankton.
3. Trial and establish a screening program for *Neoparamoeba perurans*, the causative agent of AGD.
4. Obtain measurements of primary productivity in Storm Bay and link to environmental drivers.

Of relevance is that the objectives listed above were for FRDC project 2014/031 and 24 months of funding; however, this report evaluates data collected over a five year time period to provide a comprehensive assessment of water quality in Storm Bay. Previous research was funded by a

variety of sources, including FRDC Tactical Research Fund 2009/067, Winifred Violet Scott Charitable Trust Grant and TAFI internal funding, but the sampling methodology remained consistent over the five years.

Five to six sites were sampled monthly in Storm Bay for over five years from November 2009 to April 2015, except on rare occasions when weather conditions were unsuitable, and bimonthly at times in 2013 when external funding was not available. Temperature, salinity, fluorescence and dissolved oxygen were profiled through the water column using multiprobe water quality profilers. Water samples were taken at just below the surface, at 10 m depth and close to the bottom at each site and subsamples taken for later analysis for chlorophyll *a*, nitrate, nitrite, phosphate, ammonium and silicate concentrations. A 200 µm mesh bongo net deployed to within 5 m of the bottom collected zooplankton samples, and phytoplankton were collected in an integrated sample from the surface to 10 m depth. Plankton species identification and abundance were recorded later in the laboratory. In the last 12 months of the program we also trialled a Fast Repetition Rate Fluorimeter to provide primary productivity measurements and collected water samples for a screening program for *N. perurans*.

Our results confirm previous reports that Storm Bay is a complex system, influenced by the influx of warmer, saltier and nutrient poor waters of the East Australian Current (EAC), especially during the summer-autumn period, by the Leewin Current with relatively warmer, more saline and higher nitrate inshore waters compared to shelf waters during winter and spring, and thirdly by periodic intrusion of cooler and nutrient rich subantarctic waters. In addition, freshwater outflow from the Rivers Derwent and Huon can alter the water properties of Storm Bay, especially during winter. Conditions in Storm Bay are largely determined by the dominant water body at the time, and significant interannual variability was observed.

A comparison of water quality at our central Storm Bay site with that collected by CSIRO at the same site in 1985-89 showed an overall increase in summer maximum and winter minimum temperatures, which concurs with other studies that this region is an ocean warming hotspot. Nitrates showed similar seasonal trends but no periodic peaks over summer in our data, indicating the stronger influence of the EAC.

Phytoplankton abundance and distribution in Storm Bay also revealed complex patterns with considerable interannual variation. The expected distinct spring and/or autumn peaks in diatom biomass were not observed in all years. We did record highest chlorophyll concentrations (as a proxy for biomass) in the first two years of the study, coinciding with a strong La Nina period. Diatoms were the dominant phytoplankton group for much of the year; dinoflagellates were also present but at lower concentrations. The harmful algal bloom forming species, *Gymnodinium catenatum*, was occasionally observed but it was unclear what triggered pulses of this species. *Noctiluca scintillans*, also a HAB species, was periodically found in our samples, indicating the biological influence of the EAC.

The abundance and distribution of zooplankton in the bay also fluctuated seasonally and annually, and did not always conform to predictions based on ENSO climatic conditions.

Gelatinous Hydrozoans (typical jellyfish) tended to be most abundant during years of warmer, low productivity waters. Other gelatinous zooplankton, Thaliaceans such as salps and doliolids, reached highest abundances during average temperature years. Krill, *Nyctiphanes australis*, an important component in the diet of many marine species including seabirds and commercial fisheries, were observed in moderate abundance throughout most of the study, which is notable as blooms of this species have not been observed since the 1980's.

A pilot survey for *Neoparamoeba perurans*, the causative agent of amoebic gill disease in salmon, found low concentrations of this species at sites sampled near to salmon farms and at the most oceanic site. They were most abundant in early autumn and in shallower water. Although concentrations were low, they were considered sufficient to induce AGD in salmon under suitable conditions.

Primary productivity and phytoplankton biomass were measured in Storm Bay using new equipment, a flat repetition rate fluorometer (FRRF), during the last few sampling trips and proved to be an effective and efficient means of providing real time, depth profiled productivity data. Our results indicated moderate productivity in the euphotic zone and a healthy, unstressed community.

The results from our research form a comprehensive baseline for the potential expansion of salmon aquaculture into Storm Bay. They are critical to future assessments of impacts on water quality and to effective management of salmon farming operations. The data have already been utilized by the three salmon farming companies operating in Tasmania to develop Environmental Impact Assessments for their proposed developments. The Tasmanian Government are also applying these data to the development of a monitoring program and setting threshold levels for water quality in relation to salmon farming in Storm Bay.

The information provided from our study is also important to all users of Storm Bay and more generally of south-eastern Tasmanian coastal waters, including recreational and commercial fishing. The data enable increased understanding of the influence of the three major oceanic currents to the region and associated effects on productivity, which is important to local fisheries and shellfish aquaculture. This longer-term dataset is also of significant importance to predictive modelling of anthropogenic activities, including salmon farming, and climate change in the region.

Keywords *Atlantic salmon Salmo salar, Storm Bay, south-eastern Tasmania, coastal waters, nutrients, coastal waters plankton, climate change*

1. Introduction

Farming of Atlantic salmon, (*Salmo salar*) in Tasmania commenced in the mid-1980s and has rapidly expanded to become Tasmania's most valuable primary industry. Current production of salmonids (Atlantic salmon plus a small quantity of rainbow trout) is almost 55,000 tonnes per annum, with sales approaching \$665 million wholesale (Tasmanian Salmon Growers Association website 9/8/16, available at <http://www.tsga.com.au/>). These salmon are primarily produced on marine farms located in the D'Entrecasteaux Channel/Huon Estuary region and Macquarie Harbour. Limits on salmon production in these areas have been imposed by the Tasmanian Government to minimise effects on the environment, and both regions have reached or are nearing capacity. The salmonid industry is looking to increase production to meet largely Australian market demands, and Storm Bay, on Tasmania's south east coast, is a region that has been recognised as suitable for expansion. Storm Bay has the advantages of deep, well-flushed waters with oceanic input, in close proximity to existing salmon farms in the D'Entrecasteaux Channel. It is also downstream of the city of Hobart, with easy access to mainland Australia and overseas markets and to a skilled workforce. It is, however, more exposed to oceanic conditions and requires stronger, more robust cage infrastructure and growing techniques that can withstand these more extreme conditions.

Pilot trials to assess suitable farm sites and to develop culture techniques appropriate to the environmental conditions of Storm Bay have been underway over the last couple of years by the Tasmanian salmon farming industry and one company has commenced commercial production in a lease area originally approved in 1998. However, before new or revised marine farming leases can be allocated in Storm Bay, comprehensive baseline environmental data are required to inform site selection, to provide background environmental data before large scale farming commences, and to support the development of a scientifically relevant, and cost-effective environmental monitoring program.

Storm Bay is a large deep bay that receives freshwater inflow from the River Derwent on its north-western boundary and exchanges water with Frederick Henry Bay on its north-eastern boundary. The eastern and western boundaries are defined by the Tasman Peninsula and Bruny Island, respectively, and the southern boundary connects with the Tasman Sea. This area is a mixing zone between the River Derwent outflow and oceanic waters.

The oceanography in Storm Bay is complex and is characterized by large fluctuations in temperature, salinity and nutrients on variable temporal and spatial scales. This is due to the southerly extension of warm nutrient-depleted sub-tropical waters transported via the East Australian Current (EAC) down the east coast of Tasmania over summer, whilst the south and south-west coasts are influenced by cooler, nutrient-rich sub-Antarctic waters from the south and the Leeuwin Current from the north-west (Buchanan et al. 2014). These water masses all impact on coastal waters of south-eastern Tasmania, including Storm Bay. Climate models predict that the most pronounced seawater warming in the Southern Hemisphere over the coming century will be off south-eastern Australia (Ridgeway and Hill 2009). The EAC has extended its southward penetration over the past 60 years and there has been clear change in temperature and salinity in the region, with mean positive trends of 2.28 °C century⁻¹ and 0.34 psu century⁻¹ over the 1944-2002

period (Ridgeway and Hill 2009). Sea surface temperature (SST) in winter has also increased over the last 10 years. Oke and England (2004) observed changes in the latitude of subpolar westerly winds, whereby there was a poleward shift of the westerly wind belt by about 5.4°S. Their studies agreed well with reports of patterns in the zonal winds of Hobart by Harris et al. (1988). The southward movement of the westerly wind belt displaces the EAC southward, which blocks the northward penetration of subantarctic water. This is likely to impact on marine productivity and trophic structure, which can affect salmon production through increased frequency and abundance of harmful algal blooms and gelatinous zooplankton. It is also likely to influence wild fisheries production.

Harris et al. (1991) documented the interaction between warmer EAC-derived waters and cooler temperature waters and identified associated productivity changes in Storm Bay. These included changes in both the magnitude of productivity and the composition of primary producers and consumers. Clear signals in the nutrient status of waters indicated the influence (timing and duration) of the EAC, while the magnitude and composition of primary producers (predominantly single-celled algae) highlighted the productivity of the region and the influence of westerly winds. Their research clearly demonstrated the potential for Storm Bay to act as an indicator of productivity for Southern and Eastern Tasmania.

The current project arose in response to the salmon aquaculture industry recognising the need for increased scientific knowledge to support ecologically sustainable development of Atlantic salmon (*Salmo salar*) farming operations in south-eastern Tasmania, in particular expansion into Storm Bay. The information provided will assist salmon companies to manage their operations in Storm Bay under varying environmental conditions.

Our research has also provided the opportunity to investigate changes in water quality over a quarter of a century time period as CSIRO investigated seasonal and inter-annual variability in chemical and biological parameters in Storm Bay during 1985-89. We sampled at the same “master station” in Storm Bay as CSIRO and used similar procedures where possible.

To provide a comprehensive assessment of the effects of changing climatic conditions on the Storm Bay environment we include data in this report which have been collected over a five-year time period. During this time financial support has been provided by a variety of sources, including the FRDC Tactical Research Fund 2009/067 – ‘Nutrient and Phytoplankton Data from Storm Bay to Support Sustainable Resource Planning’, from the Winifred Violet Scott Charitable Trust Grant ‘Resilience of Storm Bay, Tasmania, to Climate Change and Development: Linking Oceanographic Changes to Productivity’, from the Salmon Sub-Program FRDC 2014/031: ‘Marine currents, nutrients and plankton in the coastal waters of south eastern Tasmanian and responses to changing weather patterns’, and from internal IMAS support funding.

Objectives

1. Build on available data and establish baseline environmental conditions in south-eastern Tasmanian coastal waters to support informed expansion of finfish farming in this region.
2. Enhance risk assessments underpinning Decision Support Systems for effects of changing weather patterns on water temperature, nutrients and plankton, especially in relation to HABs and gelatinous zooplankton.
3. Trial and establish a screening program for *Neoparamoeba perurans*, the causative agent of AGD.
4. Obtain measurements of primary productivity in Storm Bay and link to environmental drivers.

2. Methods

2.1 Characteristics of water masses influencing Tasmania

The Tasmanian coastline has a complex oceanography that is characterized by large fluctuations in temperature, salinity and nutrients, which vary over many temporal and spatial scales. An early study showed a temperature difference of at least 4 °C across the State from the south-west to north-east in summer (Newell 1961). This is due to south-eastern Tasmanian waters being influenced by waters with subtropical origins from the east, while western and southern waters are influenced by cooler waters from the subantarctic and the Leeuwin (=Zeehan) Current flowing from the west (Figure 2.1; Harris et al. 1987; Clementson et al. 1989).

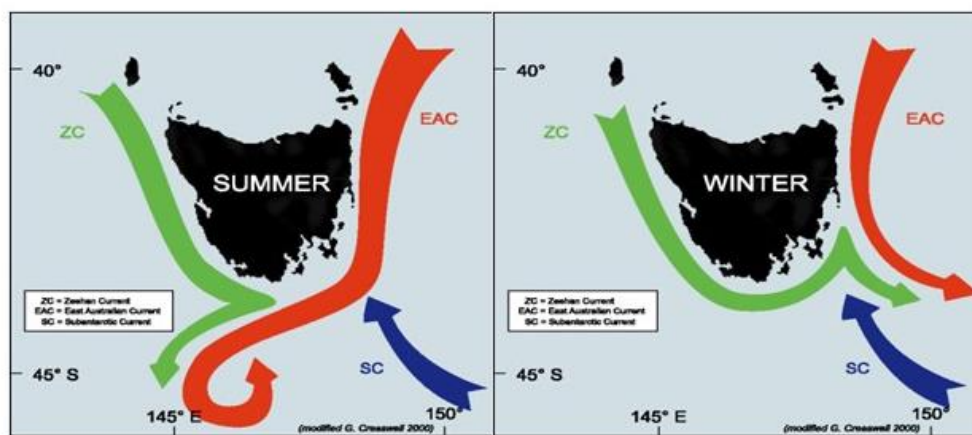


Figure 2.1 Major currents and water masses influencing the east coast of Tasmania, including Storm Bay; ZC = Zeehan Current, EAC = East Australian Current, SC = Subantarctic Current (from Cresswell 2000).

On the east coast of Tasmania there is a sharp division between the East Australian Current (EAC), which forms the western boundary of the South Pacific Ocean's subtropical gyre from the northeast and the Leeuwin Current from the northwest that centres on the Tasman Peninsula off southeast Tasmania (Baines et al. 1983; Ridgway, 2007). Western boundary currents are narrow and fast-flowing surface currents located on the western sides of subtropical gyres (Wu et al. 2012). Cresswell (2000) and Ridgway (2007) confirmed that the seasonal flow around Tasmania occurred as distinct summer and winter states. The EAC, a highly energetic and variable current, flows from tropical northern Australia down along the eastern seaboard of Australia, and is characterized by warm, saline, nutrient-poor water (Hassler et al. 2011). There is a separation point at ~32.5°S (Ridgway and Hill 2009), where the majority of the flow heads east into the Tasman Sea to become the Tasman Front and the remainder flows south. Along the Tasmanian shelf break and offshore from the break the flow is characterised by mesoscale eddies, which track in a southerly direction before turning west (Figure 2.2). The EAC traditionally exhibits its strongest influence during February and March, though it is not unknown to influence waters around Maria Island and Storm Bay well in to April in some years (K. Swadling, personal observations 2014). This extended influx of subtropical water is having ecological impacts on Tasmanian shelf waters, including sustained presence of blooms of the heterotrophic dinoflagellate *Noctiluca scintillans* (McLeod et al. 2012),

restriction of the spring diatom bloom at Maria Island (Thompson et al. 2009) and increased blooms of gelatinous species such as salps and doliolids (Ahmad Ishak 2014).

The Leeuwin Current (LC) flows from Western Australia, across the Great Australian Bight and along the west coast of Tasmania (where it is also called the Zeehan Current). It is the dominant current along the east coast of Tasmania during winter (Figure 2.3), and, unlike the EAC, remains almost entirely constrained to the continental shelf (Ridgway 2007). There are fewer descriptions of water properties along the west coast of Tasmania, and it has been suggested that the LC delivers warm (~ 12 °C), saline (34.8 – 35.2) and nitrate-rich (~ 4 μM) waters to shelf waters in winter (Buchanan et al. 2014).

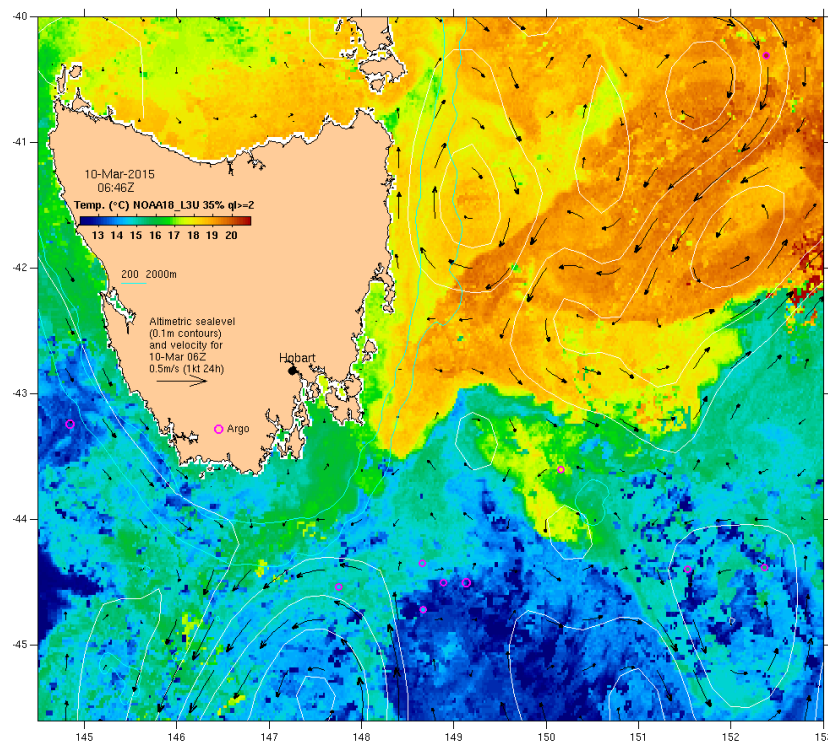


Figure 2.2 Sea surface temperature plot (10 March, 2015) showing flow down the east coast of Tasmania (black arrows), including eddy fields to the east and southwest of the island (<http://oceancurrent.imos.org.au/sst.php>. Accessed 20 October 2016).

The Derwent River flows into the Derwent Estuary and out into Storm Bay, delivering less saline (~ 25 – 30) surface waters and nitrate-rich bottom waters (~ 1 μM) in autumn and winter (Coughanowr et al. 2015). Herzfeld (2008) used particle tracking and passive tracer transport to describe mean seasonal circulation in Storm Bay. During winter and spring there is strong residual surface flow of marine origin from the Huon and Derwent Estuaries along a path on the eastern side of Storm Bay, under the influence of westerly or north-westerly winds, and exiting near

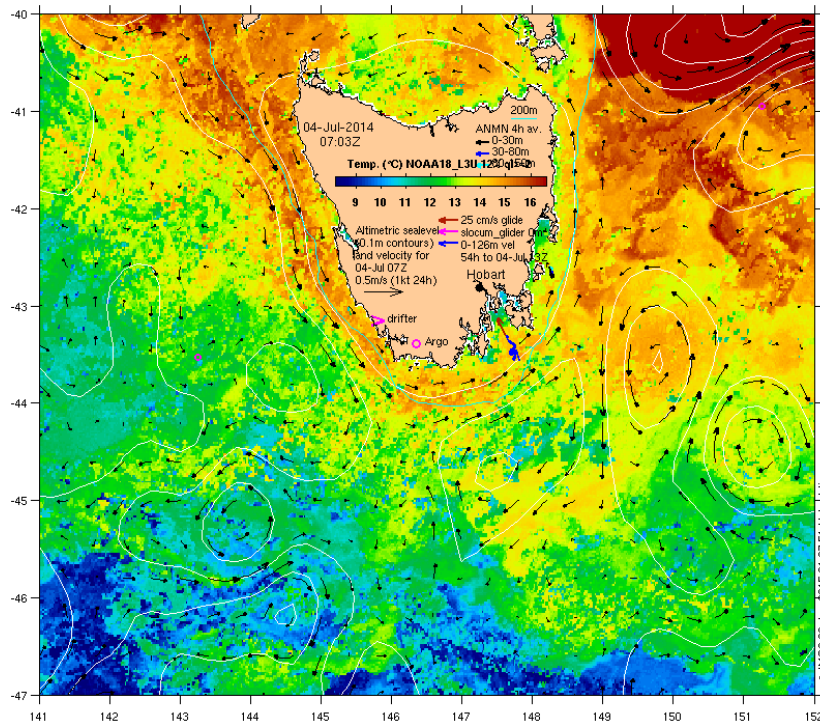


Figure 2.3 Sea surface temperature plot (4 July, 2014) showing flow across from the Great Australian Bight, along the west coast of Tasmania, around the southern tip and up the east coast (black arrows) (<http://oceancurrent.imos.org.au/sst.php>. Accessed 20 October 2016).

Tasman Island. In summer and autumn there is strong anti-clockwise circulation south of the Tasman Peninsula, which is associated with large-scale eddies that persist off the coast of south-east Tasmania. The anti-clockwise gyres are more evident in summer bottom waters, circulating across the bay from the tip of the Tasman Peninsula to the bottom of Bruny Island; this bottom circulation is still distinct in autumn, then becomes gradually less evident during winter and spring (Herzfeld 2008). Residual flow of marine water during winter is directed into the Derwent Estuary, where it travels up the bottom of the estuary as far as New Norfolk (Coughanowr et al. 2015). The surface flow in Storm Bay is generally less than 5 cm s^{-1} , in the eastward direction, though depth-averaged flows are slower, $\sim <1 \text{ cm s}^{-1}$ (Herzfeld 2008). Figures showing circulation patterns from Herzfeld (2008) are reproduced in Appendix 4.

The final water mass that has seasonal influence in Storm Bay comes from waters from the subantarctic zone (SAZ). Properties of the SAZ in the region to the east of Tasmania arise from the mixing of polar waters from the south with subtropical waters from the EAC extension and Tasman Sea (Bowie et al. 2011). SAZ-derived waters to the west of Tasmania result from mixing between water from the polar frontal zone with subtropical waters from the north (i.e. from the Leeuwin Current) (Bowie et al. 2011). Between 45.5 and 48°S surface waters ($> 150 \text{ m}$) the water temperature is typically above 10°C and salinity ~ 34.8 (Bowie et al. 2011), nitrate and phosphate values are < 5 and $0.2 \mu\text{M}$, respectively, making the water flowing northward into Storm Bay less saline and nitrate-rich relative to waters from the EAC. The CSIRO online connectivity tool CONNIE2 (CONNIE 2012) was used to determine likely sources of water into Storm Bay. CONNIE2 combines archived currents from oceanographic models with particle tracking techniques and simple models of behaviour to estimate connectivity to user-specified sink regions (Condie et al. 2012). Figure 2.4 presents output from the CONNIE2 tool, showing dispersal of

water at 5, 15 and 55 m for each season, averaged for the period 2001 - 2007. Based on the connectivity tool, water flows predominantly from the south and southwest during winter and spring. In summer and autumn, flow from the north is also strong, particularly at 5 and 15 m.

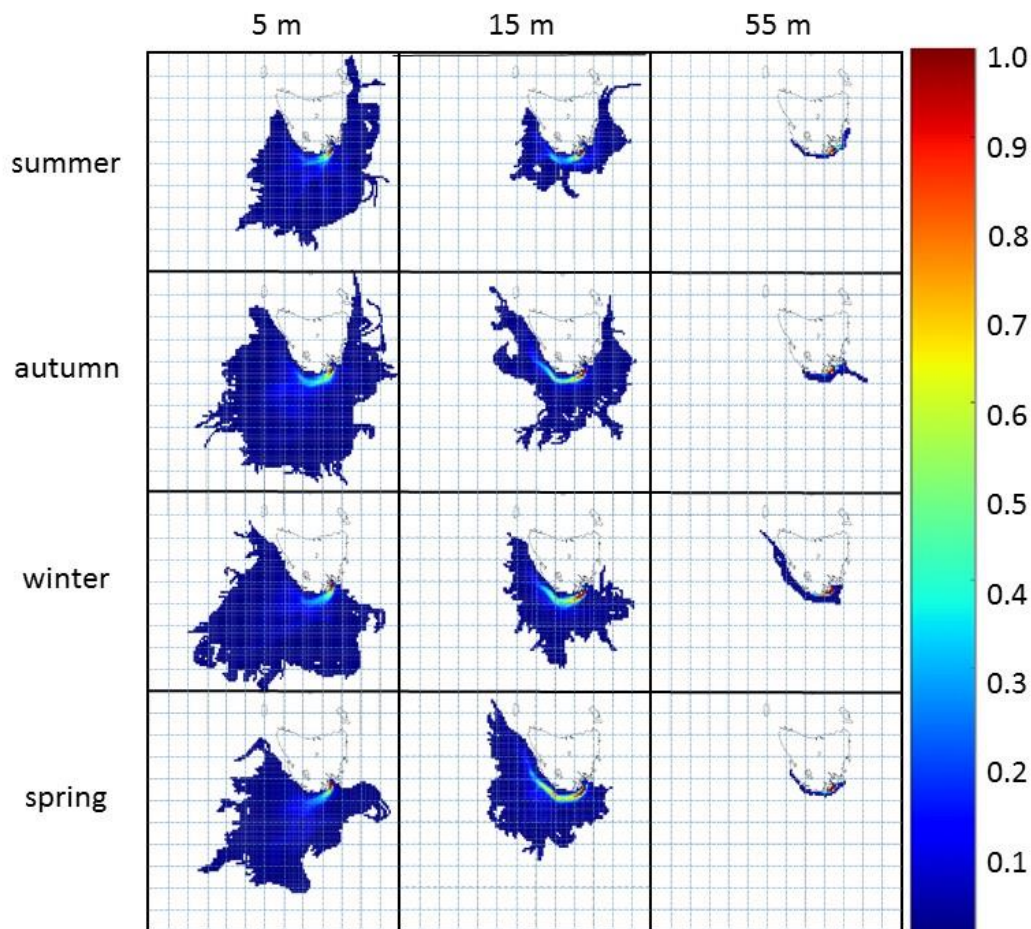


Figure 2.4 Connie 2 model results displaying the likely origins of water over a 30-day dispersal period flowing into a sink representing the study site in southern Tasmania. Dispersal of water at 5, 15 and 55 m depths were applied to winter (01/06 – 31/08), spring (01/09 – 30/11), summer (01/12 – 28/02) and autumn (01/03 – 31/05) oceanographic conditions averaged over a seven-year period (2001 – 2007). Colourbar represents the proportional likelihood of water from a region flowing into the study site.

2.2 Sampling sites in Storm Bay

Five sites were sampled monthly in Storm Bay for over five years from November 2009 to April 2015 (Table 2.1, Figure 2.5), except on rare occasions when weather conditions were unsuitable, and bimonthly at times in 2013 when external funding was not available. Site 1 was located at the mouth of the Derwent estuary and the entrance to Storm Bay, site 2 was in the same location as the 'master site' of a CSIRO study in 1985-88 (Clementson et al. 1989, Harris et al. 1991), site 3 was furthest offshore and provided the most information on oceanic currents influencing the bay, while sites 5 and 6 were requested by the salmon aquaculture industry as potential sites for expansion of salmon farming. Site 4 was further offshore and monitoring at this site was discontinued after three months because of insufficient time to collect samples from all sites in one day. An additional

site, 9, at the entrance to Frederick Henry Bay was included from 18 July 2011 at the request of the Marine Farming Branch, Department of Primary Industries, Parks, Water and Environment (DPIPWE), to provide information on water quality coming from Frederick Henry Bay. Adjacent to, and largely unaffected by the River Derwent, Frederick Henry Bay is a large marine embayment with limited freshwater input from the Coal River at its northern boundary.

Table 2.1 Longitude and latitude of sites sampled in Storm Bay, with maximum depth sampled (approximately 5 m from the bottom) at each site.

Site	Longitude, °E	Latitude, °S	Max. depth, m
1	147.3931	43.0714	15
2	147.5550	43.1700	40
3	147.6333	43.3167	90
5	147.6572	43.1132	30
6	147.4353	43.1865	30
9	147.5555	43.0591	20

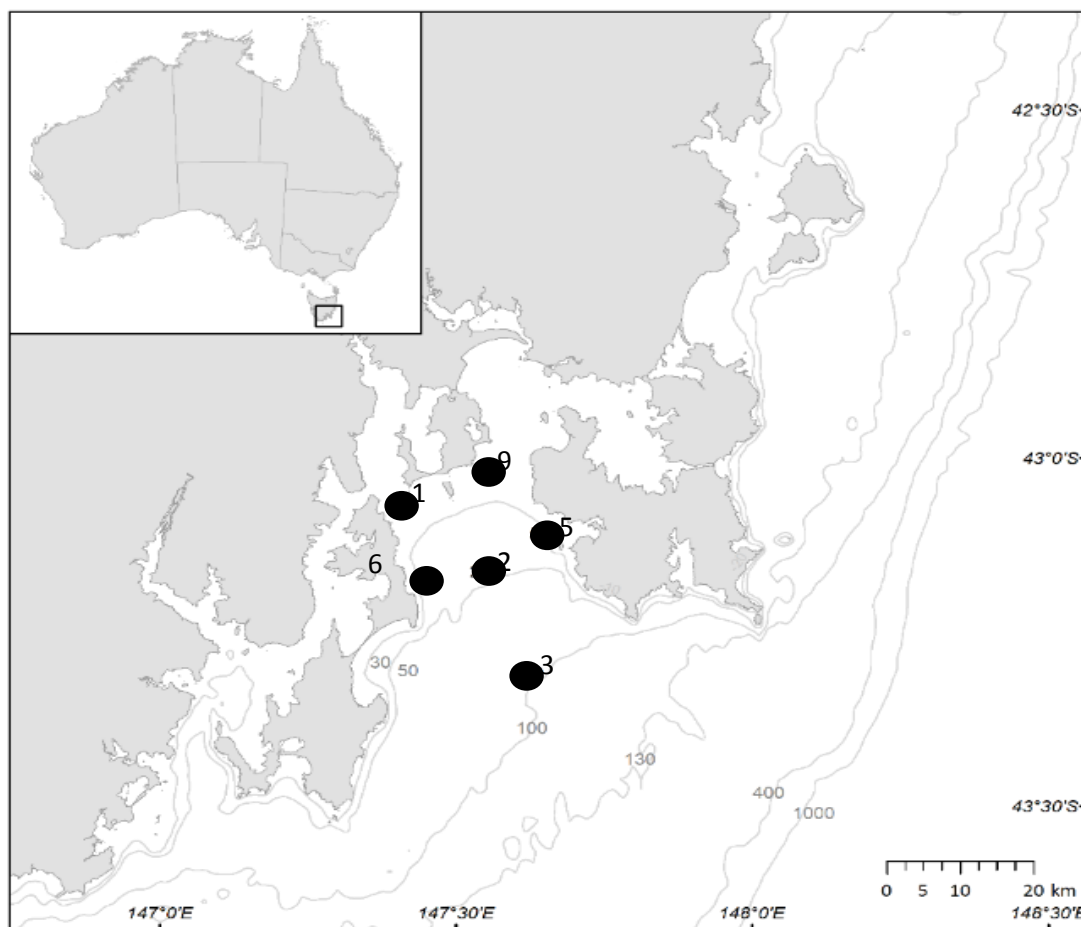


Figure 2.5 Map of Storm Bay showing site locations, and bathymetry (m).

2.3 Baseline water quality data

Prevailing weather conditions were noted at each station and degree of drift logged using GPS. Temperature, salinity, fluorescence, and dissolved oxygen were measured at each site using a Seabird SBE 19 plus CTD (full water column profile) and/or a YSI 6600 V2 Sonde CTD (profile to 30 m). The CTD was programmed to measure parameters every second on the down and upcasts. The data were depth averaged to every 0.5 m and only the upcasts were used as they showed less 'noise' in the profiles. The Secchi depth was recorded at each site by lowering a standard Secchi disk until it disappeared from sight. Water samples were collected, using a 6 L or 8 L Niskin bottle, from 0.5 – 1 m below the surface, at 10 m depth, and within 5 m of the seabed. Subsamples were taken at each depth for macronutrients (unfiltered), and were frozen and stored in the dark until processing at the CSIRO Marine and Atmospheric Laboratories, Hobart. Subsamples of 2 L were collected to measure chlorophyll *a* concentration at each depth and site. These subsamples were kept cold and in the dark until return to the IMAS laboratory, where they were filtered through 47 mm glass fibre filters (Whatman GF/F) and stored at -20 °C until analysis.

Laboratory analyses: Chlorophyll *a* concentrations were determined after extraction of photosynthetic pigments using acetone 90:10 water (vol/vol), sonification and centrifuging to remove filter paper. Absorbances were measured using a Varian CBE cintra 10E spectrometer, and standard equations were applied to determine chlorophyll concentrations (Parsons et al. 1984). The biologically relevant nutrients, dissolved nitrate+nitrite, phosphate, ammonia and silicate concentrations (μM) were measured by CSIRO Hydrochemistry laboratory using standard colorimetric methodology (Grasshoff et al. 1983) adapted for flow injection analysis on a 5-channel Lachat Quick Chem 8000 series Automated Ion Analyser. Method detection limits were 0.02 μM P, 0.05 μM N, 0.05 μM Si, and 0.05 μM ammonia.

2.4 Plankton sampling

Integrated water column samples for phytoplankton analysis were collected from the surface to 10m depth using a weighted Lund tube ("snake"). Three replicates were mixed in a bucket and a 1 L sub-sample taken for phytoplankton and immediately preserved using Lugol's acidified iodine solution at a ratio of approximately 1 mL L⁻¹ of sample. Note that Lugol's precludes the identification of some species of interest, and that examination of live samples is preferable for very fragile species such as *Chatonella* and *Heterosigma*.

Phytoplankton samples were concentrated by sequential settling over ~ 1 week, reducing the sample down to approximately 15 mL. The final volume was recorded and the sample thoroughly mixed before a 1 mL aliquot was taken and examined by phase contrast light microscopy (Leica DMLB2) in a Sedgewick-Rafter chamber. The entire chamber was scanned at low power (x50) to count large or rare species, and then re-examined at x200 until 400 squares had been inspected, or at least 200 cells of the dominant species had been counted. Thecate dinoflagellates were occasionally examined using fluorescence microscopy and Calcofluor to highlight plate structure. The identification of species was confirmed at higher magnification (x400), and a minimum of 20 squares was examined at x400 to count small flagellates (<5 μm), which were grouped into broad taxonomic categories based on shape and flagellae. Cell measurements and approximate geometric

shape were also recorded for the calculation of biovolume ($\mu\text{L cell}^{-1}$). Cell concentrations (cells mL^{-1}) were calculated from the original volume.

Zooplankton were collected with a 2-m long Bongo net (mouth diameter: 75 cm; mesh size: 200 μm). The nets were deployed to within 2 m of the seabed and hauled steadily (1 m s^{-1}) back to the surface. On-board, zooplankton samples were anaesthetised using soda water and refrigerated. The catches were returned to the laboratory and preserved in 4% formaldehyde. When necessary, samples were subsplit with a Folsom plankton splitter so that between 400 and 1000 individuals were counted. Many groups, including copepods, krill, salps and cladocerans, were identified to species. Other individuals were identified to coarser taxonomic levels.

Measurements for wind speed, rainfall and the Southern Oscillation Index (SOI) were sourced from the Bureau of Meteorology (BoM; www.bom.gov.au). Rainfall and wind data are for the Ellerslie Road (94029) weather station. The SOI is calculated using the pressure differences between Tahiti and Darwin, and can be interpreted as a measure of the intensity of El Niño or La Niña events in the Pacific Ocean. Monthly SOI data were obtained from the BoM.

2.5 Data analysis

Field and laboratory data acquired in this study were stored in a Microsoft SQL Server relational database at the University of Tasmania. Integrity of the data was managed through a combination of in-built integrity rules, stored procedures for importing and checking data and manual checks.

To examine bay-wide trends in the environmental variables over the 5-year sampling period box plots were produced. Each plot highlights the median value (black line), the 25th and 75th percentiles (horizontal edges of boxes), the 10th and 90th percentiles (capped bars), and outliers encompassing the minimum and maximum values (open circles).

Relationships between the sites and environmental factors were examined using principal components analysis (PCA) with PRIMER version 7 (Plymouth, UK). PCA is an ordination technique used to reduce the dimensionality of multivariate data sets and enable graphical presentation of the relationships between factors. Prior to analysis, the data were normalised to account for the different units of the variables under consideration, then a resemblance matrix for all sites was constructed based on Euclidean distance.

To investigate associations between the phytoplankton assemblages at the sampling sites (Q-mode analysis), phytoplankton abundances were fourth root transformed; this transformation is suitable for ecological data where there are many zeros and few large values (Quinn and Keough, 2002), and is recommended when using the Bray-Curtis index as a measure of (dis)similarity. The PERMANOVA routine of PRIMER 7 was applied to the phytoplankton assemblages, using the Bray-Curtis measure of similarity. Two random factors, YEAR and SOI, were considered in the model, with YEAR having a significant effect on phytoplankton assemblage (Pseudo-F = 5.503, $P=0.01$). A matrix of Bray-Curtis similarities (Bray and Curtis, 1957) was constructed for all sites and subjected to canonical analysis of principal coordinates (CAP), a constrained ordination method which finds the axes that best discriminate between groups; i.e. between the five sampling years.

3. Results

3.1 Storm Bay – general overview of conditions

In this section we provide information on the factors influencing Storm Bay and describe the spatial and temporal dynamics of key water column parameters.

3.1.1 SOI, rainfall and wind

A plot of the Southern Oscillation Index (SOI) during the sampling period is shown in Figure 3.1. SOI values below -7 (e.g. Summer 2010, Spring 2014) are indicative of El Niño conditions and are usually accompanied by sustained warming of the central and eastern tropical Pacific Ocean, a decrease in the strength of the Pacific Trade Winds, and reduction in winter and spring rainfall over eastern Australia (BOM 2016). In south east Australia the warm EAC does not penetrate as far south, resulting in cooler surface waters and stronger westerly winds. SOI values above +7 (e.g. July 2010 – April 2011) are typical of La Niña episodes. They are associated with stronger Pacific trade winds and warmer sea temperatures to the north of Australia. Waters in the central and eastern tropical Pacific Ocean become cooler during this time. Together these give an increased probability that eastern and northern Australia will be wetter than normal. Rainfall around Hobart (Figure 3.1) is shown for the Ellerslie Road site.

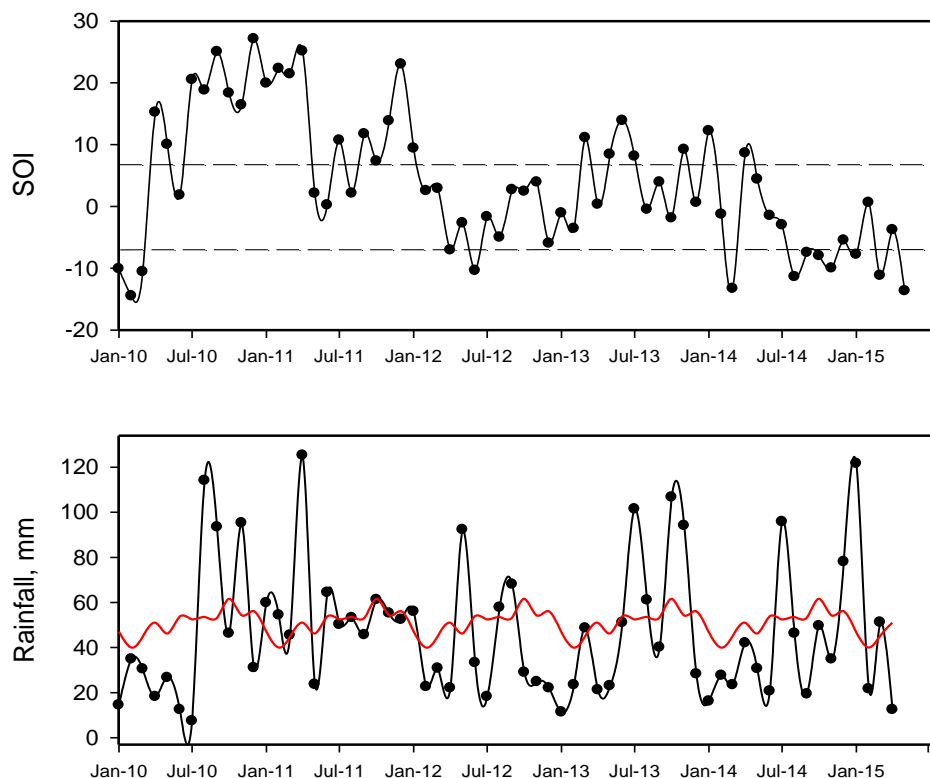


Figure 3.1 Top panel: Southern Ocean Index (SOI), 2010 – 2015 (Data from Bureau of Meteorology), dashed lines show +7 and -7; Bottom panel: Average rainfall (black line) measured at the Ellerslie Road BoM site, 2010-2015. Long-term average monthly rainfall (1885-2009) shown in red (repeated for each year of sampling).

Record rainfalls in winter and spring 2010 coincided with high SOI, whilst 2012 and 2014 were drier than long-term records, coincident with sustained negative SOI values. Note that rainfall around the Storm Bay catchment can be localised so patterns will be somewhat dependent on the weather station from where the data are sourced.

Seasonal wind roses for long term data (1958 – 2004) are shown in Figure 3.2. Based on the measurements made at 9 am the average wind direction is typically from the north-west (Figure 3.2A), whereas wind direction is generally more variable at the 3 pm measurement. During the summer afternoon sea breezes come largely from the south-east, or from a southerly direction. In autumn, wind direction is much more variable; winds in March continue to be similar to those in summer, in April there are increasing westerly and north-westerly afternoon breezes while in May the winds are predominantly from the north-west. During winter winds are principally from the north-west during June and July, but become more variable in August, generally flowing from the west, north-west and north. Finally, in spring the wind direction during September is similar to August, though a higher proportion comes from the south and south-east; this trend becomes stronger and winds during October and November come increasingly from the south-east.

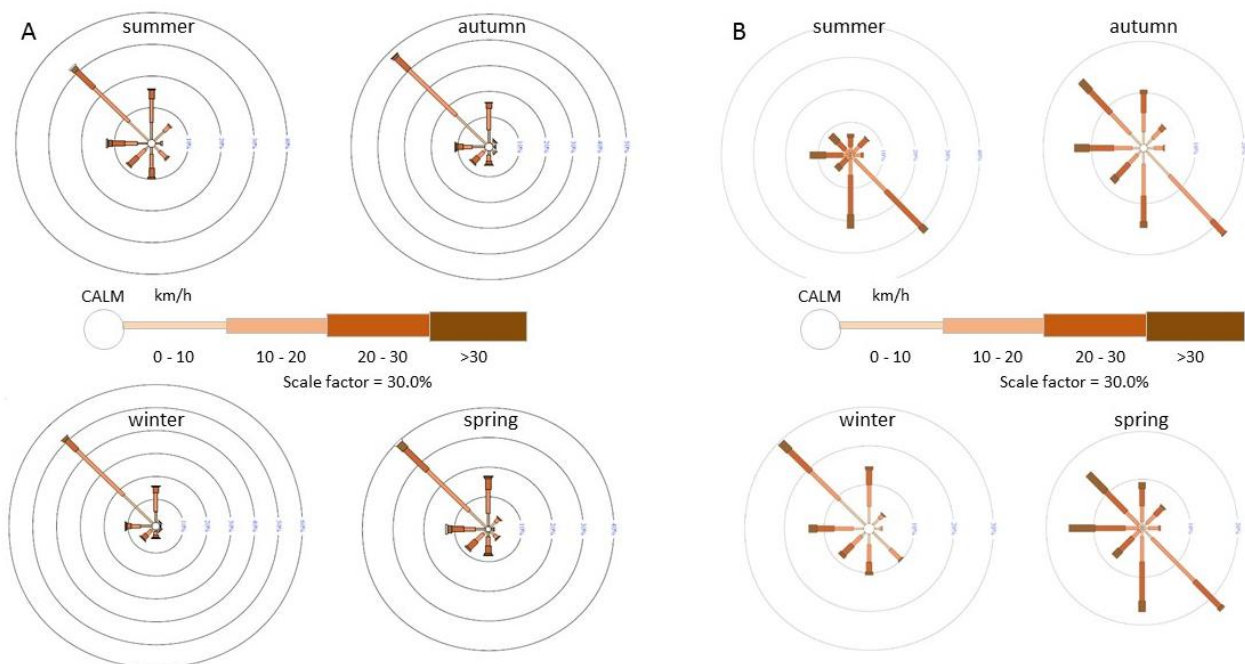


Figure 3.2 Average annual long-term wind strength and direction (1958 – 2004). Data sourced from Bureau of Meteorology weather station at Ellerslie Road, Hobart and Hobart Airport. Wind roses for all seasons at A) 9 am and B) 3 pm.

3.1.2 Temperature, salinity, DO and chlorophyll a

Water temperature, averaged across the water column (Figure 3.3), in Storm Bay followed a distinct seasonal cycle each year, reaching a low of 9 °C and a high of 19.1 °C. Warmest temperatures were in February, followed by a gradual cooling throughout autumn to a winter minimum in August, then increasing again during spring. Across the sites, the median

temperature varied little, with site 3, the most marine of the sites, showing the least spread in values.

Data available from the Integrated Marine Observing System shows results from Slocum Glider missions into Storm Bay (Figure 3.4; <https://portal.aodn.org.au>). The glider has run missions in Storm Bay since 2009, generally around 2 to 3 weeks per deployment and covering up to 1000 km.

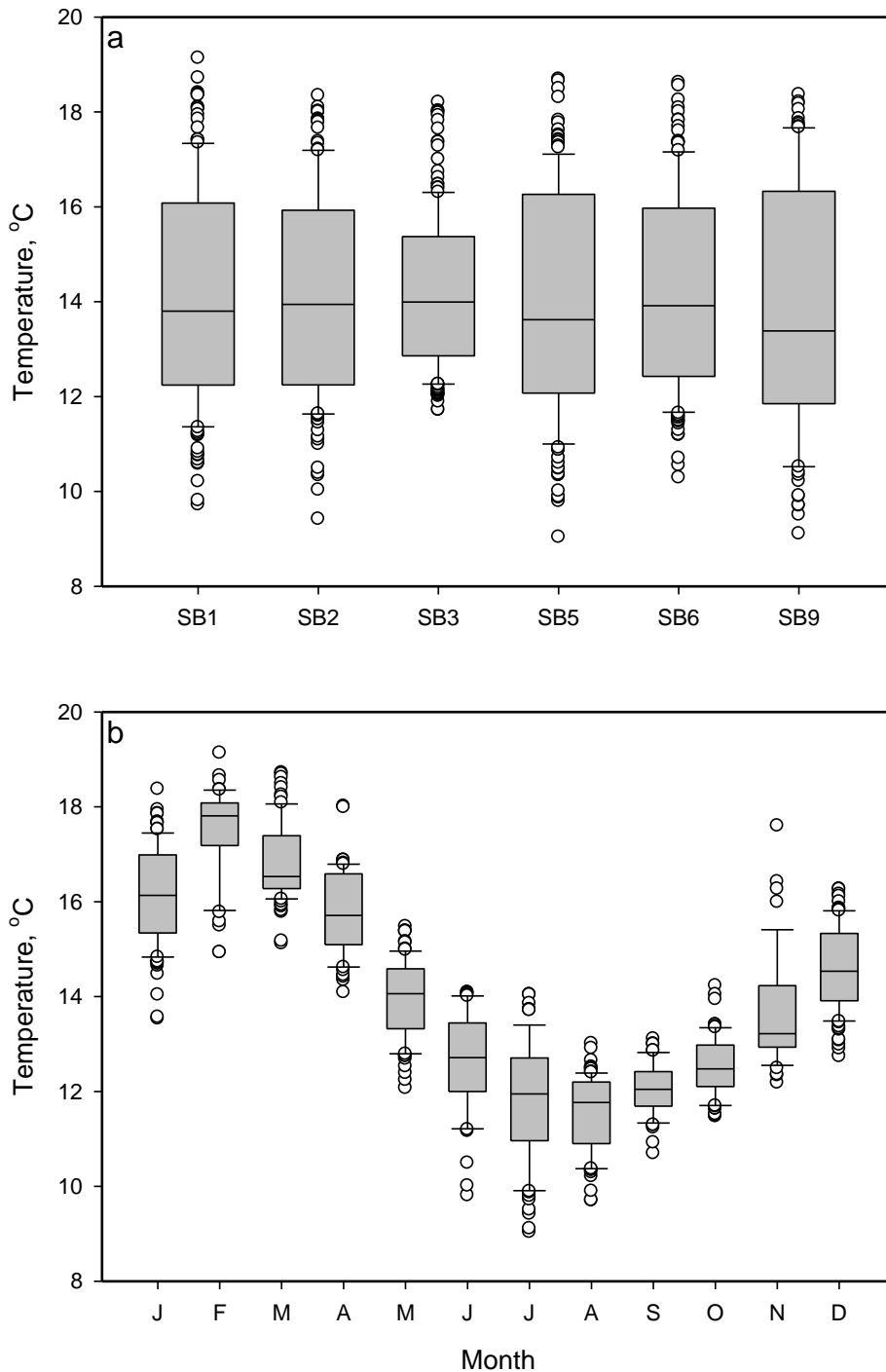


Figure 3.3 Water temperature (°C) across all sites (a) and months (b) in Storm Bay, 2009 – 2015. Box plots show the median temperature (50th percentile, black line), the 25th and 75th percentiles (horizontal edges of boxes), the 10th and 90th percentiles (capped bars), and outliers (open circles).

It moves through the water column in a zig-zag fashion, traversing the water column from the surface to within 10 m of the bottom, providing high resolution (5 second sampling interval) profiles of water properties (Rizwi et al. 2010). IMOS routinely undertake quality control: data are compared with calibrated CTD casts and bottle samples at the beginning and end of the deployment (Rizwi et al. 2010).

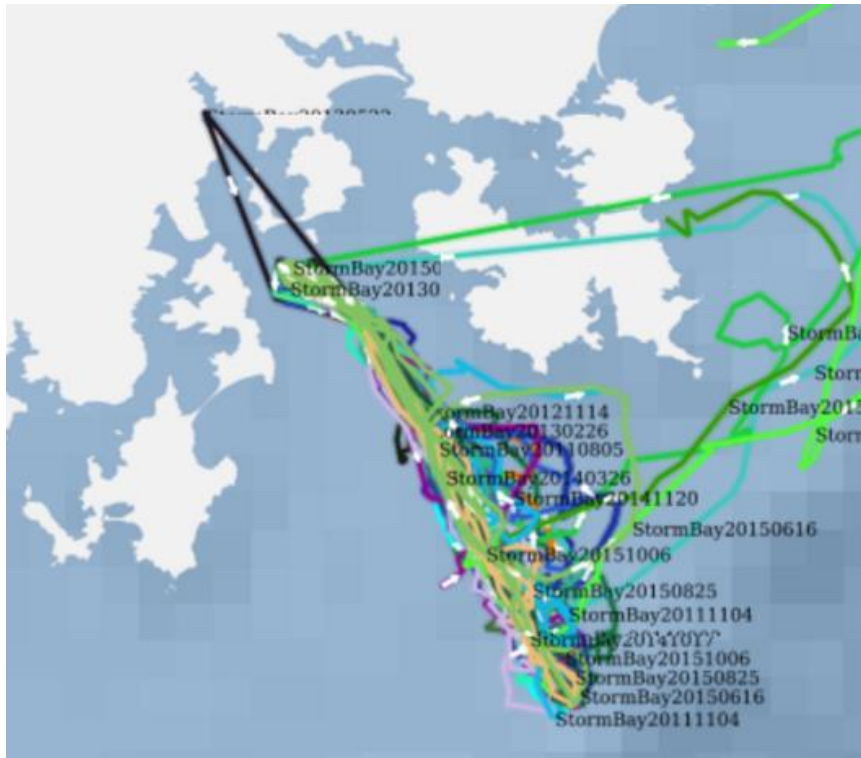


Figure 3.4. Map of Storm Bay, showing glider tracks. Slocum Gliders have been deployed by the ANFOG (Australian National Facility for Ocean Gliders) for IMOS, from the mouth of the Derwent Estuary to the continental shelf, passing close to sites 1, 2 and 3 in the present study.

Representative glider profiles of temperature from each season are shown in Figure 3.5. Stratification is strongest in summer, with the warmest temperatures generally in regions where the water is shallowest (20 – 40 m). Towards the edge of the shelf (depths of 120 – 160 m) temperatures are cooler, though stratification remains strong. The thermocline deepens in autumn, as highlighted by warmer temperatures towards the edge of the shelf. Increased mixing in winter results in little stratification, though surface waters are cooler over the shallow waters at the mouth of the Derwent Estuary. Lastly, in spring the waters are well-mixed throughout the water column across the shelf.

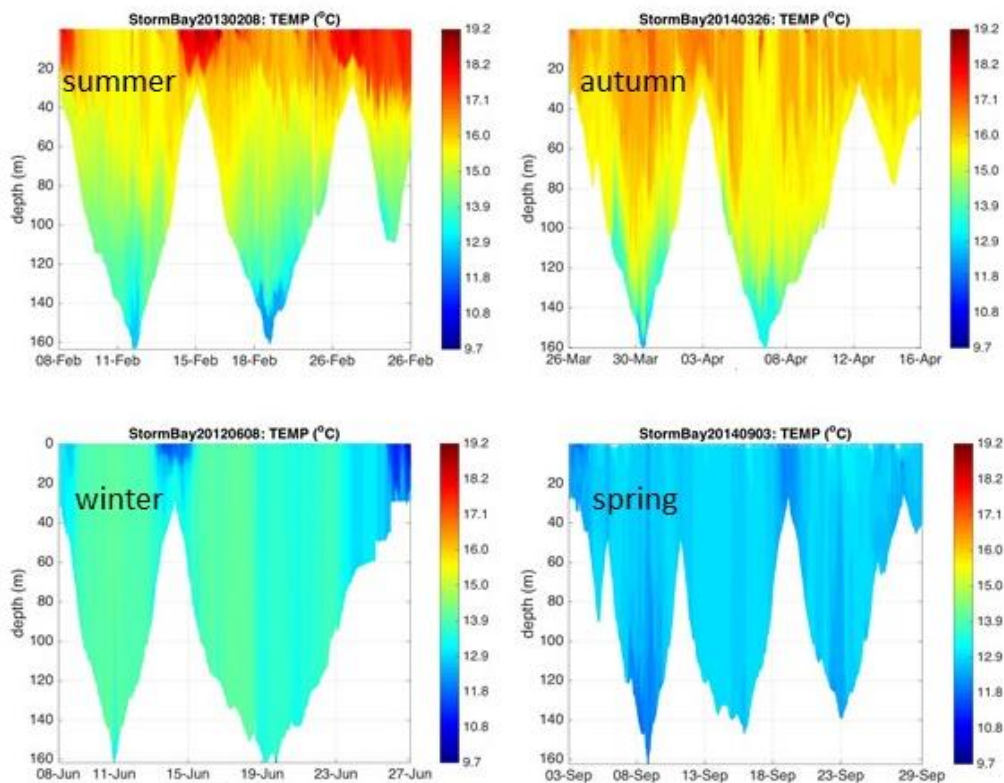


Figure 3.5 Glider transects of temperature with starting dates: 8 February 2013 (summer), 26 March 2014 (autumn), 8 June 2012 (winter) and 3 September 2014 (spring). Colourbars range from 9.7 °C to 19.2 °C.

Median salinity varied little across Storm Bay, being slightly higher at sites 3 and 6, highlighting the marine nature of site 3 and the patterns of seawater circulation in Storm Bay. The lowest salinities were recorded at site 1 (Figure 3.6), where less saline surface waters flow into the bay from the Derwent Estuary. Seasonally, salinity was highest in autumn, with slightly fresher water present in Storm Bay in spring. Some lower salinity values were recorded in July and August, suggesting the presence of less saline subantarctic water flowing into the bay, or freshwater flow from the Derwent. Glider transects show slight lower salinity in summer, then mild stratification in autumn to spring, especially in the shallow regions near the mouth of the Derwent (Figure 3.7).

Plots of temperature versus salinity, based on CTD profiles throughout the water column on each sampling date, for each of the sites are presented in Figure 3.8. The colourbar in the figure represents the density layers (as a function of salinity and temperature). Fresher surface waters were common at site 1 and, to a lesser extent, sites 2 and 5. This reflects circulation in Storm Bay, where fresh surface waters flow from the Derwent into site 1, then flowing out past sites 2 and 5. There is a clear gradient from river-influenced estuarine waters at site 1 through to the marine waters of site 3.

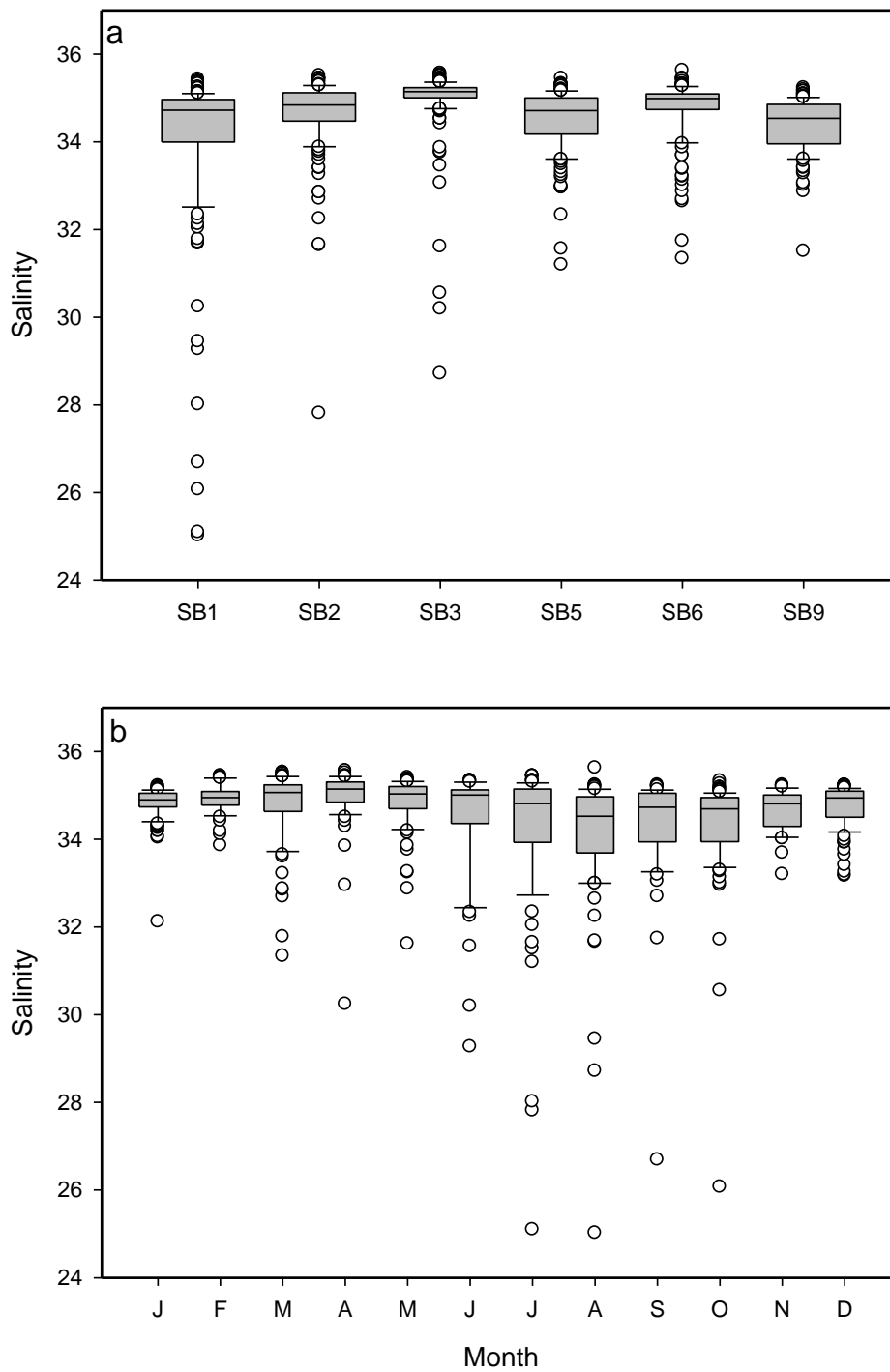


Figure 3.6 Salinity across all sites (a) and months (b) in Storm Bay, 2009 – 2015. Box plots show the median salinity (black line), the 25th and 75th percentiles (horizontal edges of boxes), the 10th and 90th percentiles (capped bars), and outliers (open circles).

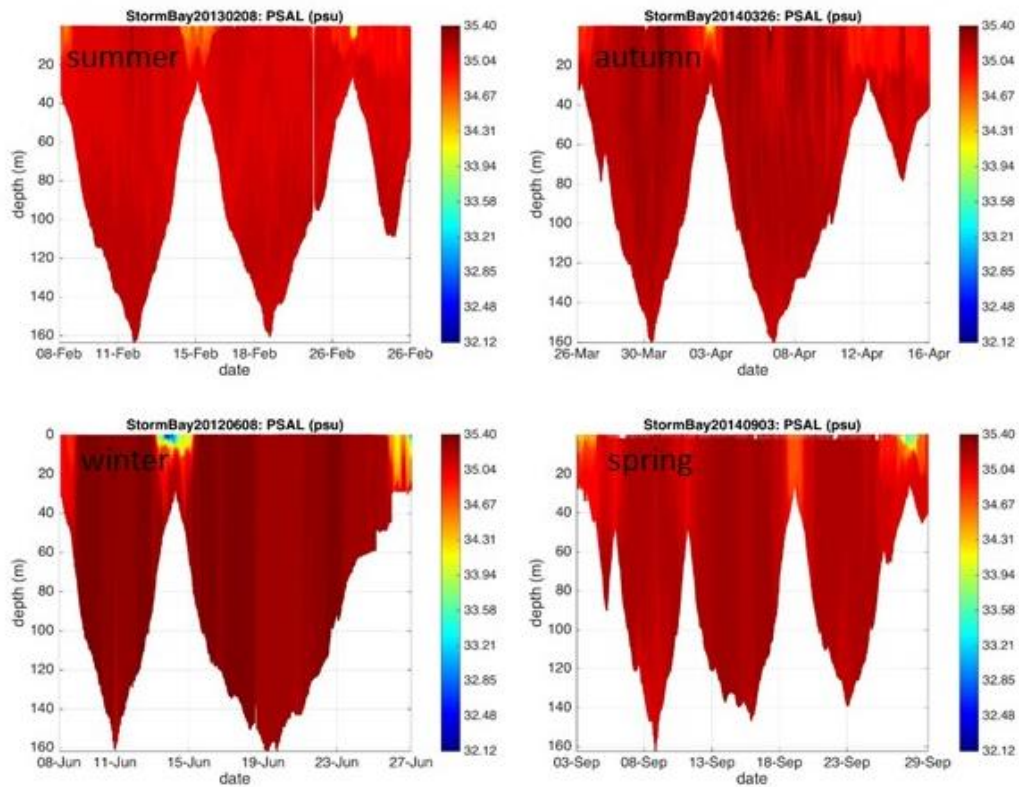


Figure 3.7 Glider transects of salinity with starting dates: 8 February 2013 (summer), 26 March 2014 (autumn), 8 June 2012 (winter) and 3 September 2014 (spring). Colourbars range from 32.12 to 35.40.

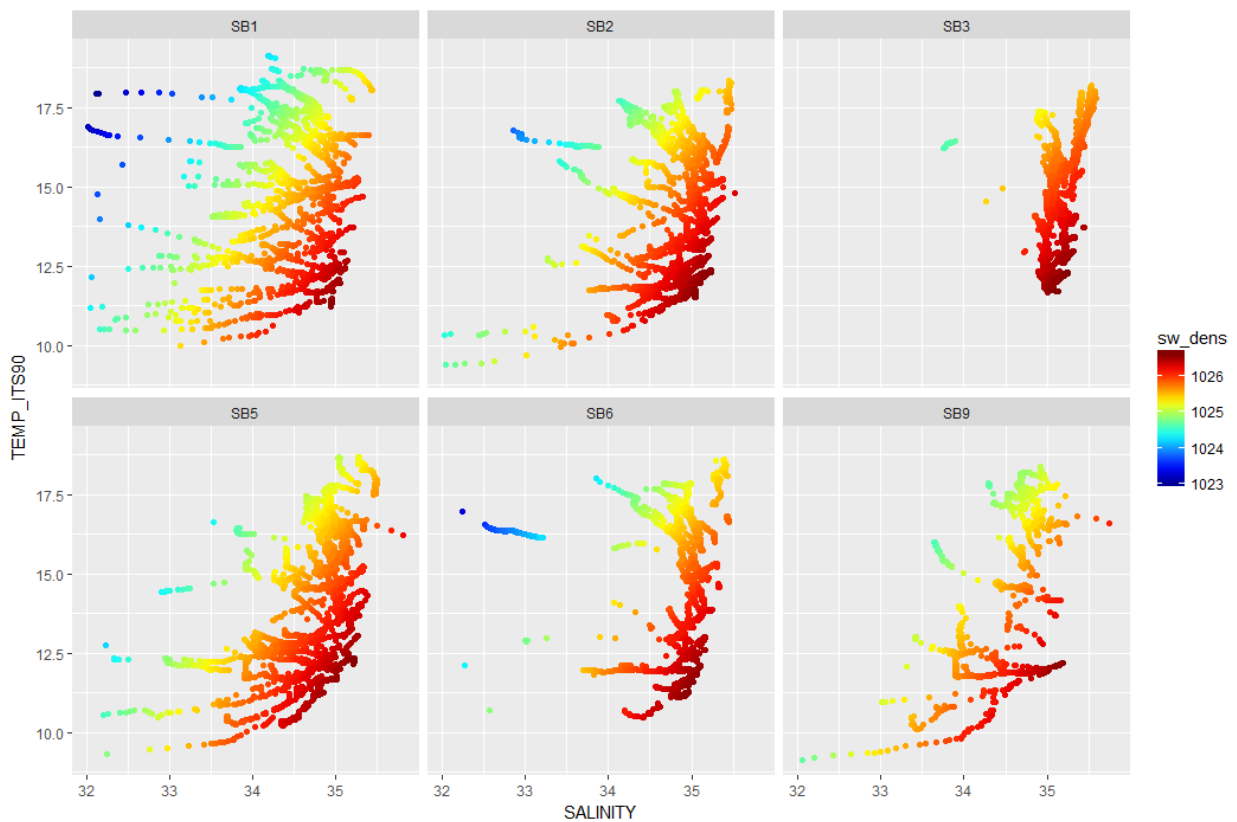


Figure 3.8 Temperature-salinity plots. Points show data from each CTD deployment on every sampling date for each site. Colourbar is seawater density, with less dense water layers showing to the left of each plot.

Dissolved oxygen results were not accurate for the first ten months and have not been included in any of the analyses. Dissolved oxygen was uniform across Storm Bay (Figure 3.9), with the median around 7.8 mg L⁻¹. Most of the values fell between the 25th and 75th percentiles, and site 3 again

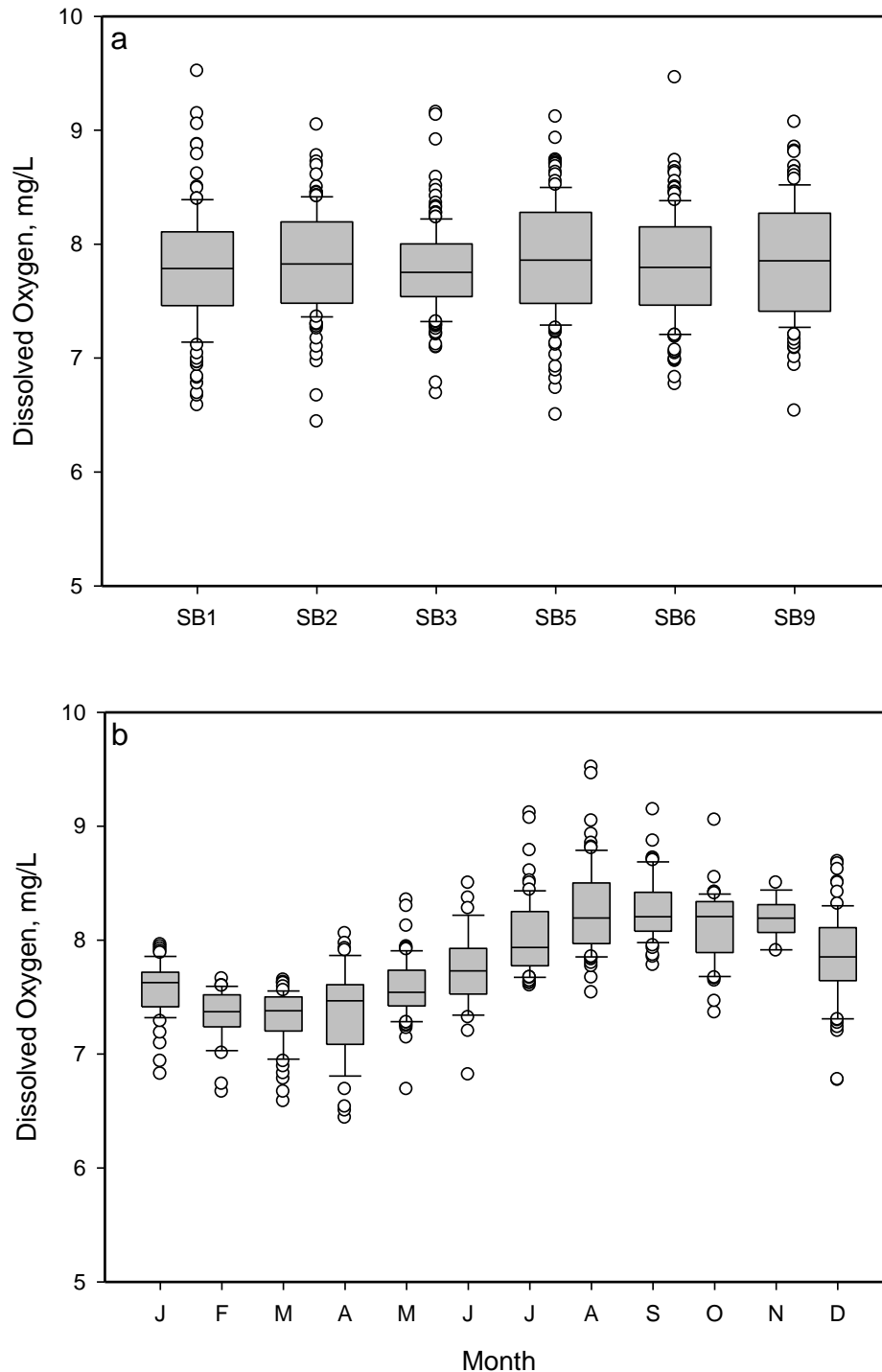


Figure 3.9 Dissolved oxygen across all sites (a) and months (b) in Storm Bay, 2010 – 2015. Box plots show the median DO (black line), the 25th and 75th percentiles (horizontal edges of boxes), the 10th and 90th percentiles (capped bars), and outliers (open circles). Note that trips 11 – 54 only were plotted due to instrument unreliability during the first 10 sampling trips.

showed the least amount of spread around the median. Seasonally, dissolved oxygen was lowest in late summer and autumn when temperatures were highest, indicating net respiration in Storm Bay during January to April. Dissolved oxygen increased to a spring maximum, highlighting net productivity and well mixed waters, then began to decrease again in late spring. Glider transects show similar trend, with lower dissolved oxygen present in the bay in summer and autumn, gradually increasing through winter and reaching a maximum in spring (Figure 3.10).

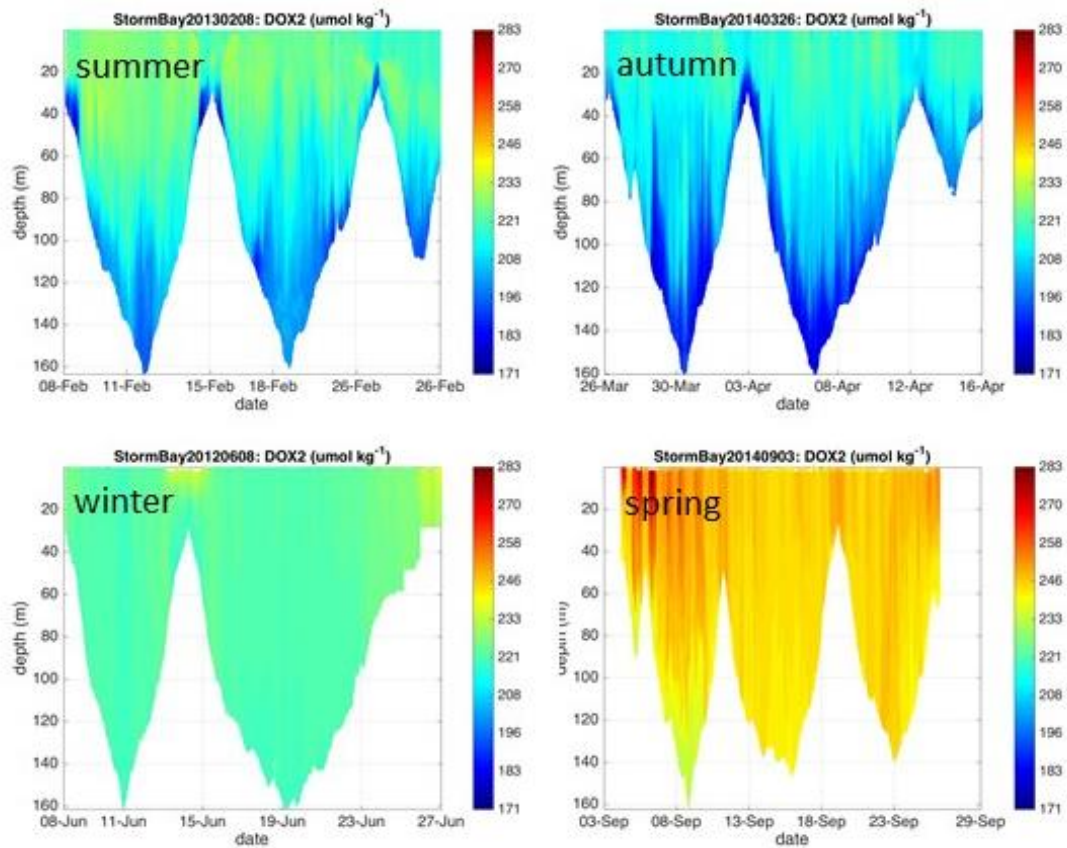


Figure 3.10 Glider transects of dissolved oxygen with starting dates: 8 February 2013 (summer), 26 March 2014 (autumn), 8 June 2012 (winter) and 3 September 2014 (spring). Colourbars range from 171 to 283 $\mu\text{mol kg}^{-1}$.

3.1.3 Chlorophyll *a* and Secchi depth

The concentration of chlorophyll *a* showed surprisingly little variation across the seasons (Figure 3.11). There was a gradient in concentration from site 1 to site 3, where chlorophyll *a* decreased slightly. It was highest and most variable at the inshore sites 1 and 9, and lowest at site 3, furthest out in the bay. There was no clear annually recurrent seasonal bloom, although data suggests higher values in spring and autumn (see later time series). Average chlorophyll *a* was quite low, $0.84 \mu\text{g L}^{-1}$, with a maximum value of $5.82 \mu\text{g L}^{-1}$ recorded at 10 m at site 9 in August 2011, and the minimum of $0.05 \mu\text{g L}^{-1}$ at site 3 in winter. Chlorophyll *a* was generally inversely related to Secchi depth (Figure 3.12). This is to be expected, as an increased number of particles in the water column will decrease transparency, leading to shallower Secchi depths. Secchi values tended to be shallower in summer, and chlorophyll *a* concentration higher. Shallow Secchi depths are more

likely to occur in winter and spring (Figure 3.12). Glider transects clearly show increased chlorophyll *a* in spring, especially during the first few days of the mission, 3-6 Sept, 2014 (Figure 3.13). There was also a clear bloom in autumn in the top 30 m, while these surface blooms in summer tended to be over the shallower waters near the mouth of the Derwent.

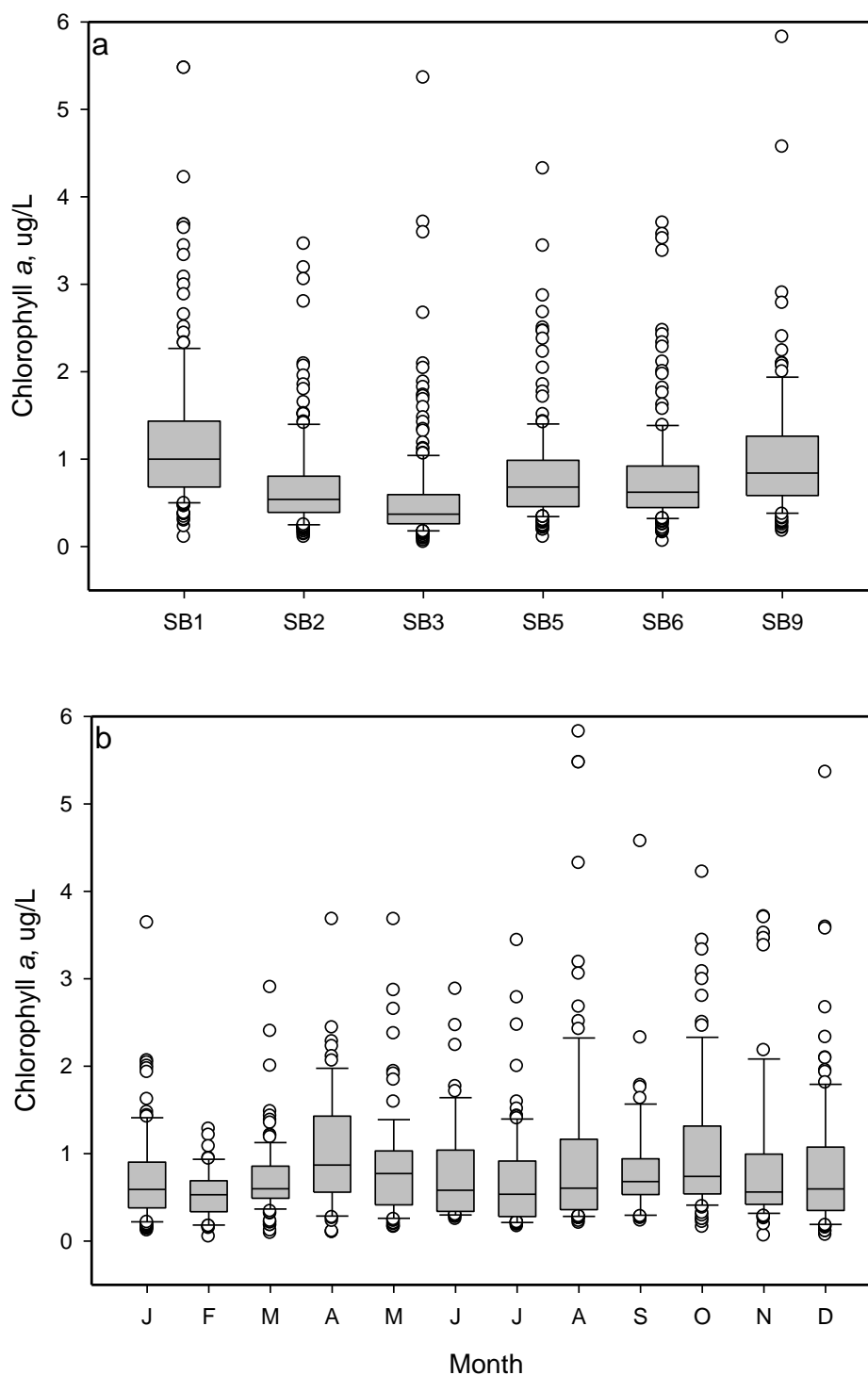


Figure 3.11 Concentration of chlorophyll *a* across all sites (a) and months (b) in Storm Bay, 2009 – 2015. Box plots show the median chlorophyll (black line), the 25th and 75th percentiles (horizontal edges of boxes), the 10th and 90th percentiles (capped bars), and outliers (open circles).

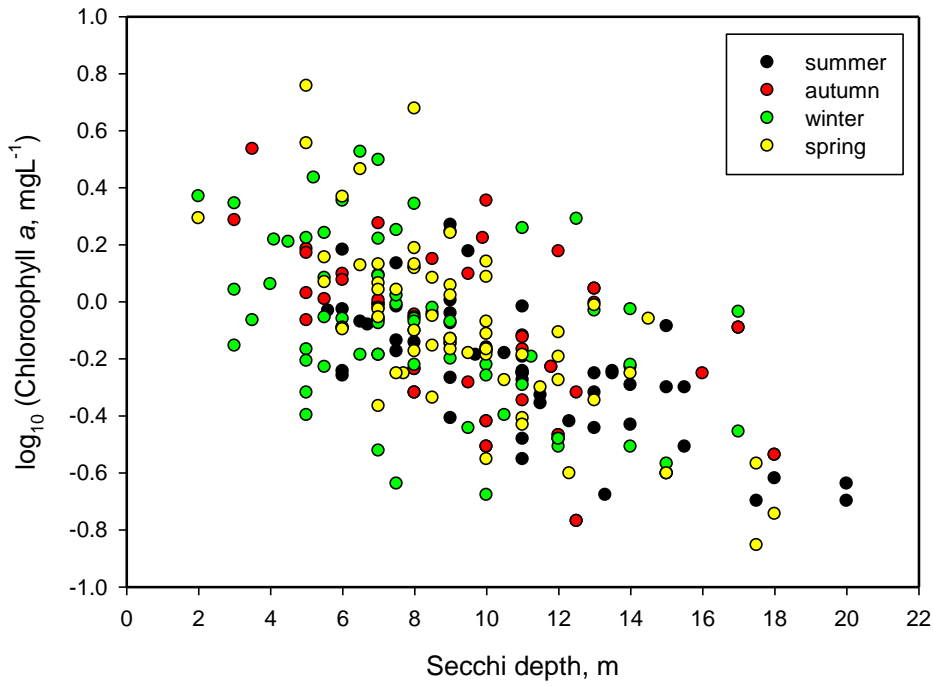


Figure 3.12 Concentration of chlorophyll a (log₁₀) versus Secchi depth across all sites for each season.

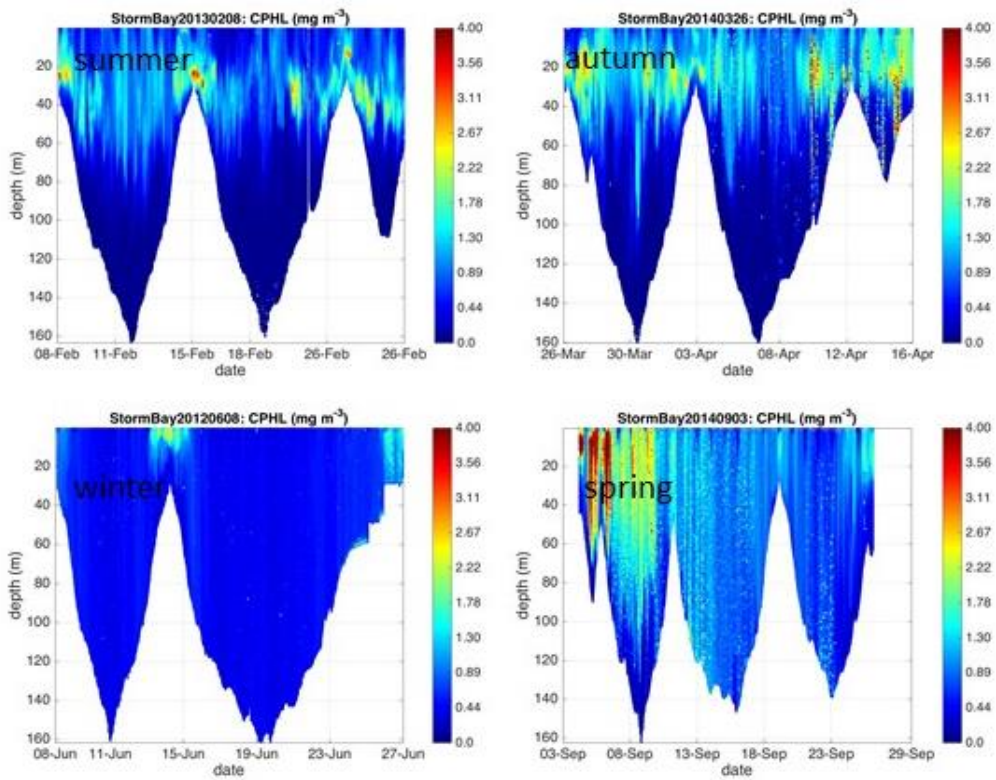


Figure 3.13 Glider transects of dissolved oxygen with starting dates: 8 February 2013 (summer), 26 March 2014 (autumn), 8 June 2012 (winter) and 3 September 2014 (spring). Colourbars range from 0.0 to 4.0 mg m⁻³.

3.1.4 Nutrients

Nitrate + nitrite values (NO_x) at the surface showed clear seasonal trends, peaking over winter at values of 3 – 5 μM (Figure 3.14) and drawing down to near zero in summer and autumn. This distinct seasonal cycle shows evidence of nitrogen input into Storm Bay during winter, the result of intrusion of subantarctic bottom water. Highest values were mostly recorded at sites 1 and 3,

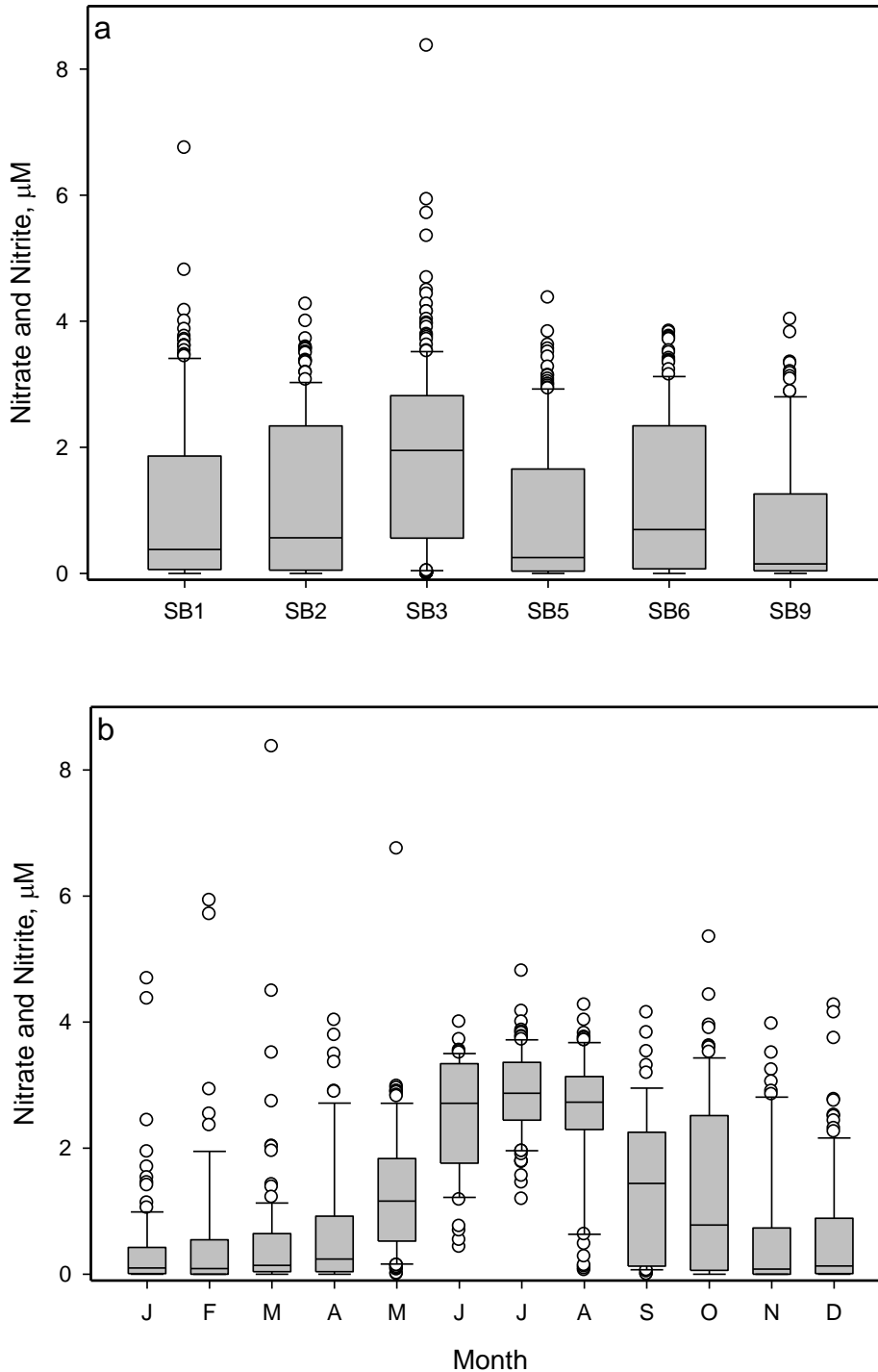


Figure 3.14 Concentration of nitrate + nitrite across all depths for sites (a) and months (b) in Storm Bay, 2009 – 2015. Box plots show the median NO_x (black line), the 25th and 75th percentiles (horizontal edges of boxes), the 10th and 90th percentiles (capped bars), and outliers (open circles).

with the highest median value clearly at site 3. Bottom water NO_x values at site 3 were regularly the highest. There was an increasing gradient in NO_x from site 1 to site 3, while sites 1, 5 and 9 were lower than sites 3 and 6.

Phosphate concentrations (Figure 3.15) also reached a peak in winter, at approximately 0.4 μM, that was associated with Southern Ocean influence. The highest phosphate values generally occurred at site 1, although overall there was little variation in median values between sites (the

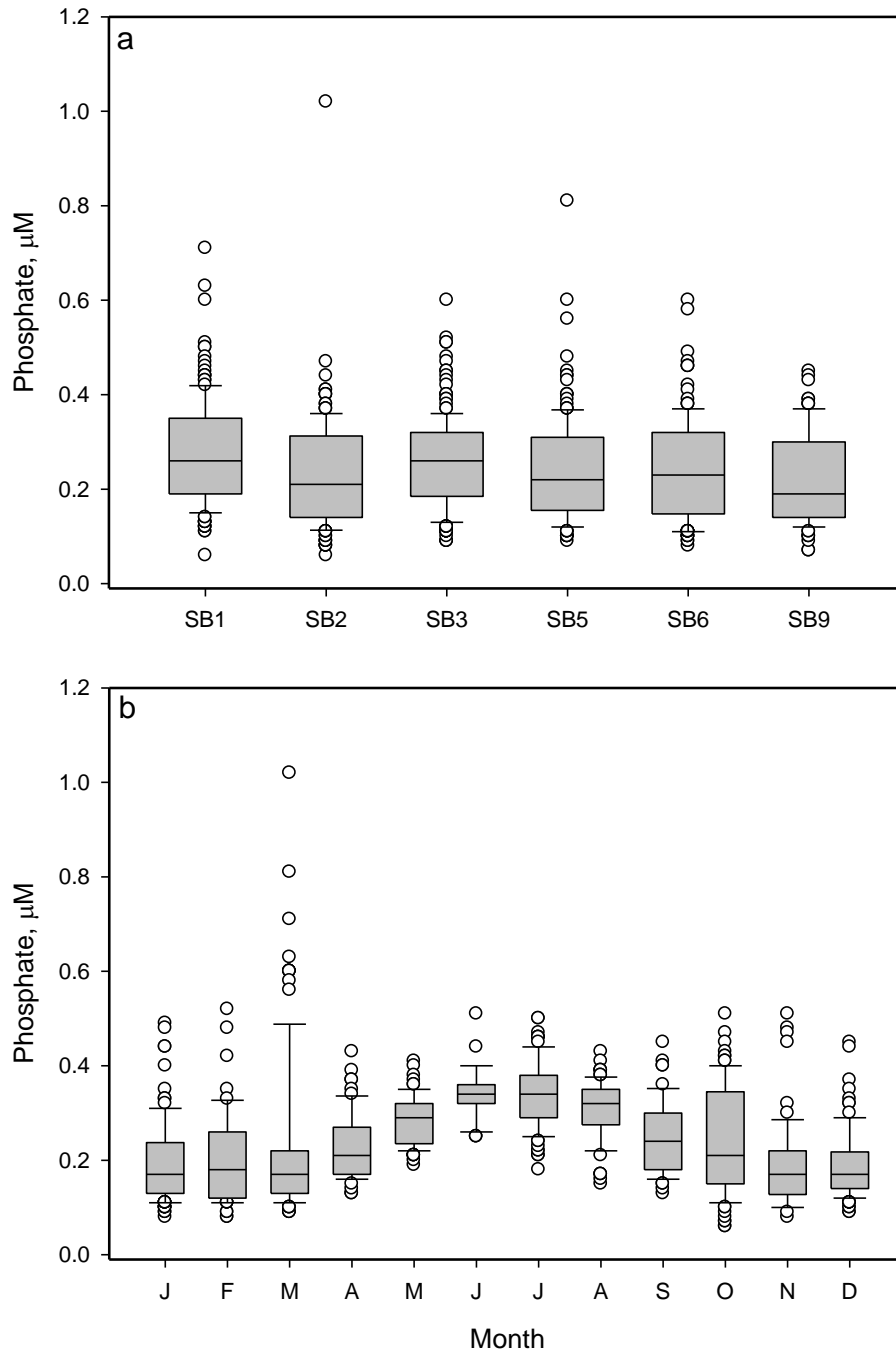


Figure 3.15 Concentration of phosphate across all depths for all sites (a) and months (b) in Storm Bay, 2009 – 2015. Box plots show the median phosphate (black line), the 25th and 75th percentiles (horizontal edges of boxes), the 10th and 90th percentiles (capped bars), and outliers (open circles).

median at site 9 was a little lower than the other sites). Summertime surface phosphate levels at all sites were around or below 0.2 μM . Bottom water phosphate levels were generally between 0.2 and 0.4 μM , with no clear seasonal trends.

Median ammonium concentrations (Figure 3.16) at all sites were generally $<0.5 \mu\text{M}$, with no clear peaks in any season or month. Overall, the lowest values were measured in August and other months showed reasonable spread around the median.

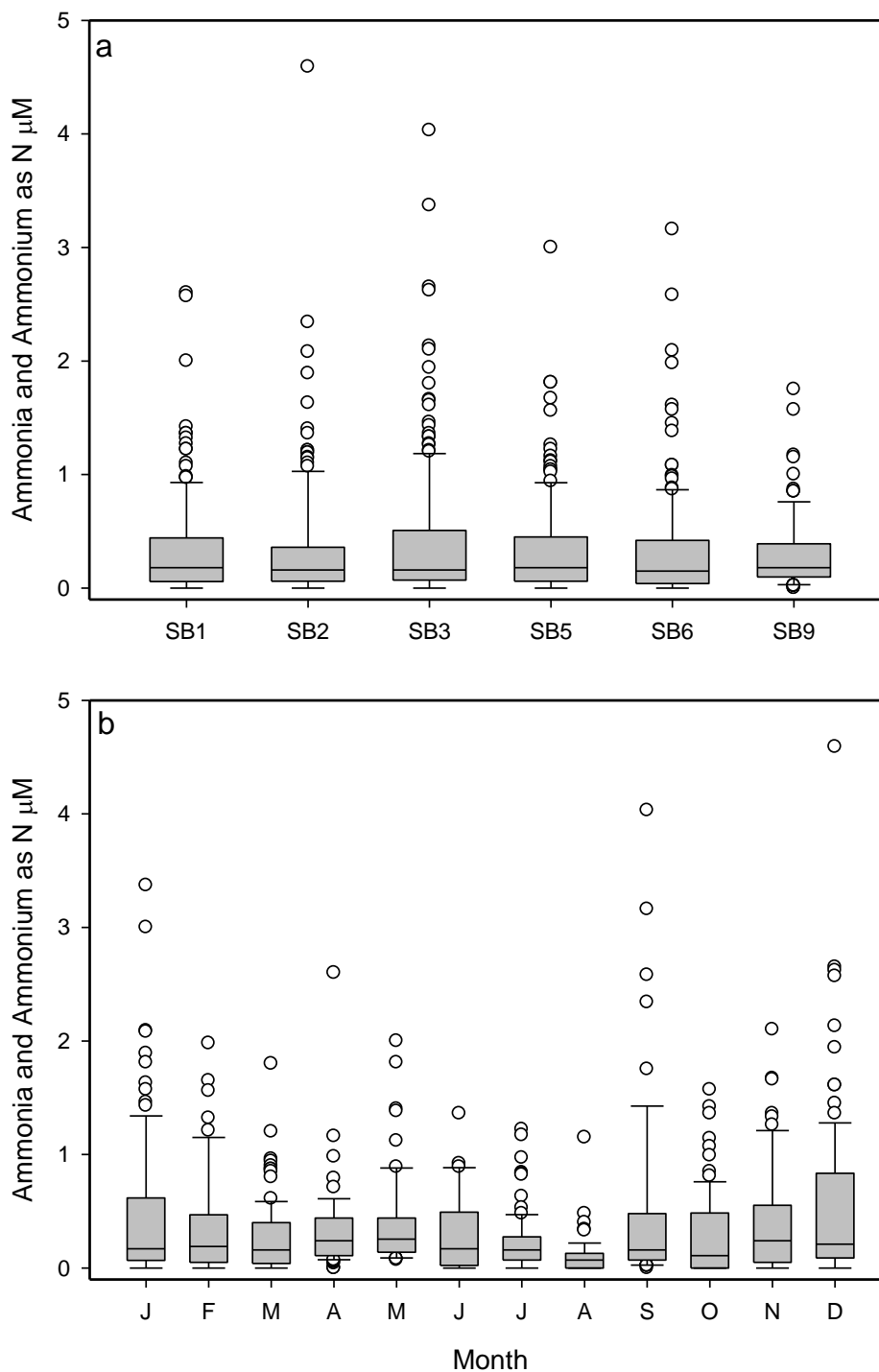


Figure 3.16 Concentration of ammonium across depths and all sites (a) and months (b) in Storm Bay, 2009 – 2015. Box plots show the median ammonium (black line), the 25th and 75th percentiles (horizontal edges of boxes), the 10th and 90th percentiles (capped bars), and outliers (open circles).

Median silicate concentrations (Figure 3.17) were consistently highest at sites 1 and 9, followed by site 5. Water from the River Derwent flows through site 1, then tracks east towards site 9 then site 5 (Herzfeld 2008). The lowest and least variable silicate concentrations were at site 3. Seasonally, silicate was generally highest in winter when the River Derwent outflow is also greatest.

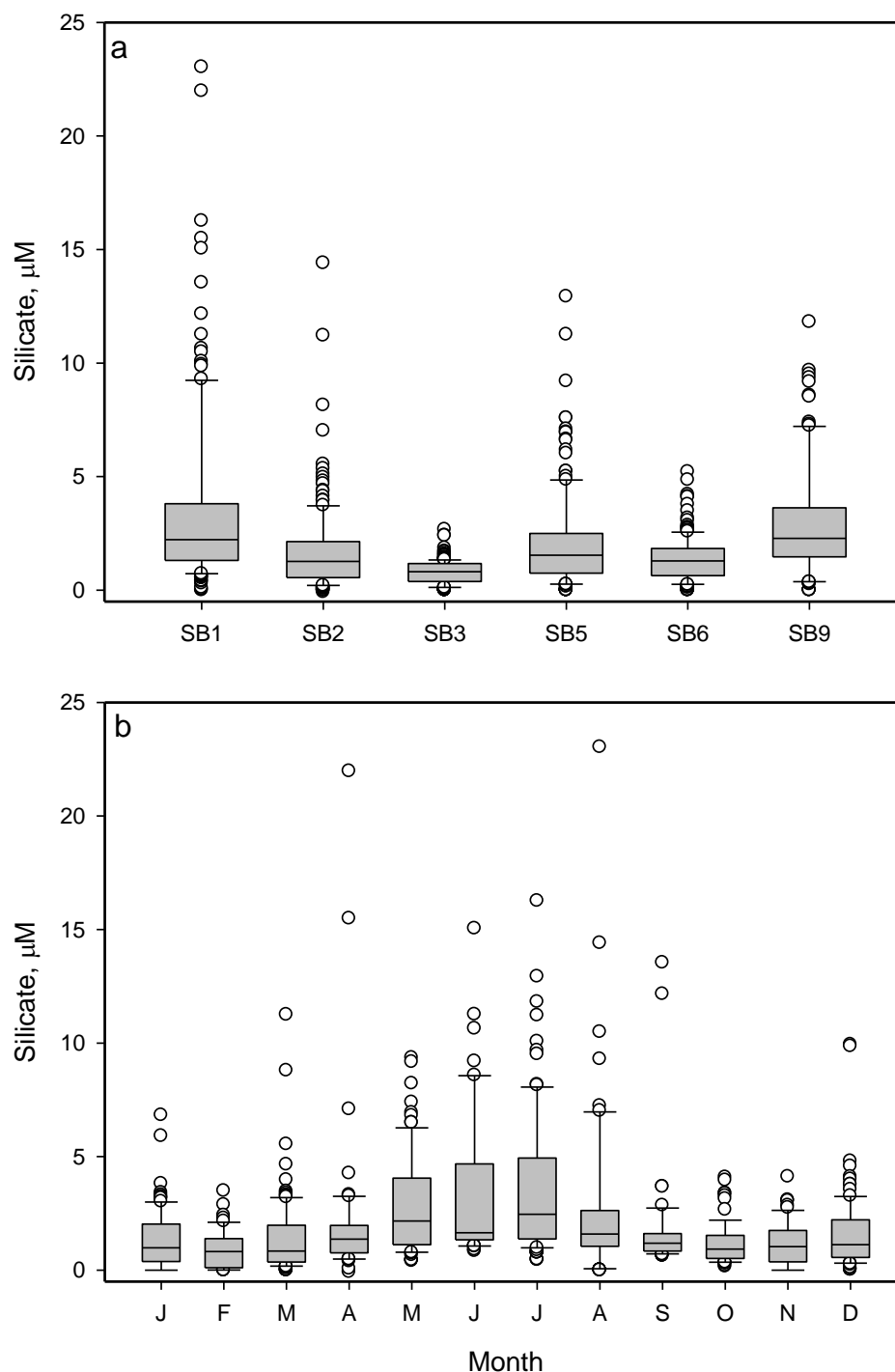


Figure 3.17 Concentration of silicate across all depths and sites (a) and months (b) in Storm Bay, 2009 – 2015. Box plots show the median silicate (black line), the 25th and 75th percentiles (horizontal edges of boxes), the 10th and 90th percentiles (capped bars), and outliers (open circles).

A principal components analysis (PCA) of the environmental variables at all sites is presented in Figure 3.18). Length of the vectors on the plot indicates their strength as drivers of the variation in

the sites, and the closer the vectors the stronger the correlation between variables. Season had a stronger influence on the PCA than site or month, so we have presented only the data for season. The first two principal components accounted for 64% of the variation in the data. Samples from the winter clustered in the bottom right quadrant, and were influenced by high concentrations of phosphate and NO_x. Samples from summer and spring clustered to the left of the ordination and were influenced by high temperatures and drawdown of nutrients. Autumn samples crossed the plot, perhaps indicating the transition between water states from the summer to the winter.

Based on draftsman plots of correlations between environmental variables (all years, data not shown), nitrate and phosphate were highly correlated in winter ($R=0.7035$) and spring ($R = 0.8647$) following recharge from Southern Ocean influences, with low correlation in summer ($R < 0.01$) and autumn ($R=0.2514$) when nutrient draw-down resulted in nitrate depletion. Nitrate is widely believed to be the limiting nutrient in marine systems, limiting phytoplankton growth.

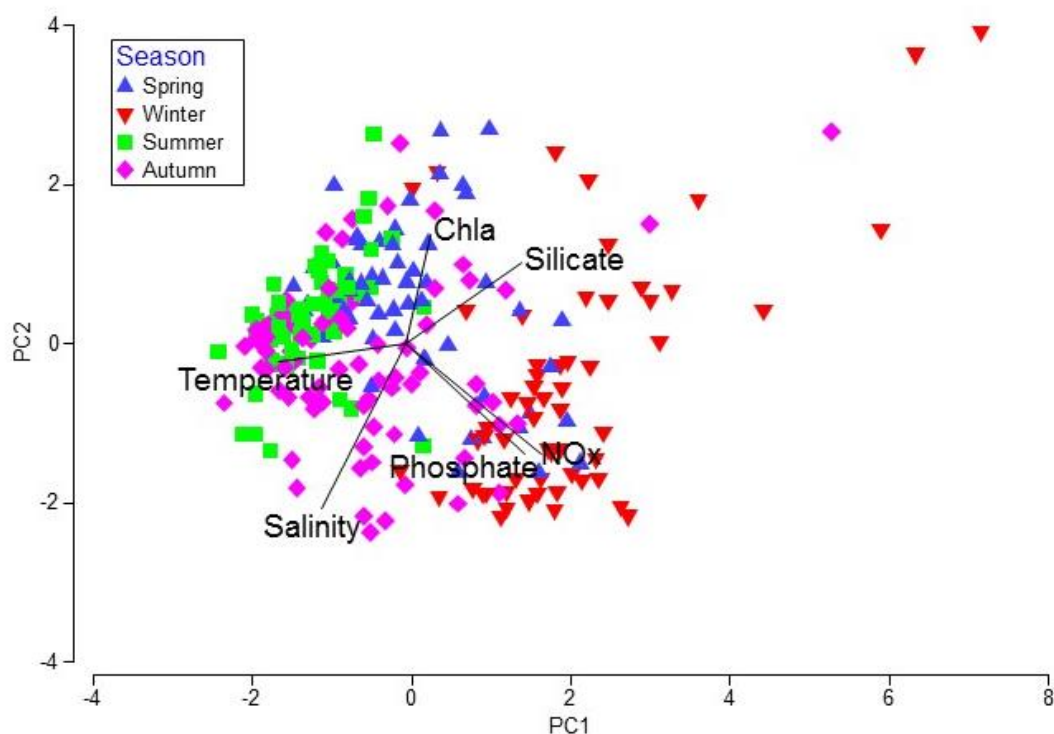


Figure 3.18 Principal Components Analysis of the six physical and chemical factors measured at the six sites between November 2009 and April 2015. PC1 accounted for 42% of the variation in the data, and PC2 accounted for 22%.

3.2 Sites in Storm Bay

This section focusses on the six sites in Storm Bay, showing temporal trends in variables for both surface and bottom waters.

3.2.1 Site 1 (43.07S, 147.39°E)

Site 1 was located close to the mouth of the Derwent River (Figure 2.5). Water temperature varied in a predictable manner, reaching highs of almost 20 °C in summer and lows of ~10 °C in winter

(Figure 3.19 a). Generally surface temperatures were warmer than near the bottom in summer, and cooler in winter. Surface salinity was influenced by freshwater flow from the river, decreasing to ~ 25 each Spring, except in 2014 when there was only a small decrease (Figure 3.19 b). Bottom salinity was largely invariant over the sampling period. Dissolved oxygen showed corresponding increases at the same periods, and was regularly lower in bottom than surface waters (Figure 3.19 c). Chlorophyll *a* concentrations were variable at site 1, with no clear seasonal trends over the years (Figure 3.19 d). NO_x showed a fairly regular seasonal cycle at Site 1 (Figure 3.20 a), with replenishment in winter and drawdown in summer. In winter 2013 bottom NO_x (6.75 μM) was

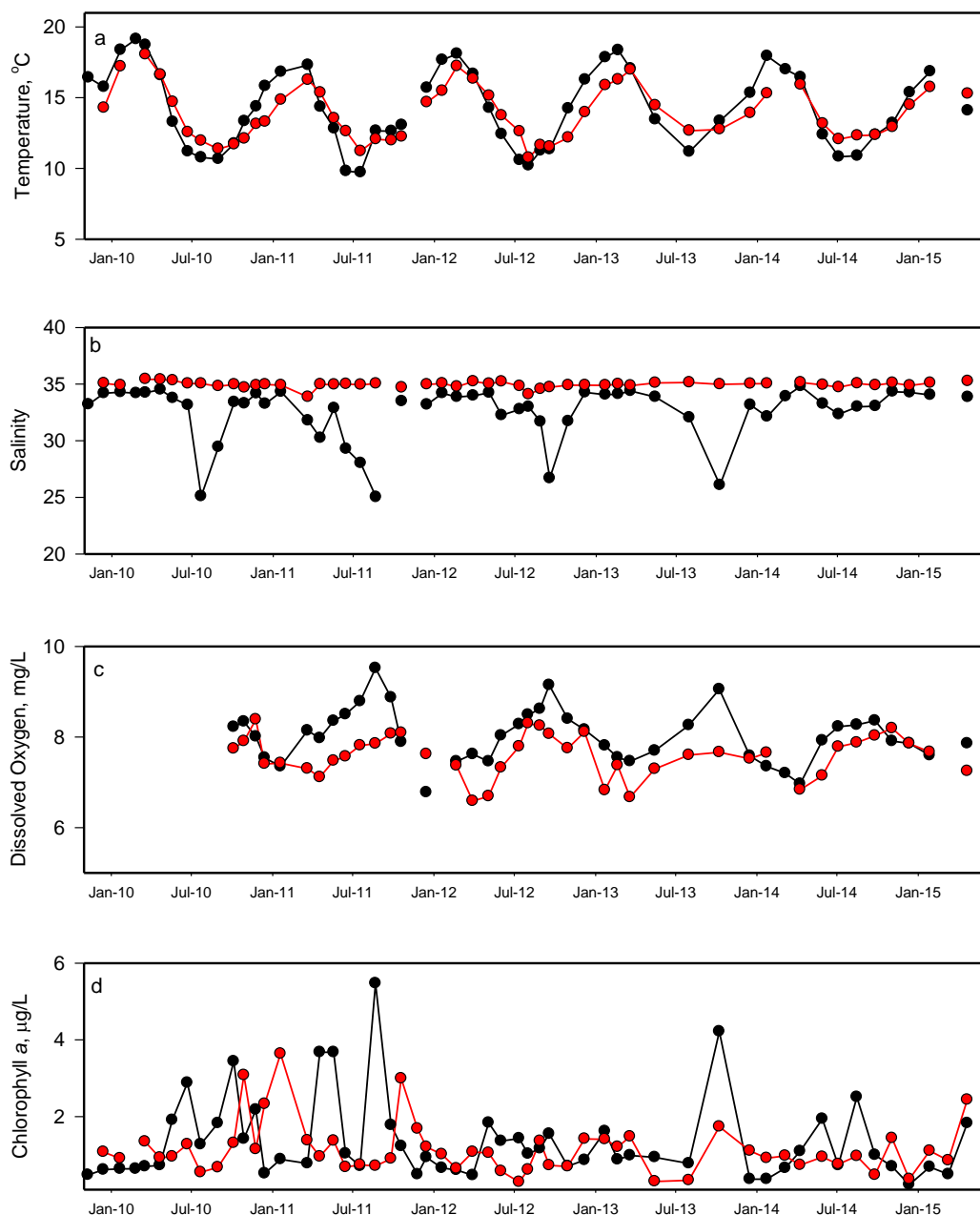


Figure 3.19 Temperature, salinity, dissolved oxygen and chlorophyll *a* concentration at site 1, 2009 – 2015. Surface measurements (black circle and line) were at 0.5 m and bottom measurements (red circle and line) at 15 m. The first 10 months of oxygen measurements were omitted due to technical errors with the instrument.

approximately twice as high as surface NO_x , and it is not clear whether this is indicative of water mass influence or simply contamination of the sample. Ammonium was often higher in the bottom waters than at the surface (Figure 3.20 b), perhaps due to processes in the sediments, and did not show such a distinct seasonal cycle. Silicate tended to be drawn down during the summer, although it remained high in surface waters during summer 2011 (Figure 3.20 c), a period when chlorophyll *a* concentrations were low (Figure 3.19 d). There was high rainfall (120 mm) in the summer of 2011 (Figure 3.1), which could possibly explain the high silicate at that time. Silicate values were routinely higher in surface waters at site 1 than any of the other sites. Finally, phosphate showed a similar seasonal cycle to NO_x , with higher concentrations in winter and draw down in summer (Figure 3.20 d). Site 1 surface waters regularly had the highest phosphate values of all the sites, suggesting an influence from the River Derwent.

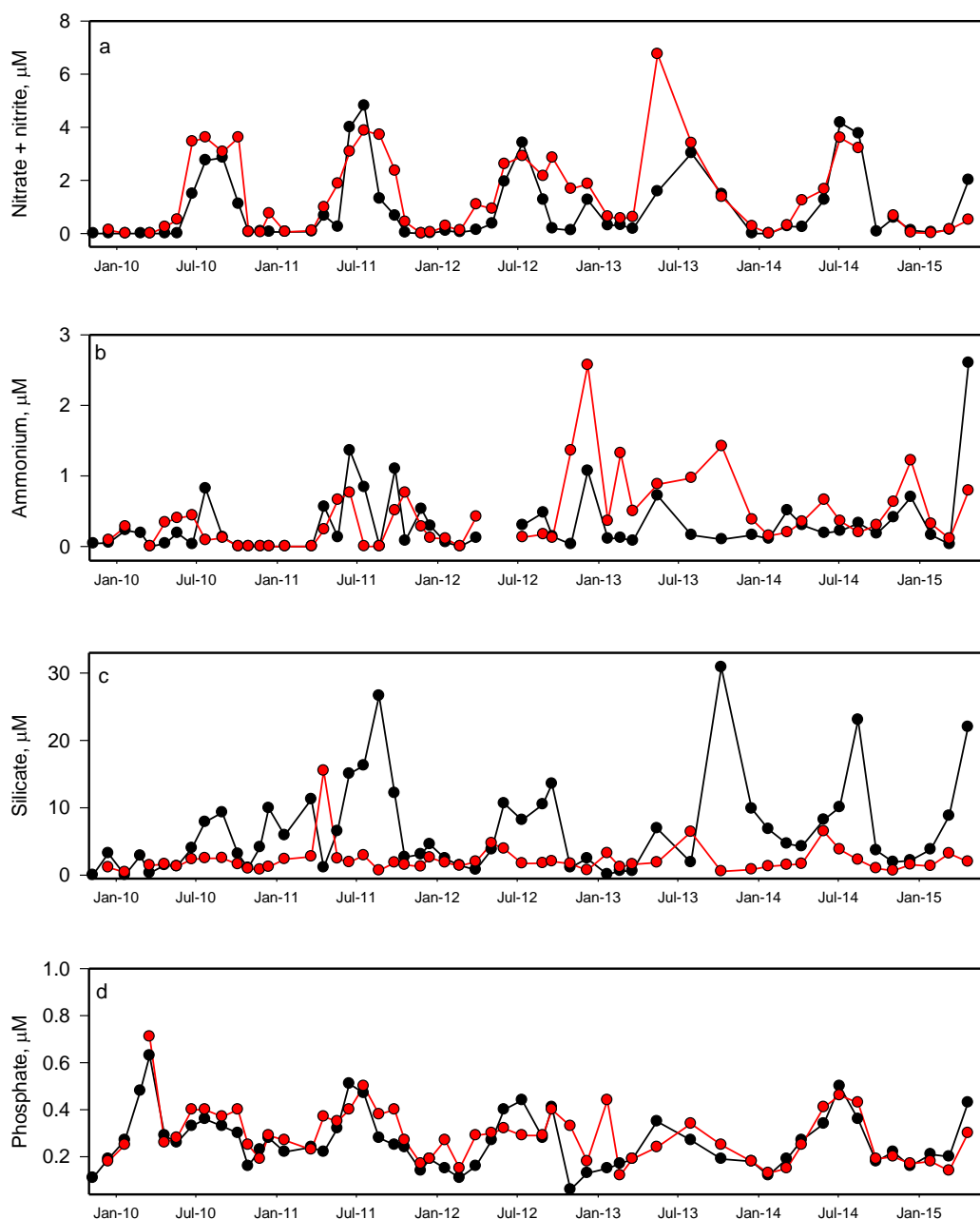


Figure 3.20 Concentration of nutrients at site 1, 2009 – 2015. Surface measurements (black circle and line) were at 0.5 m and bottom measurements (red circle and line) at 15 m.

3.2.2 Site 2 (43.17°S, 147.17°E)

Site 2 was located in the middle of Storm Bay, away from close proximity to the coast. This site was the location for an intensive study by CSIRO in the early 1980s (Harris et al. 1987; Clementson et al. 1989), and was chosen for the present study to enable comparison between the two studies (see Section 3.6 'Historical comparison'). Temperature cycles (Figure 3.21a) were similar to Site 1, while salinity remained more 'marine', with a few times in winter (notably 2010) when surface waters were less saline and indicative of freshwater flowing from the Derwent (Figure 3.21b). Dissolved oxygen followed a seasonal cycle (Figure 3.21c), with water remaining well-oxygenated.

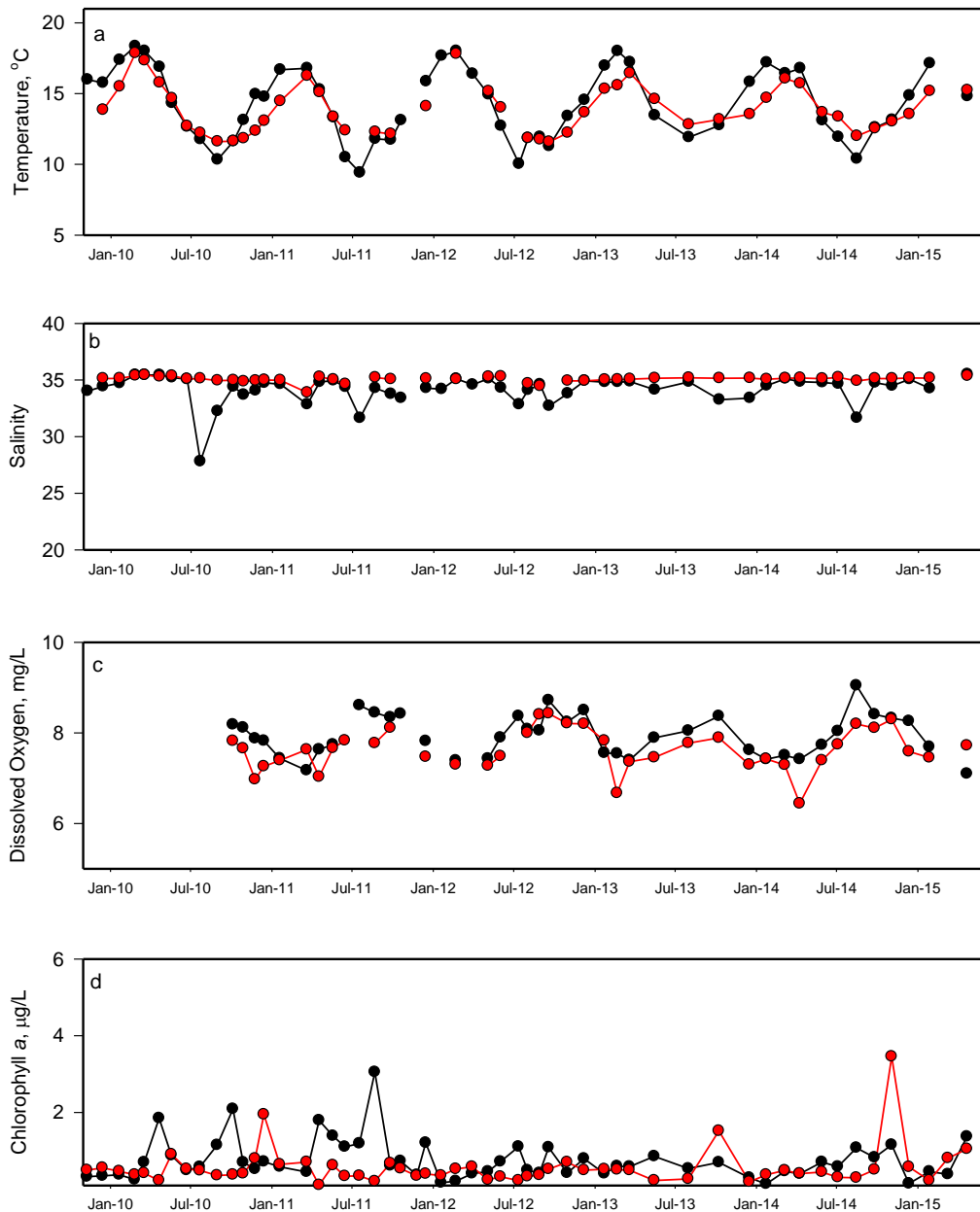


Figure 3.21 Temperature, salinity, dissolved oxygen and chlorophyll a concentration at site 2, 2009 – 2015. Surface measurements (black circle and line) were at 0.5 m and bottom measurements (red circle and line) at 20 m. The first 10 oxygen measurements were omitted due to technical errors with the instrument.

Chlorophyll *a* at Site 2 was less than measured for site 1, not reaching above 3 $\mu\text{g L}^{-1}$ (Figure 3.21d). It was typically higher in surface waters, although occasionally bottom chlorophyll *a* exceeded surface values in spring – summer.

The NO_x cycle was seasonal though less strongly drawn down in bottom waters in summer (Figure 3.22a); this concurs with the low chlorophyll *a* concentration in bottom water at Site 2. Ammonium concentrations at Site 2 were generally below 2 μM , with the highest value recorded in late 2014 (Figure 3.22b). Peak ammonium values often occurred in deeper bottom waters at sites 2 and 3. Surface silicate showed a seasonal cycle (Figure 3.22c), while bottom silicate at site 2 remained relatively low (< 3 μM) throughout the sampling period. Phosphate remained below 0.5 μM , with one high value in autumn 2010 (Figure 3.22d).

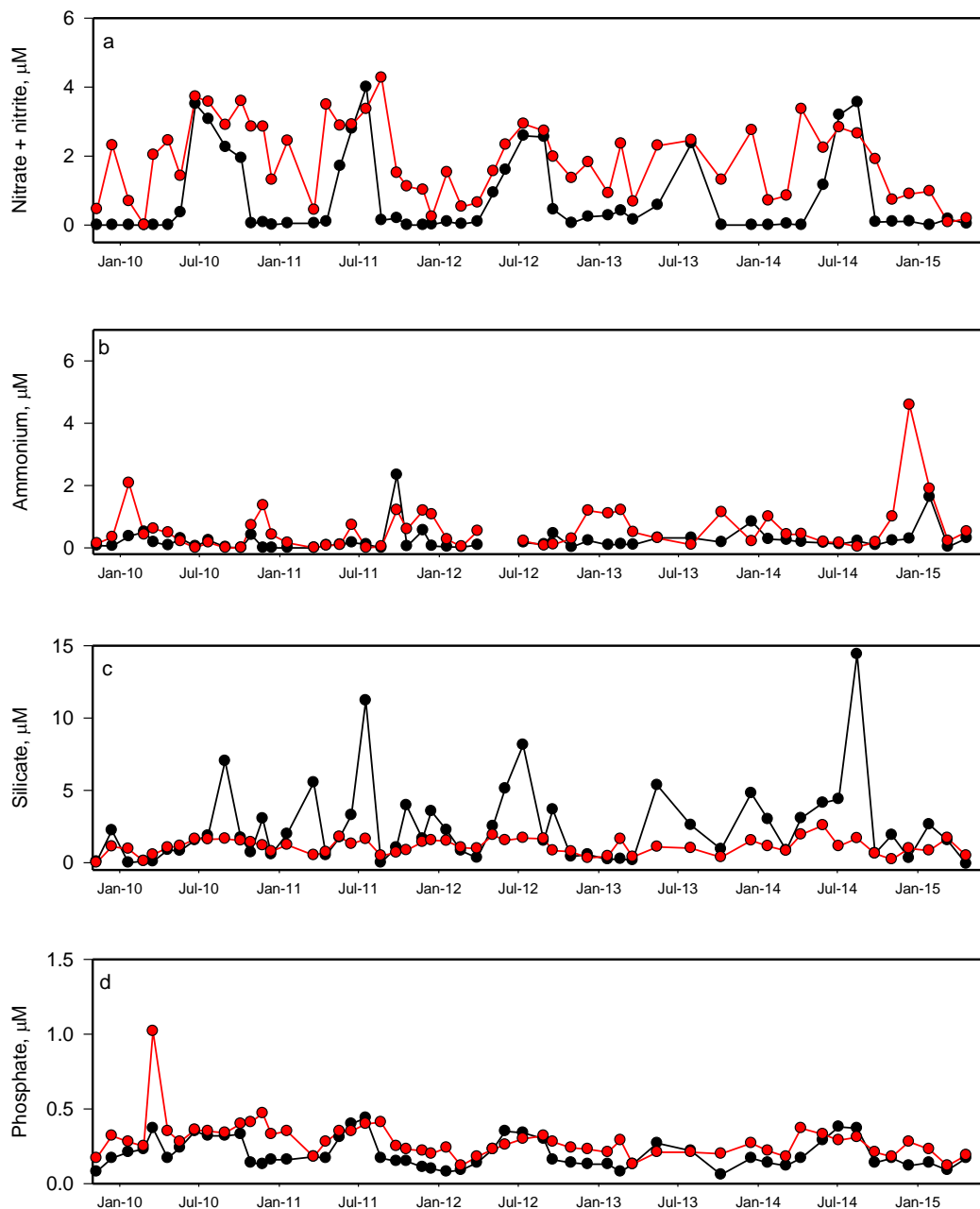


Figure 3.22 Concentration of nutrients at site 2, 2009 – 2015. Surface measurements (black circle and line) were at 0.5 m and bottom measurements (red circle and line) at 20 m.

3.2.3 Site 3 (43.31°S, 147.31°E)

Site 3 was located furthest out on the continental shelf and was the most marine of the sites. The water depth was approximately 90 m, and so an intermediate depth (50 m) was also sampled at this location. The water was well-mixed, based on water temperature (Figure 3.23a), except during the summer of 2010 when La Niña conditions were forming. Water temperatures at site 3 were consistently higher in winter and lower in summer than at all the other sites. Salinity was largely indicative of marine waters (Figure 3.23b), except for occasions between winter 2010 and winter 2011 when rainfall was high (Figure 3.1). Dissolved oxygen generally did not vary over the water column (Figure 3.23c), while chlorophyll *a* was low, especially in bottom waters, apart from during the spring and summer of 2010-2011 (Figure 3.23d).

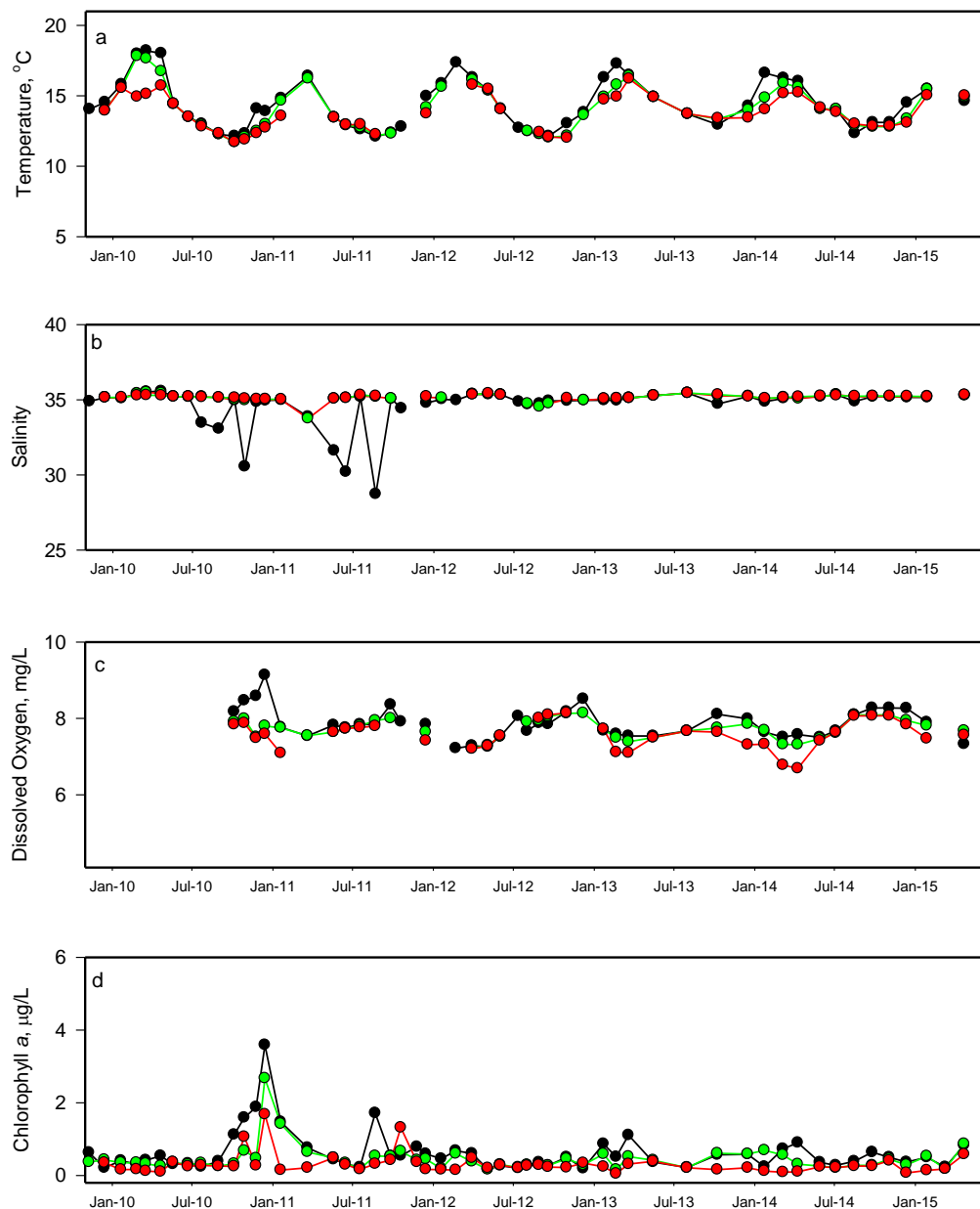


Figure 3.23 Temperature, salinity, dissolved oxygen and chlorophyll *a* concentration at site 3, 2009 – 2015. Measurements were at 0.5 m (black circle and line), 50 m (green circle and line) and 90 m (red circle and line). The first 10 oxygen measurements were omitted due to technical errors with the instrument.

Nutrients at Site 3 showed a stronger seasonal cycle than observed for Site 2, with high bottom NO_x in autumn of most years, and regularly the highest NO_x values of all the sites (Figure 3.24a). There were periods of increased ammonium (Figure 3.24b), particularly in summers when zooplankton was abundant. Silicate values were consistently lower than at other sites. Phosphates showed a similar pattern to site 2, with highest values often in bottom waters and peaks in winter at the surface.

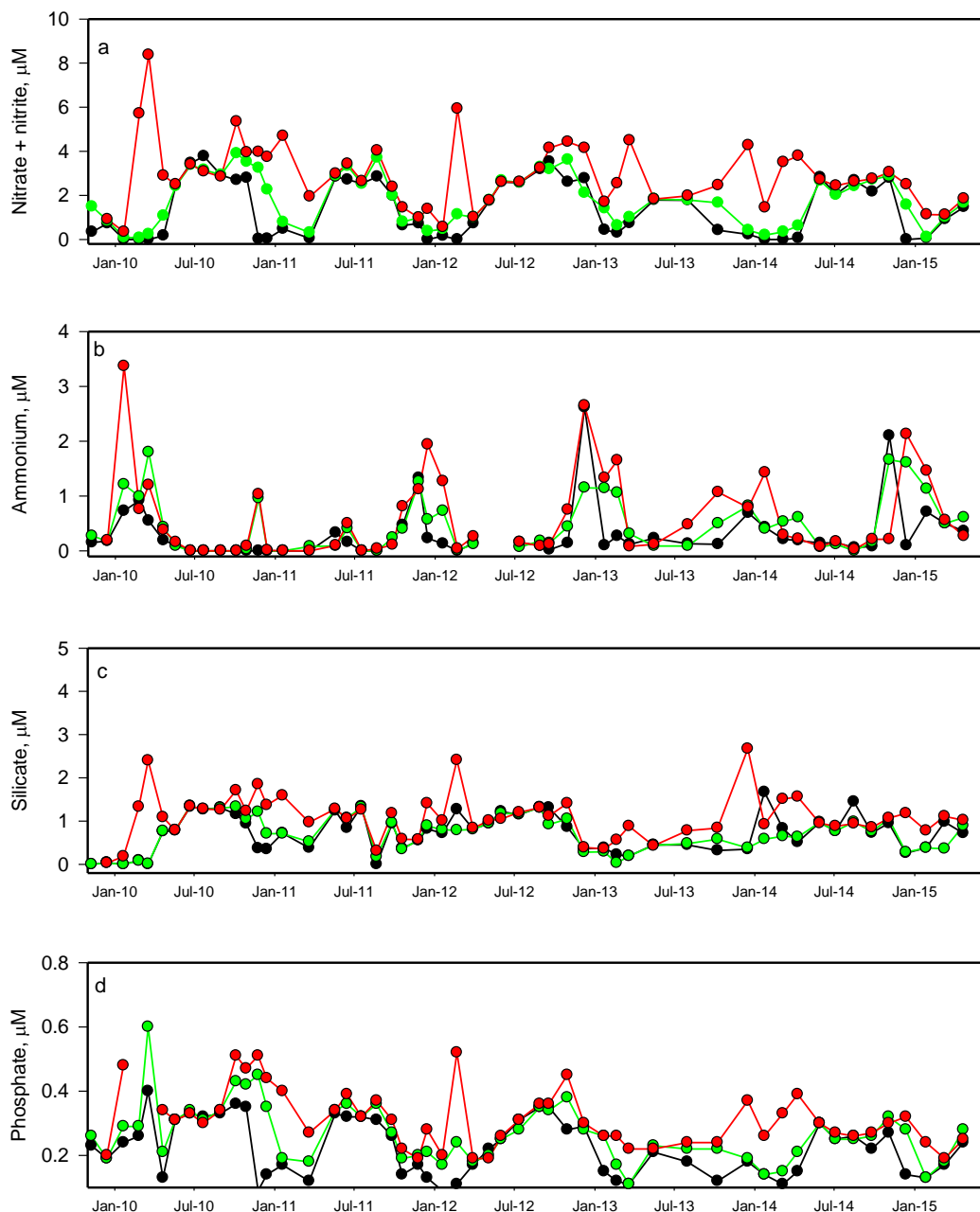


Figure 3.24 Concentration of nutrients at site 3, 2009 – 2015. Measurements were at 0.5 m (black circle and line), 50 m (green circle and line) and 90 m (red circle and line).

3.2.4 Site 5 (43.11°S, 147.11°E)

Site 5 was located near Nubeena. It often had cooler and less salty surface waters in winter when compared to bottom waters (Figure 3.25a,b), while dissolved oxygen was rarely lower than 7 mg L⁻¹ (Figure 3.25c). Chlorophyll *a* tended to be higher in surface waters (Figure 3.25d) and reached similar values to those at Site 2, with a maximum of 3.44 µg L⁻¹.

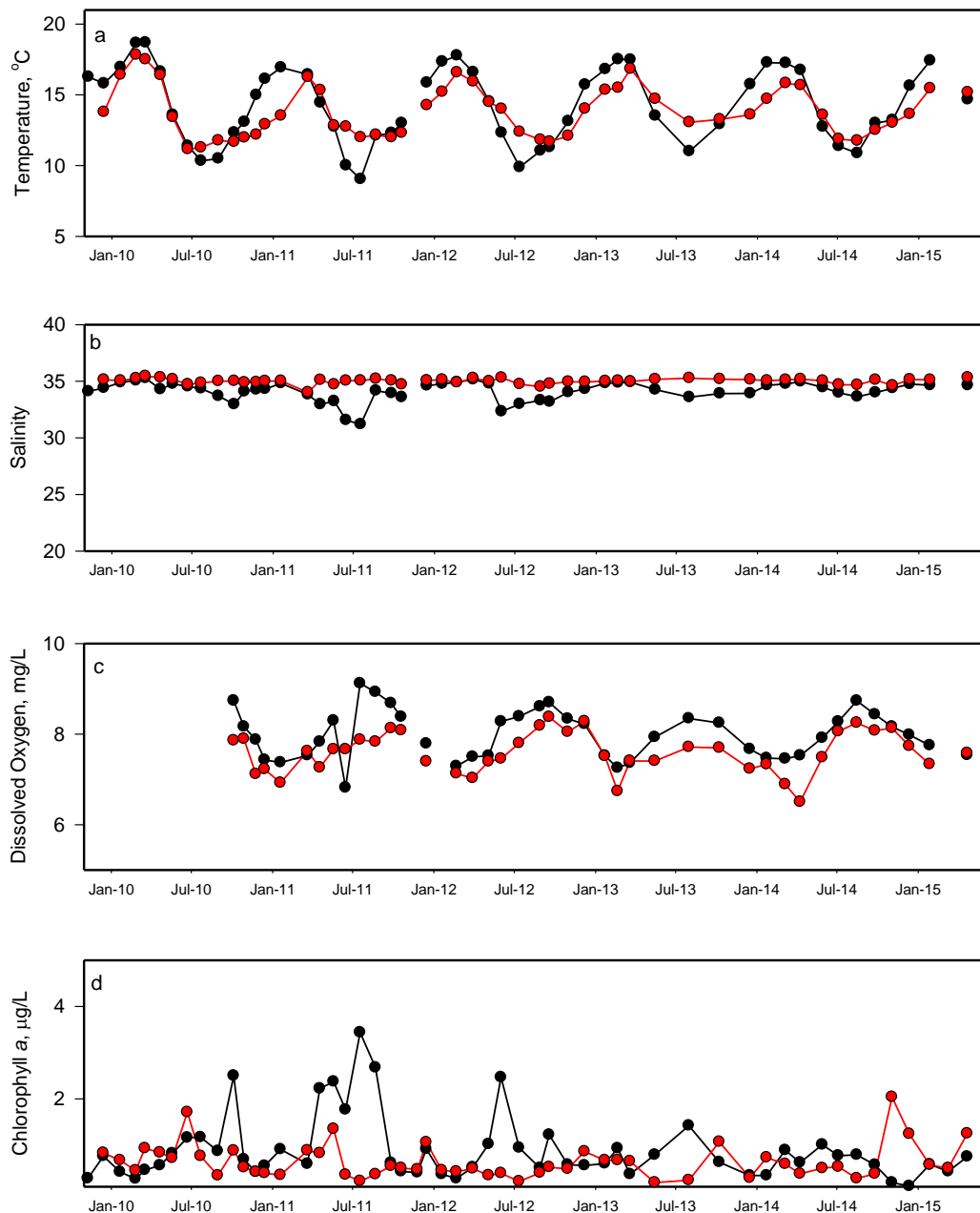


Figure 3.25 Temperature, salinity, dissolved oxygen and chlorophyll *a* concentration at site 5, 2009 – 2015. Surface measurements (black circle and line) were at 0.5 m and bottom measurements (red circle and line) at 30 m. The first 10 oxygen measurements were omitted due to technical errors with the instrument.

NO_x concentrations showed similar patterns to site 2, although winter time peak values tended to be slightly lower. Bottom water ammonia values were often higher than at the surface and highly variable. Similar to other sites, silicate and phosphate generally peaked over winter in surface

waters, although silicate is influenced by freshwater flowing from the River Derwent whilst phosphate is likely affected by the influx of nutrient-rich oceanic waters.

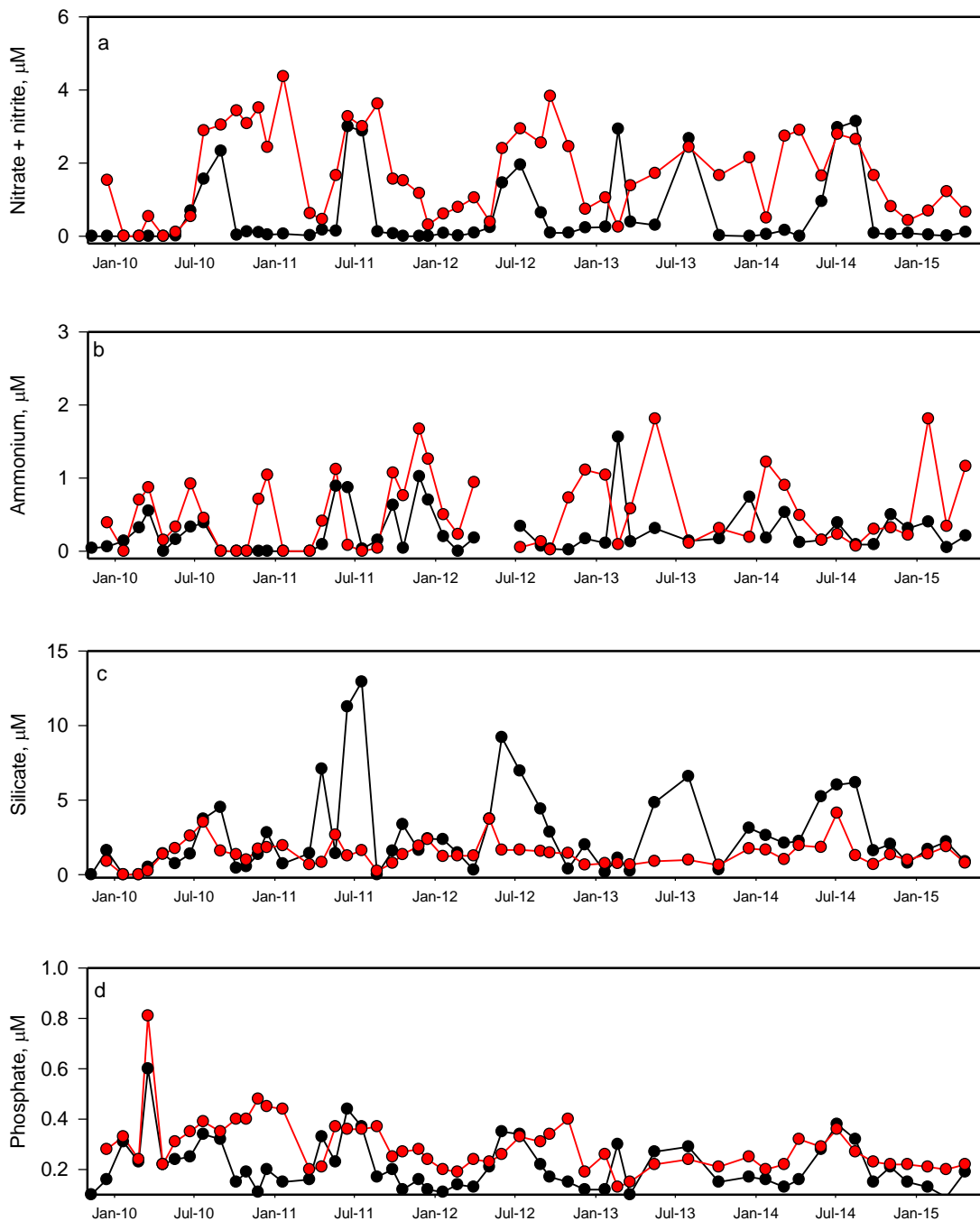


Figure 3.26 Concentration of nutrients at site 5, 2009 – 2015. Surface measurements (black circle and line) were at 0.5 m and bottom measurements (red circle and line) at 30 m.

3.2.5 Site 6 (43.18°S, 147.18°E)

Site 6 was located near Trumpeter Bay on Bruny Island. It is on the western edge of the bay, almost on a straight line from site 5 on the eastern side and site 2 in the middle. The water characteristics of this site (Figure 3.27) were very similar to sites 2 and 5, except that surface and bottom water values were more closely aligned for most characteristics than at other sites, indicating a well-

mixed water column. This is also indicated by the low variation in salinity at site 6 in Figure 3.6. The exception is ammonia values, which were high in bottom waters from August 2011 until the end of sampling (Figure 3.28).

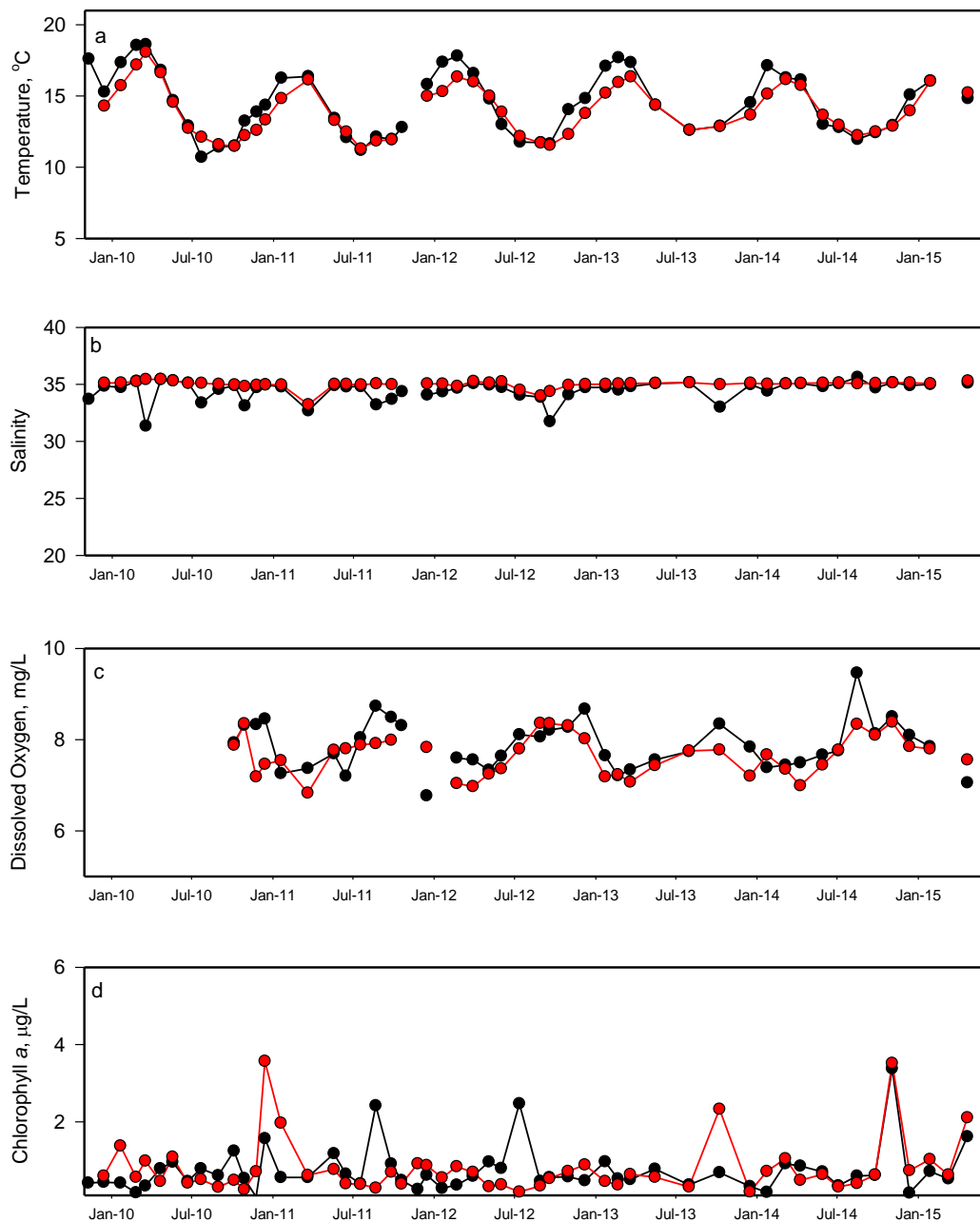


Figure 3.27 Temperature, salinity, dissolved oxygen and chlorophyll a concentration at site 6, 2009 – 2015. Surface measurements (black circle and line) were at 0.5 m and bottom measurements (red circle and line) at 30 m. The first 10 oxygen measurements were omitted due to technical errors with the instrument.

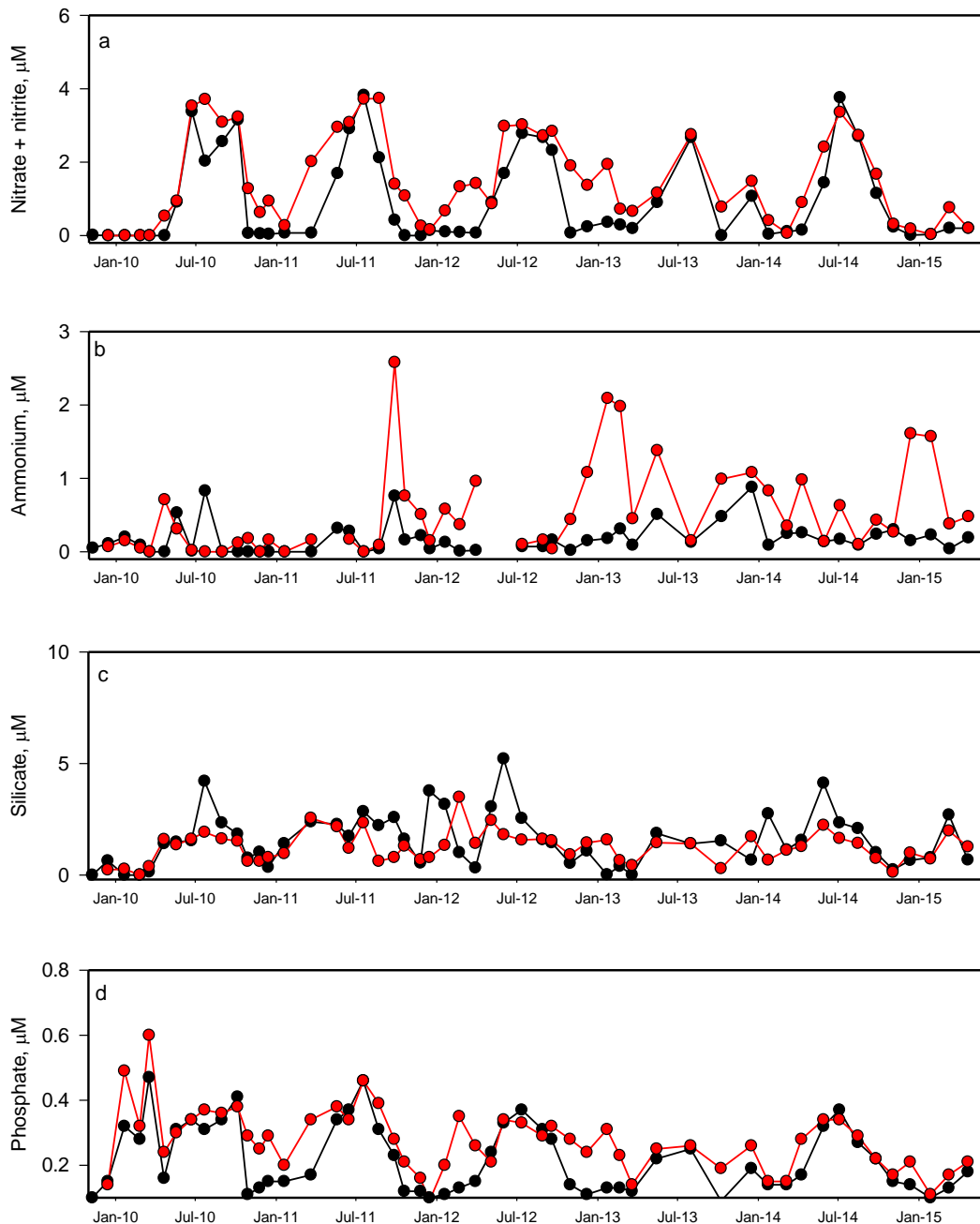


Figure 3.28 Concentration of nutrients at site 6, 2009 – 2015. Surface measurements (black circle and line) were at 0.5 m and bottom measurements (red circle and line) at 30 m.

3.2.6 Site 9 (43.05°S, 147.05°E)

Site 9 was in the mouth of Frederick-Henry Bay, and sampling began there in mid-2011. The characteristics of this site (Figure 3.29) were similar to the other inshore sites, with temperature and salinity showing little variations between surface and bottom, indicating a well-mixed water column. Chlorophyll a was regularly highest in bottom waters, and often had the highest value of all the sites. Nitrate values were amongst the lowest recorded in Storm Bay; ammonia was more variable but also often amongst the lowest values. Surface and bottom waters had similar silicate concentrations, which peaked when bottom waters were less saline. Phosphate was similar to site 2 (Figure 3.30).

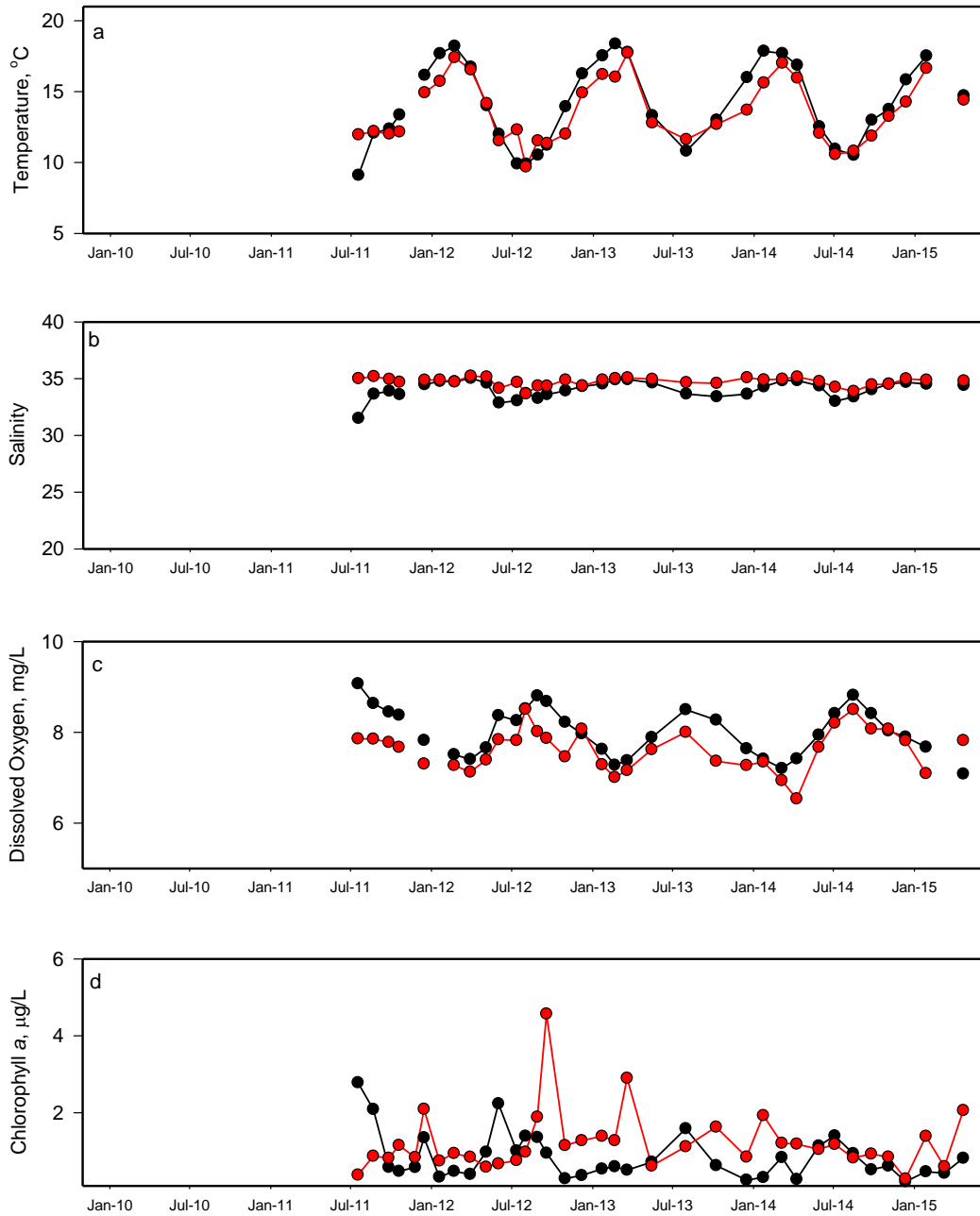


Figure 3.29 Temperature, salinity, dissolved oxygen and chlorophyll a concentration at site 9, 2011 – 2015. Surface measurements (black circle and line) were at 0.5 m and bottom measurements (red circle and line) at 20 m.

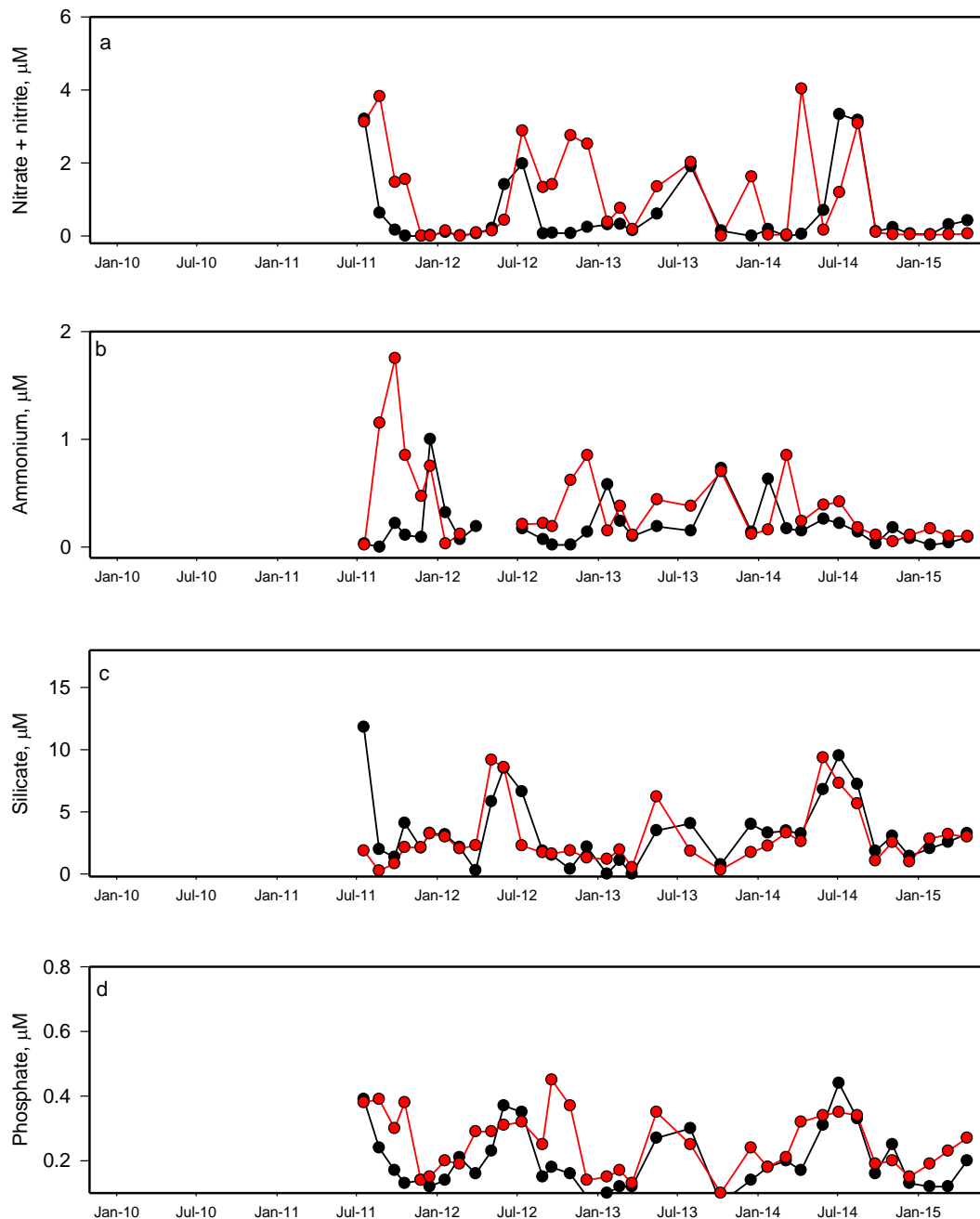


Figure 3.30 Concentration of nutrients at site 9, 2011 – 2015. Surface measurements (black circle and line) were at 0.5 m and bottom measurements (red circle and line) at 20 m.

3.3 Phytoplankton and Zooplankton

3.3.1 Chlorophyll *a* biomass

Chlorophyll *a* results integrated over 0-10 m for Storm Bay Sites 1-6 are presented in Figure 3.31. Sites 1, 2 and 3 were broadly similar with respect to seasonality, however the timing and magnitude of the minima and maxima did not always coincide. Sites 1 and 2 had two seasonal maxima in 2010-2011, with Site 1 at the base of the Derwent estuary recording the highest surface chlorophyll ($5.7 \mu\text{g L}^{-1}$, October 2010). Site 3, the most oceanic site did not show the same bi-modal

patterns, with highest chlorophyll levels occurring in December 2010 ($4.7 \mu\text{g L}^{-1}$). Site 5, near the Tasman Peninsula showed similar trends to Site 2, for the first two years of the study. Site 6, off

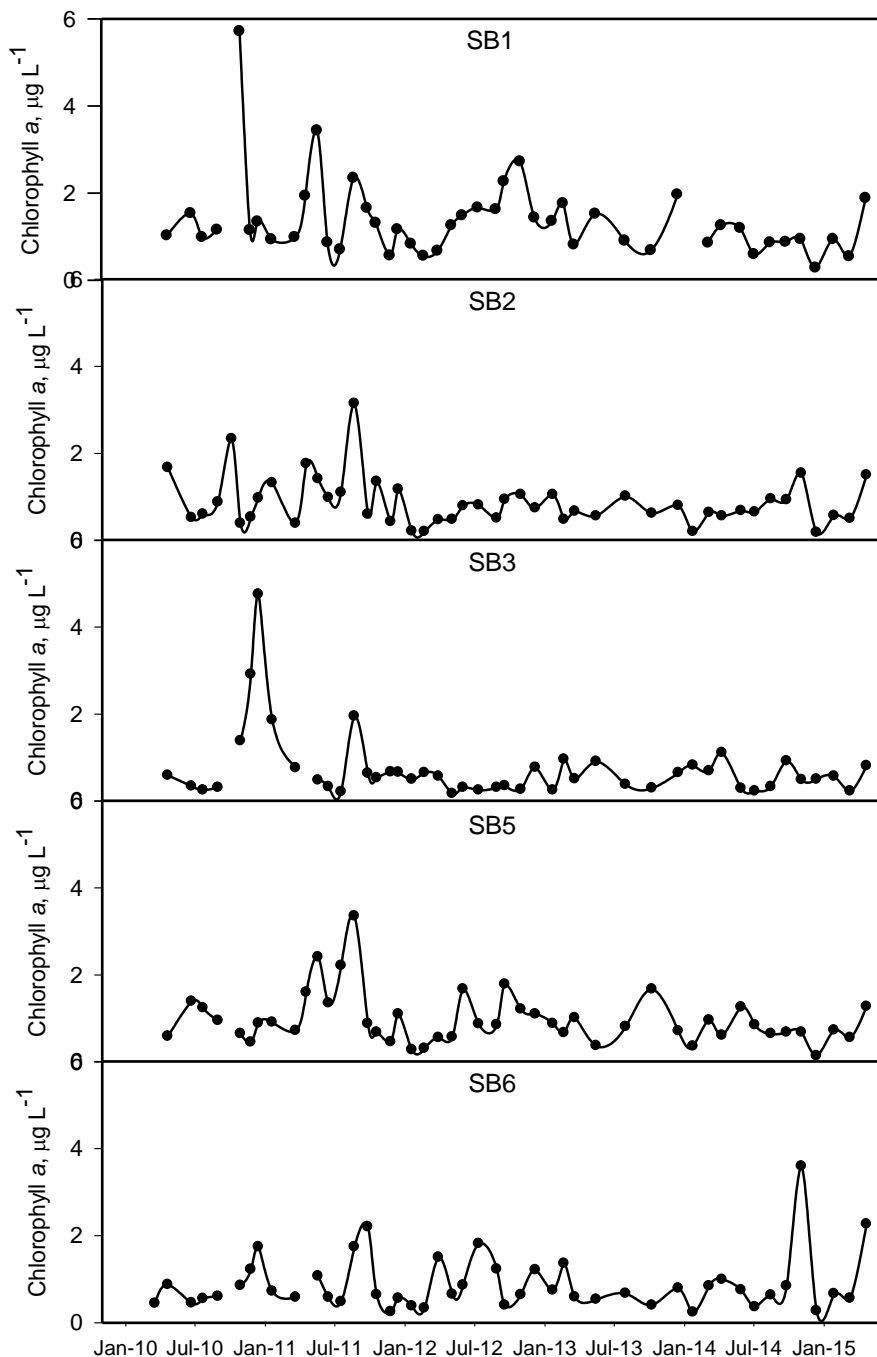


Figure 3.31 Chlorophyll *a* concentration for each site from January 2010- April 2015. Data from integrated 'snake' tube, 0 – 10 m.

Bruny Island, had lower chlorophyll *a* concentrations overall, and a single maximum was evident, typically occurring in winter.

Little seasonality was evident at sites 1 to 3 in 2012 and 2013, with the exception of the spring peak in September 2013, although this was poorly defined due to bad weather preventing sampling the months either side. In contrast, both sites 5 and 6 had a late autumn/early winter peak in 2012 that was not evident in the estuary to ocean transect. There were no clear seasonal patterns common to

all sites in 2014, however Site 6 had a classical spring bloom peaking at $3.5 \mu\text{g L}^{-1}$, followed by a summer minimum.

The “snake” sample, shown above, integrates water collected over the upper 10 m of the water column. Comparison of surface ($\sim 0.5\text{m}$ depth) with the depth-integrated sample (Figure 3.32) showed a strong coupling between the samples, with only occasional instances where surface chlorophyll *a* was higher than the snake data.

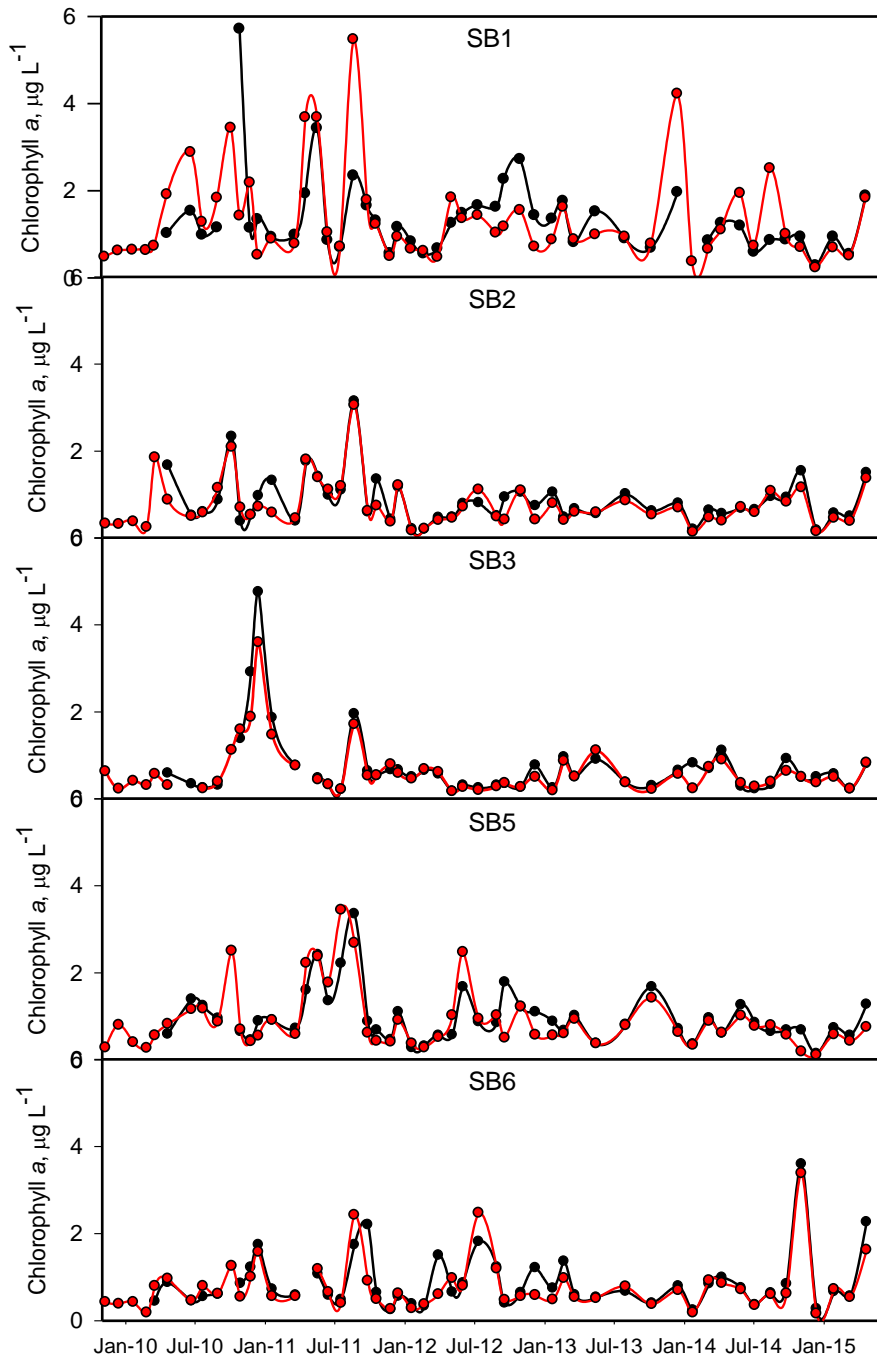


Figure 3.32 Surface and depth-integrated chlorophyll *a* time series for Sites 1-6, January 2010 to December 2015. Red line and circles are surface samples; black line and circles are integrated snake samples.

3.3.2 Main phytoplankton groups

Phytoplankton data are summarised as total cell counts, and also by major taxonomic groups (diatoms, dinoflagellates) in the first instance. Only data for the snake samples are presented. Total phytoplankton abundance for sites 1-6 is shown in Figure 3.33. There was no clear seasonal trend in total phytoplankton community, however Site 1 closest to the Derwent estuary tended to have the highest total cell counts compared to other sites, while Site 3 (oceanic) tended to have the lowest total cell counts. Periodically, site 5 (Tasman), site 6 (Bruny) and site 2 (mid-transect) all had higher total cell counts than the estuarine site. Total cell counts were most frequently influenced by small flagellates (< 5 µm size class), at the limit of clear taxonomic discrimination beyond broad functional groups, or shape by light microscopy.

For species other than nanoflagellates, diatoms typically dominated the phytoplankton community in Storm Bay, with dinoflagellates contributing a smaller and temporally variable proportion of the total cell counts. Site 1, (lower estuarine), usually had the highest concentration of diatoms, with lower abundances at sites 2 and 3 respectively (Figure 3.34). This is a similar pattern to that observed in chlorophyll *a* data. Periodically, numbers of diatoms were highest at site 5 on the Tasman Peninsula. Some seasonality was evident in La Niña years (2010-2011, Figure 3.1) and neutral periods (2012-2013), but this was suppressed in El Niño years (2014). Dominant diatom genera from Storm Bay include *Skeletonema*, *Pseudo-nitzschia*, *Chaetoceros*, *Ceratoneis* (+ *Nitzschia*), *Guinardia*, *Leptocylindrus*, *Thalassiosira*, *Dactyliosolen*, and *Rhizosolenia*. Rarer genera include *Coscinodiscus*, *Eucampia*, *Lauderia*, *Asterionellopsis*, *Ditylum*, *Hemiaulus*, *Melosira*, *Navicula*, *Proboscia* and *Corethron*.

Total dinoflagellate concentrations were 1 to 2 orders of magnitude lower across the survey period, with site 1 samples typically having the highest concentrations (Figure 3.34). As with the diatoms, site 5 occasionally had the highest dinoflagellate counts. Peaks in dinoflagellate abundance tended to occur immediately after a distinct diatom peak, illustrating how quickly community composition can change in a dynamic region such as Storm Bay. As with diatoms, total dinoflagellate numbers tended to be greatest in La Niña and neutral cycles, and lowest in El Niño conditions. Under El Niño conditions, the penetration of the EAC is reduced with cooler surface waters and stronger westerly winds influencing growing conditions for phytoplankton. A distinct peak in total dinoflagellates occurred in spring 2012 at site 1, dominated by small gymnodinioid cells (< 10 µm) and *Alexandrium*-like species. Most common dinoflagellate genera were *Tripos* (*Ceratium*), *Protoperidinium*, *Dinophysis*, *Prorocentrum*, *Scripsiella*, *Gymnodinium* and *Gyrodinium*. Less common genera included *Alexandrium*, *Dissodinium*, *Oxytoxum*, *Gonyaulax*, *Pyrocystis*, *Karenia*, *Heterocapsa* and *Polykrikos*.

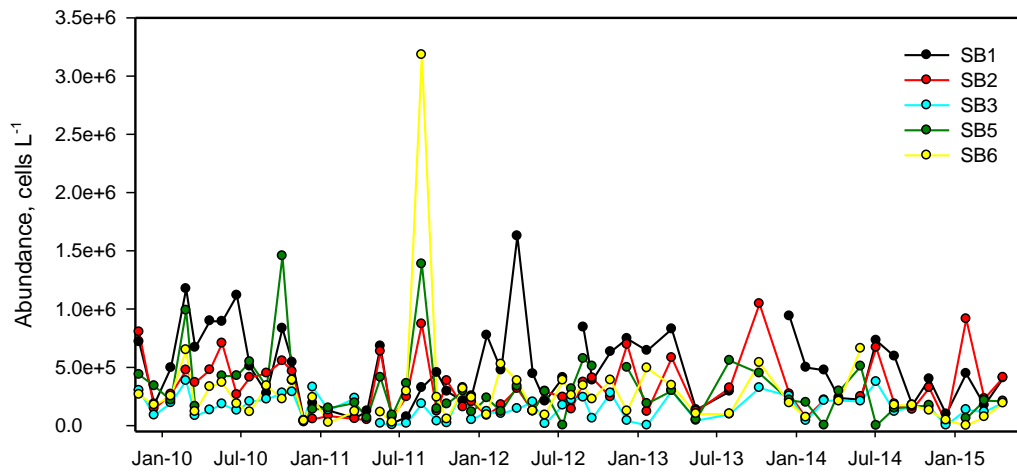


Figure 3.33 Total phytoplankton abundance (cells L⁻¹) at Sites 1-6 in Storm Bay (integrated snake sample) from November 2009 to April 2015.

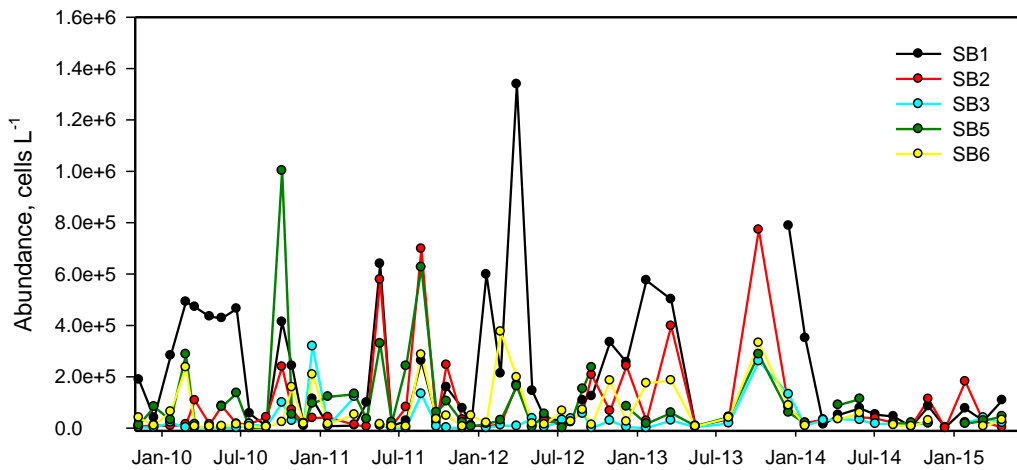


Figure 3.34 Total diatoms (cells L⁻¹) at sites 1-6 in Storm Bay (integrated snake sample).

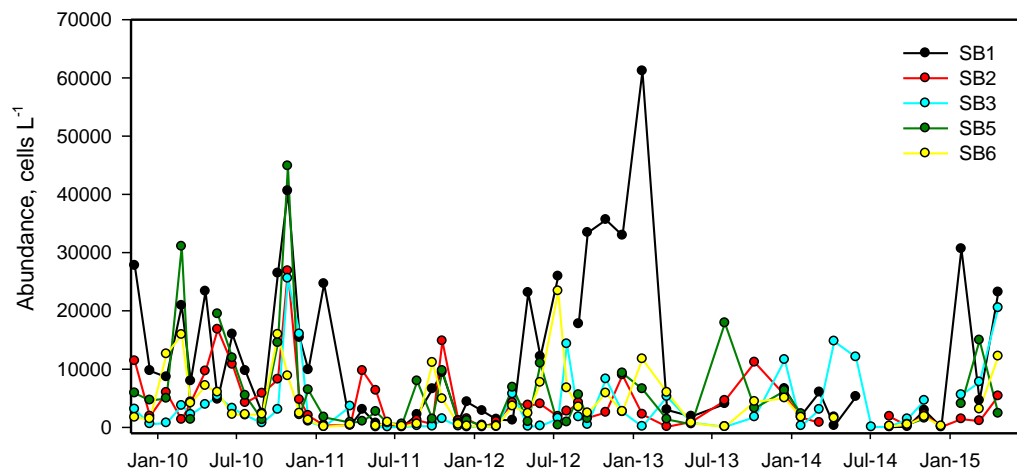


Figure 3.35 Total dinoflagellates (cells L⁻¹) at sites 1-6 in Storm Bay (integrated snake sample).

Canonical Analysis of Principle Coordinates (CAP) for the entire study period is plotted in Figure 3.36, for the phytoplankton depth-integrated (snake) samples from all sites (1,2,3,5,6). CAP allows us to discriminate between *a priori* groups, in this case sampling year which had a stronger influence than season or site on community composition. The CAP groups similar samples, and shows the results in 2-dimensional space (i.e. an x-y plot), using distance, so that samples that cluster closely together are more similar than samples that are more distant on the plot. Figure 3.36 shows that there was a reasonable discrimination between sampling years, and that the phytoplankton community composition appeared to follow a trajectory, with each year occupying

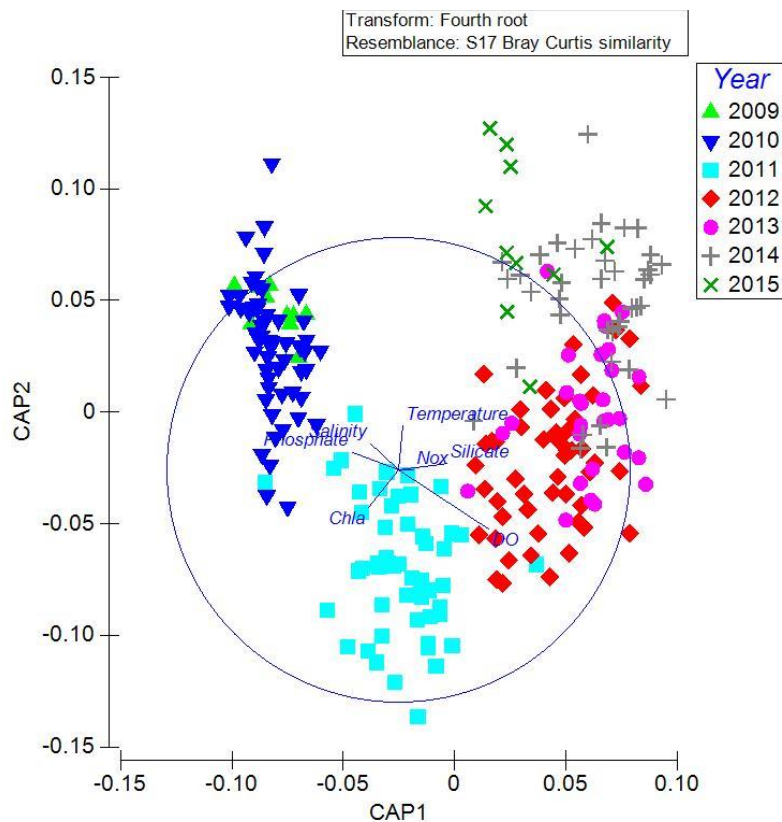


Figure 3.36 Canonical analysis of principle components of all phytoplankton species from sites 1,2,3, 5 and 6.

a different “space” on the CAP plot. Years that are characterised by high positive SOI values (La Niña years, 2010-2011) clustered to the left of the plot, while years that are characterised by negative SOI values (El Niño years, 2014-2015) were clustered to the right of the plot. Intermediate or neutral years were in-between. The vectors overlaid on the CAP are the environmental variables associated with every phytoplankton sample on the plot. They showed that nitrate and silicate were closely correlated, and explained some of the discrimination on axis 1, along with DO. Chlorophyll *a* and temperature explained some of the discrimination on axis 2, with an inverse relationship between the two variables.

3.3.3 Important species of HABs

Several phytoplankton genera and species are of interest because of their potential to cause harm to humans through consumption of affected shellfish, or by direct toxicity to fish, inflicting

significant economic impact on the harvest of both wild and cultured species. A small group of phytoplankton produce harmful toxins that can bio-accumulate in filter feeding shellfish, potentially resulting in a suite of poisoning syndromes, depending on the causative phytoplankton. Other phytoplankton act more specifically on fish, either by direct-acting toxins, or by physical damage to the gills through features such as barbs, mucilage or ammonia production. Yet another group can cause discolouration and deoxygenation of the water column from the rapid build-up of biomass.

Not all of the species of interest can be routinely discriminated by light microscopy, so groupings here may represent several toxic species within a single genus. No toxin or meat testing was undertaken as part of the Storm Bay study, so trends presented here are indicative of baseline populations of selected HAB groups over the period of the study. To further elucidate the potential presence of harmful species of the genus *Alexandrium*, samples from Sites 1,2,3,5 and 6 (Trips 52 - 56) were collected and preserved in the field for subsequent genetic analysis at the University of Technology Sydney. The results of those samples are discussed in the report for FRDC project 2014/032: 'Improved understanding of Tasmanian harmful algal blooms and biotoxin events to support seafood risk management', and are not presented here.

Pseudo-nitzschia were often the most dominant genus, and were classified into two size classes (< 3 µm, > 3 µm) with total *Pseudo-nitzschia* presented in Figure 3.37. The genus is associated with Amnesic Shellfish Poisoning, through the production of domoic acid. Fish and crustaceans

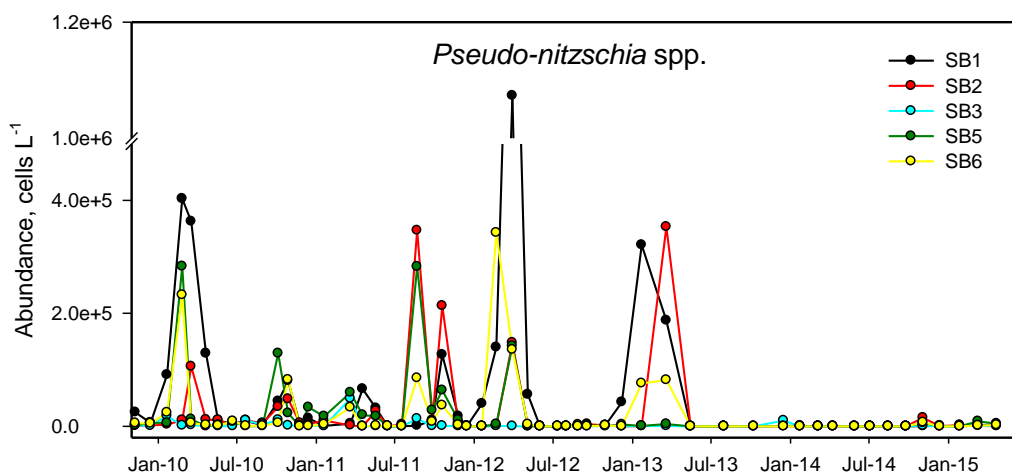


Figure 3.37 Time series for *Pseudo-nitzschia* spp. at Sites 1,2,3,5 and 6 from depth-integrated snake samples.

grazing on *Pseudo-nitzschia* can also accumulate the toxins, causing higher food-web effects. *Pseudo-nitzschia* was typically in highest abundance at sites 1 and 2, during summer although increased populations were also observed in spring and autumn. No blooms of the genus were observed in the later part of the time series.

The genus *Dinophysis* genus includes several species associated with Diarrhetic Shellfish Poisoning (DSP), including *D. acuminata*, *D. acuta*, *D. caudata*, and *D. fortii*, which are primarily associated with the production of okadaic acid. *Dinophysis acuminata*, *D. acuta*, and *D. fortii* were routinely

observed in low concentrations, while *D. caudata* was absent during the period of the study. *Dinophysis* were typically most abundant at site 1, with no clear seasonal pattern (Figure 3.38). On rare occasions *D. truncata* was observed, indicative of penetration of sub-Antarctic water (Hallegraeff et al. 2010).

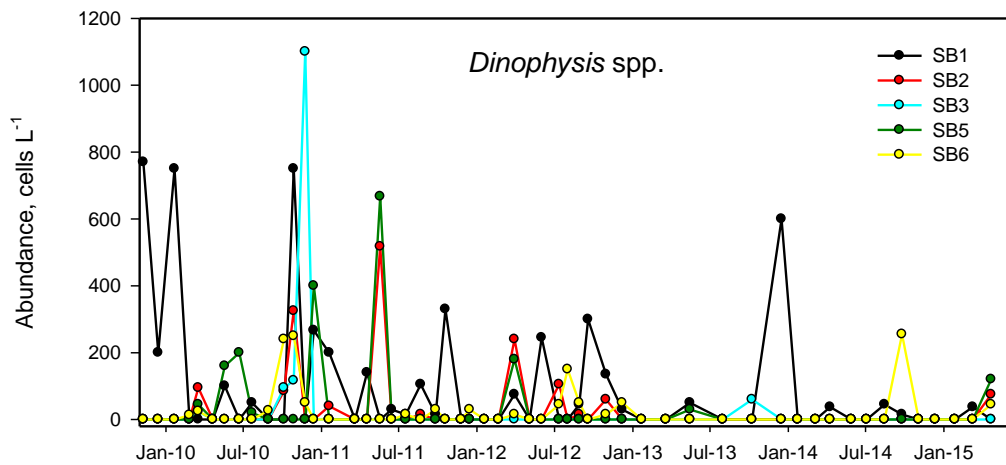


Figure 3.38 Time series for *Dinophysis* spp. at Sites 1,2,3,5 and 6 from the depth-integrated snake sample.

Cerataulina is associated with blooms or high biomass events, but was only ever present in low concentrations in Storm Bay during the period of the study. Highest concentrations were recorded at site 1 and site 5, with concentrations typically below 1000 cells L⁻¹ (Figure 3.39).

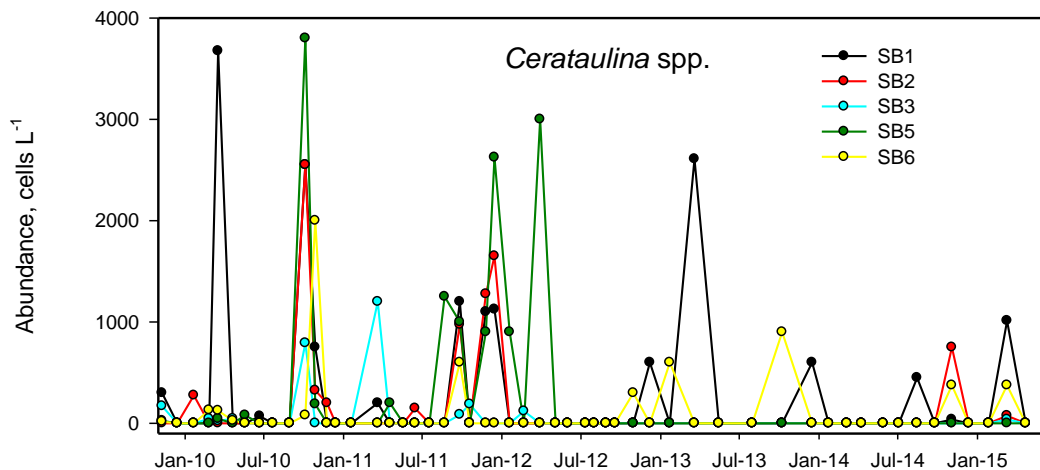


Figure 3.39 Time series for *Cerataulina* at Sites 1,2,3,5 and 6 from the depth-integrated snake sample.

The most common red-tide species, *Noctiluca scintillans*, is an “iconic” EAC species associated with well documented range expansion and southward penetration of EAC (McLeod et al, 2012). High biomass blooms are particularly obvious, due to their large cell size (up to 2mm), distinctive red colouration of the water as positively buoyant cells accumulate at the surface of the water column, and spectacular displays of bioluminescence at night as cells accumulate in lee shorelines and

respond to physical disturbance from waves and dogs. Blooms are spatially patchy and potentially undersampled with the depth-integrated snake, with only low concentrations of cells recorded in exposed waters of Storm Bay (Figure 3.40). Spectacular blooms made international headlines in 2015, immediately after the final sampling round in April.

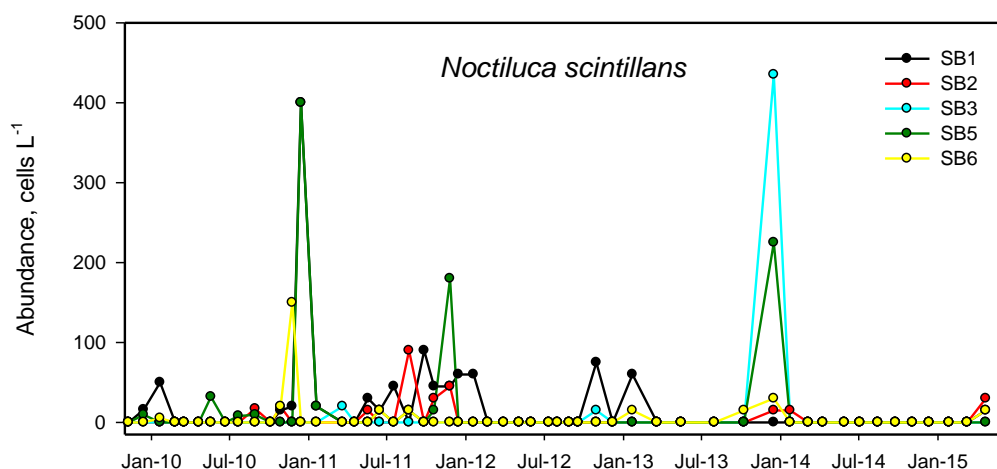


Figure 3.40 Time series for *Noctiluca scintillans* at Sites 1,2,3,5 and 6 from the depth-integrated snake sample.

As with other high biomass blooms, water quality can deteriorate due to increased biological oxygen demand, and discolouration and potentially high concentrations of ammonia produced by *N. scintillans* cells.

The genus *Karenia* comprises several species associated with harm to both shellfish (*K. breve*) and finfish (*K. mikimotoi*, *K. umbella*, and *K. papilionacea*). Occurrences of *K. cf breve* were isolated and only very low concentrations were recorded (Figure 3.41).

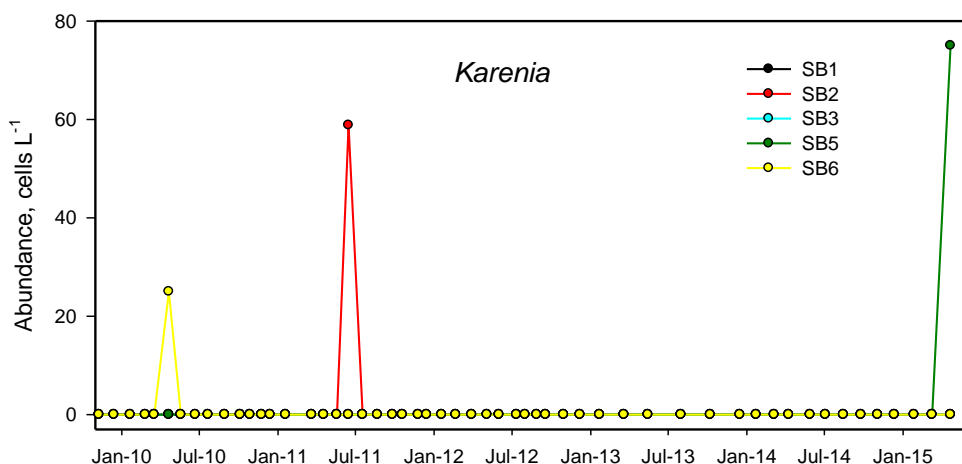


Figure 3.41 Time series for the genus *Karenia* at Sites 1,2,3,5 and 6 from the depth-integrated snake sample.

One of the most studied species in Tasmania, the dinoflagellate *Gymnodinium catenatum* is a causative species in Paralytic Shellfish Poisoning. This species is more problematic in estuaries than exposed areas such as Storm Bay, with complex life cycle including a cyst stage. Occurrences

of *G. catenatum* were rare, with peaks typically associated with site 6 (Bruny) (Figure 3.42). Concentrations were below the TSQAP alert levels for mussels (1000 cells L⁻¹) on all occasions, except the final sampling period in April 2015, coincident with high numbers of *Noctiluca scintillans* (Figure 3.41).

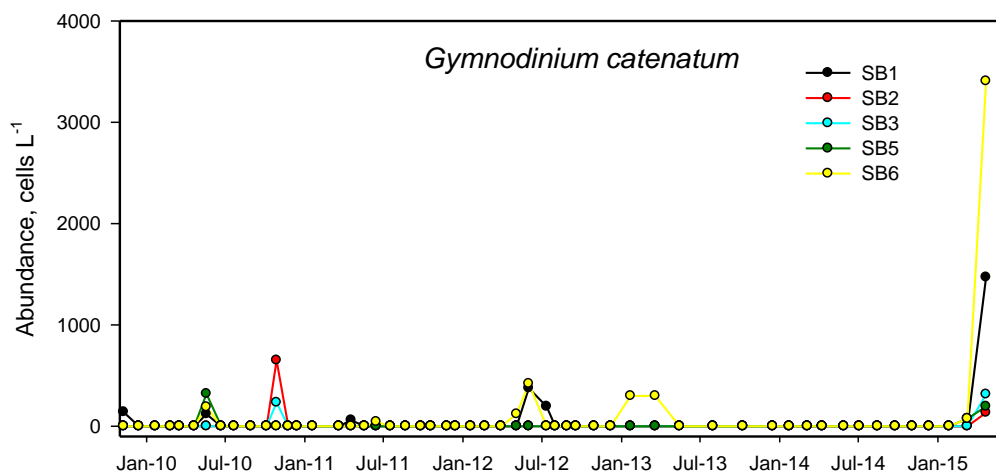


Figure 3.42 Time series for *Gymnodinium catenatum* at Sites 1,2,3,5 and 6, from the depth integrated snake sample.

The genus *Chaetoceros* includes barbed species that can cause gill damage and infection via excessive mucilage secretion in affected fish. A highly diverse genus, *Chaetoceros* was always present in low concentrations, with a notable event in spring 2013 (Figure 3.43).

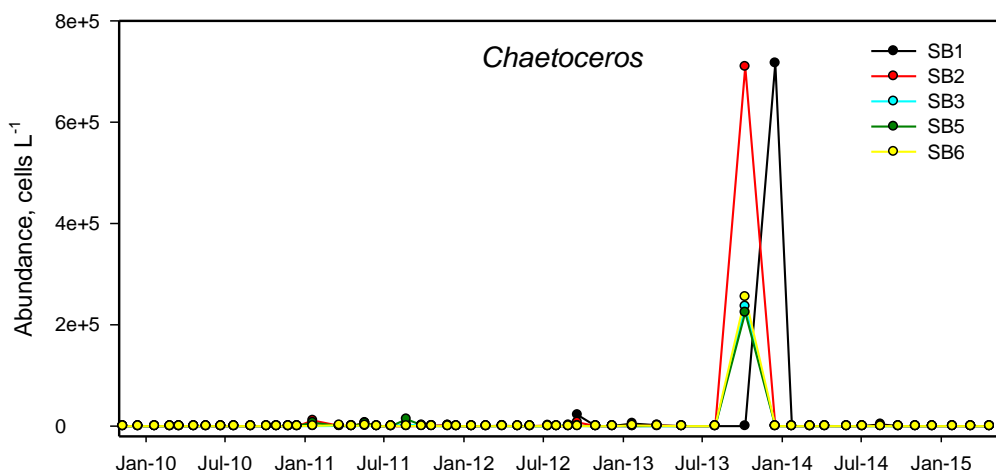


Figure 3.43 Time series for the genus *Chaetoceros* at Sites 1,2,3,5 and 6 from the depth-integrated snake sample.

3.3.4 Zooplankton

Zooplankton distribution and abundance was determined for 3 sites, namely 2, 5 and 6, while lack of resources prevented sites 1 and 3 from being processed. A canonical analysis of principal

coordinates (CAP), based on all zooplankton from sites 2, 5 and 6 is presented in Figure 3.44. There was clear separation between the seasons, with each having characteristic zooplankton present. ANOSIM showed that these four groups based on season were statistically significantly different. Summers were dominated by gelatinous species, such as Doliolids and the salps *Thalia democratica* and *Salpa fusiformis*. *Nyctiphanes australis*, the euphausiid species found in coastal temperate waters, was also abundant in summer. In autumn, species that are characteristic of more northerly, subtropical waters, e.g. the cladoceran *Penilia* and the copepods *Temora turbinata* and *Acartia danae*, were dominant, especially during autumns when the presence of the EAC remained strong in Storm Bay. Species present during winter and spring were more typical of cool temperate waters and included a mixed assemblage of copepods associated with cooler temperatures e.g. *Neocalanus tonsus*, *Centropages australiensis* and *Euterpina acutifrons*.

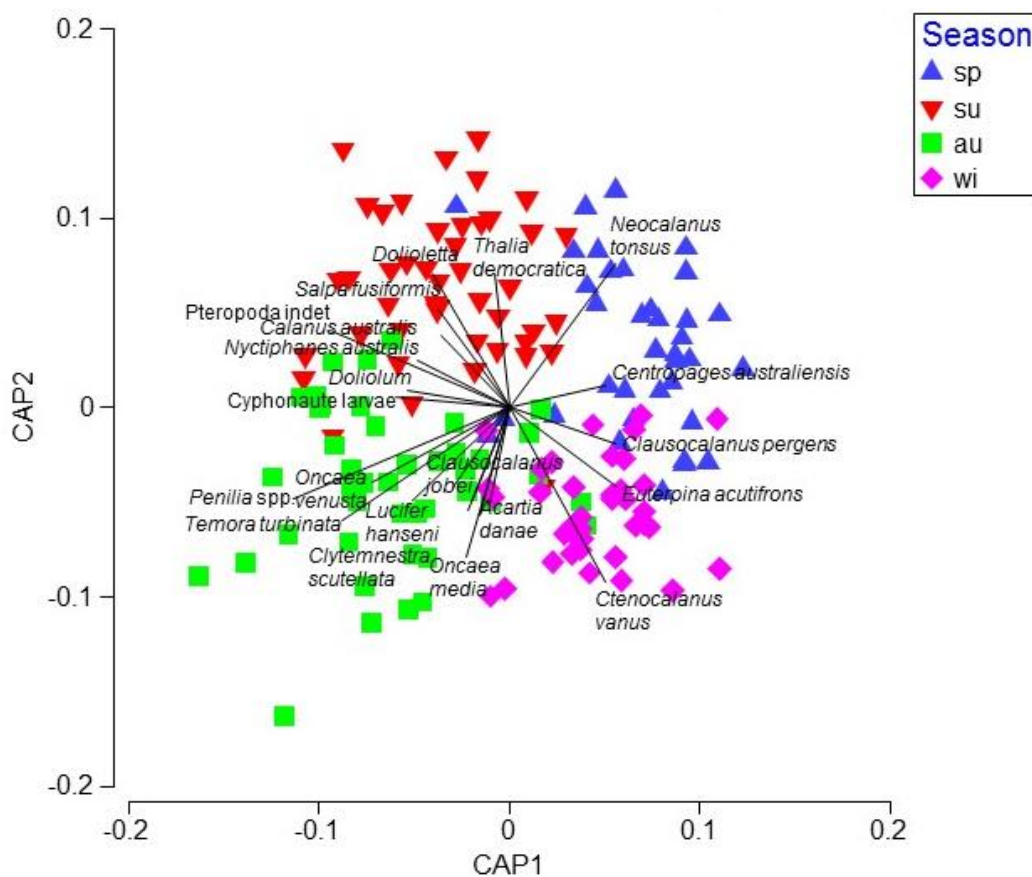


Figure 3.44 Plot showing canonical analysis of principal coordinates for zooplankton-sample relationships for sites 2, 5 and 6 for 2009-2015.

Zooplankton showed more regular cycles in abundance (Figure 3.45) than were observed for the phytoplankton. There were peaks in abundance in spring and summer, with lowest numbers occurring in winter. This is a typical pattern for coastal temperate zooplankton. Site 6 generally had the highest abundances of the three sites examined. Copepods dominated total zooplankton abundance (Figure 3.46); other dominant groups included euphausiids, predominantly *Nyctiphanes australis*, cladocerans and gelatinous species.

In September 2014 copepod abundance reached a maximum of greater than 120,000 individuals m^{-3} at site 6, at least three times the maxima recorded at other times. This figure mainly comprised the small calanoid copepods *Acartia tranteri* and *Paracalanus indicus*, both of which are very abundant in coastal waters of south eastern Australia. Phytoplankton were low at that time, suggesting a significant grazing impact by the copepods.

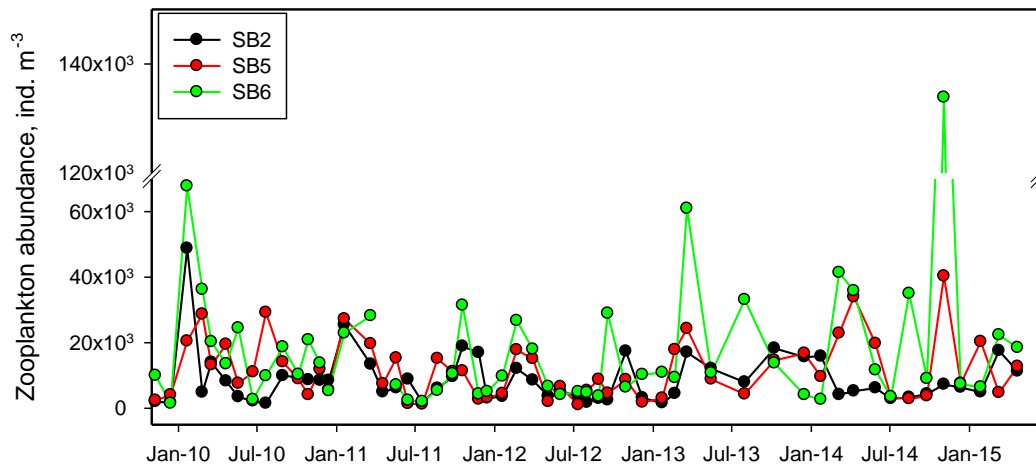


Figure 3.45 Total zooplankton abundance at three sites in Storm Bay, for the period November 2009 to April 2015.

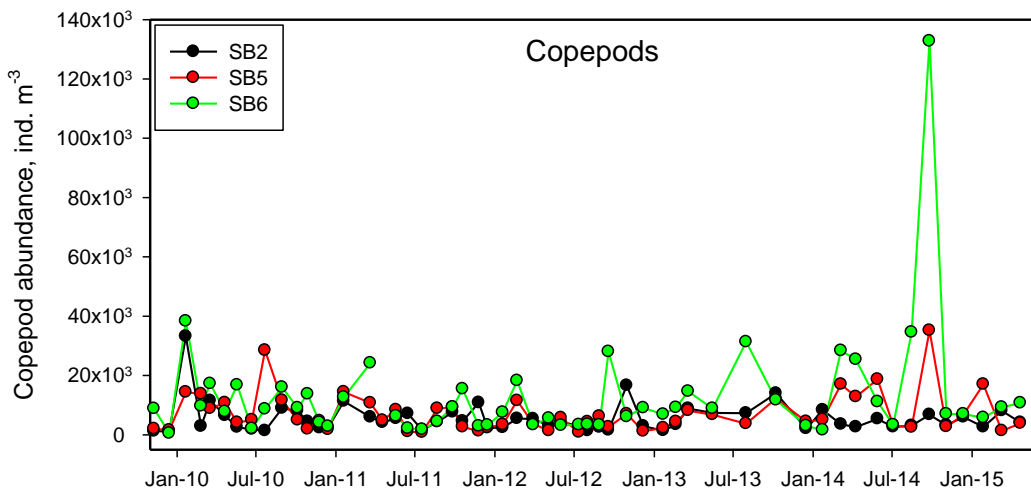


Figure 3.46 Total copepod abundance at three sites in Storm Bay, for the period November 2009 to April 2015.

The only common euphausiid recorded in Storm Bay was *Nyctiphanes australis*, a species that occupies a key position in coastal food webs and is the major prey item of predators such as jack mackerel, barracouda, mutton birds and pygmy blue whales. The krill were particularly abundant during the summer of 2013 (Figure 3.47), following a period of neutral SOI. Krill and salps tend to dominate under different conditions, with El Niño conditions favouring the growth of krill. Cladocans, small crustaceans sometimes called water fleas, were another periodically dominant group (Figure 3.48). There are three main marine groups of cladocerans, and these bloom

periodically in response to localised conditions. For example, input of nutrients or influxes of warm waters can promote large numbers of cladocerans in short time frames

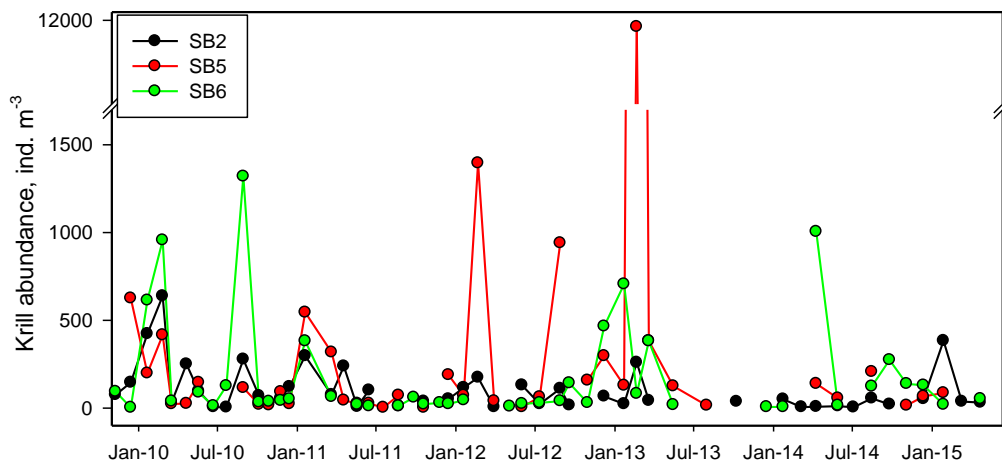


Figure 3.47 Total euphausiid abundance at three sites in Storm Bay, for the period November 2009 to April 2015.

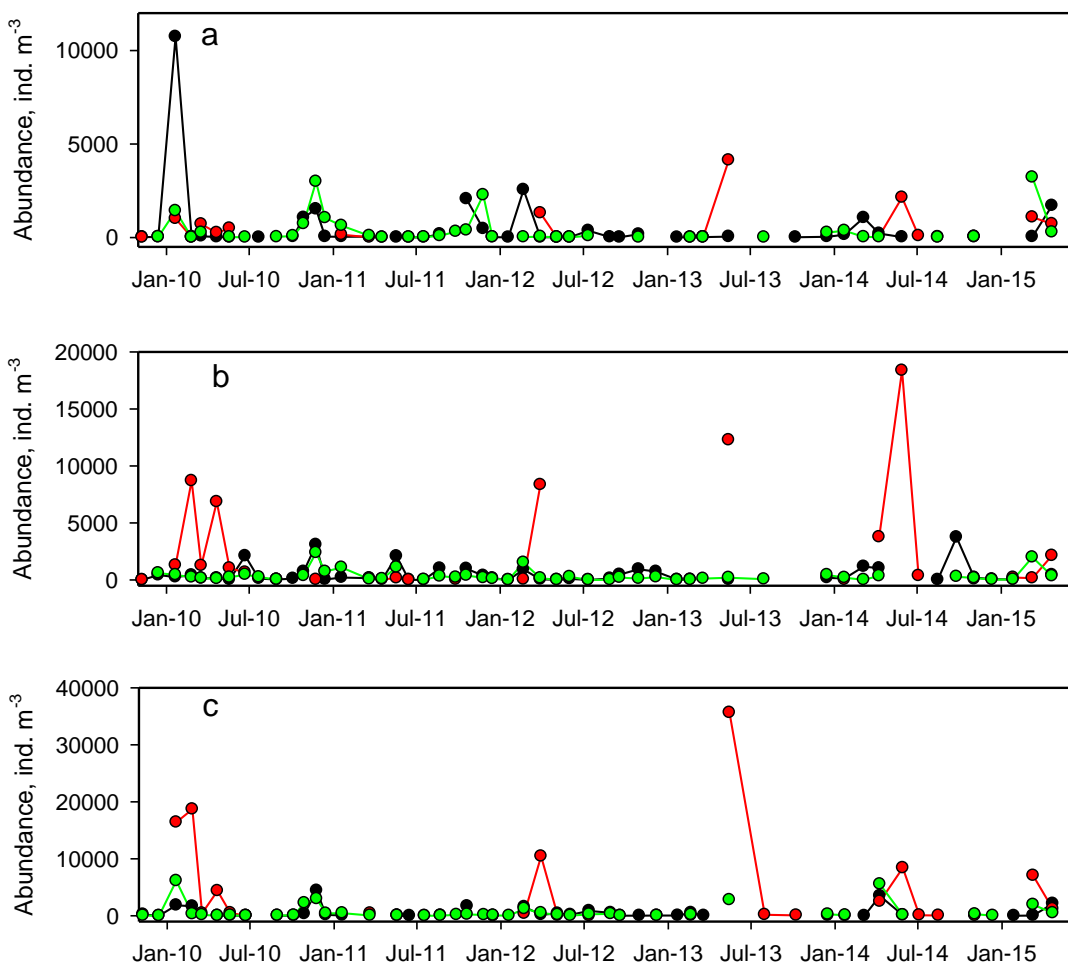


Figure 3.48 Total cladoceran abundance at three sites in Storm Bay, for the period November 2009 to April 2015. Black lines and dots are *Evadne* sp., red are *Penilia* sp. and green *Podon* sp. (a) site 2, (b) site 5 and (c) site 6.

3.3.5 Gelatinous zooplankton

Gelatinous zooplankton can be an important component of the Storm Bay zooplankton. Figure 3.49 shows total counts for hydrozoans and Thaliaceans. Hydrozoans are typical jellyfish, killing their prey with the use of nematocysts (= stinging cells). Hydrozoans found in Storm Bay were typically small, largely represented by the genera *Obelia* and *Clytia*. Their highest abundance was reached in autumn 2011, when 4000 individuals m^{-3} were recorded. Thaliaceans, on the other hand, are gelatinous animals that are not related to jellyfish. They are represented in the zooplankton by salps, doliolids and pyrosomes.

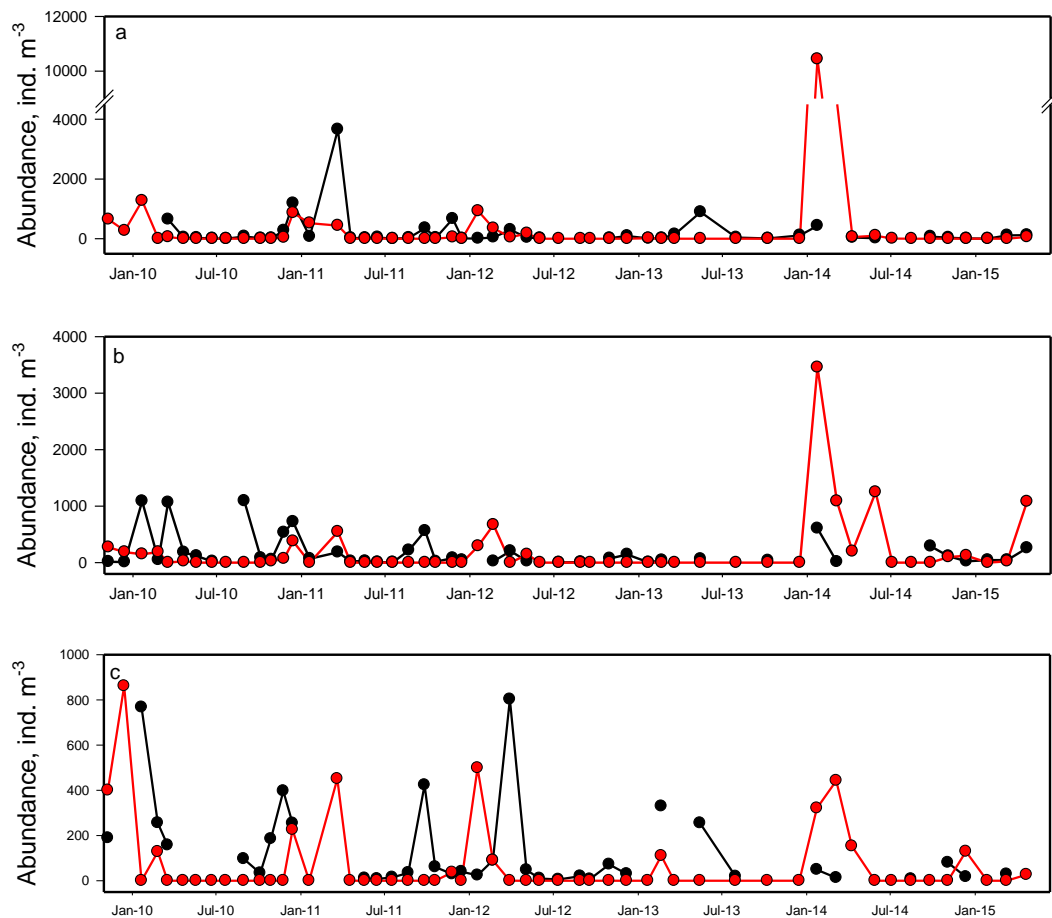


Figure 3.49 Total gelatinous groups at three sites in Storm Bay, for the period November 2009 to April 2015. Black lines and dots are hydrozoans and red are Thaliaceans (a) site 2, (b) site 5 and (c) site 6.

3.4 Detection of *Neoparamoeba perurans* in Storm Bay

Barbara Nowak

3.4.1 Introduction and Methods

Neoparamoeba perurans is a parasitic marine amoeba that is the causative agent for amoebic gill disease (AGD, Young et al. 2008). It was first described in Tasmania during the 1980s, when it was detected in sea-caged salmonids (Munday 1986, cited in Oldham et al. 2016). *Neoparamoeba perurans* was only quite recently proven to cause AGD (Crosbie et al. 2012). Since that time it has been confirmed in most salmon-producing regions, and represents a serious health challenge for the salmon industry in Tasmania. A thorough review of the incidence and distribution of AGD is available in Oldham et al. (2016).

Water samples were collected on four occasions to analyse for the presence of *N. perurans*, at sites 3, 5 and 6 from 10 m and 50 m (Table 3.1). Water samples were collected with a 6 L Niskin bottle (General Oceanics) and transferred to 10L carboys that had been sterilised (1/10 household bleach rinsed with freshwater). Water was filtered on board through a sterilised (1/10 household bleach rinsed with freshwater) filtration unit. Each sample was filtered onto a 47 mm, GF/C Whatman filters (pore size: 1.2 µm), and the filters stored in 5 mL vials with 1 ml lysis buffer. Wright et al. (2015) provide details of processing of the filters to test for the presence of *N. perurans*.

3.4.2 Results and Discussion

Water samples were collected on four occasions to analyse for the presence of *N. perurans*, at sites 3, 5 and 6 from 10 m depth, and 50 m at site 3 (Table 3.1). Low numbers of *N. perurans* were detected in 25% of the samples analysed, particularly in water collected during April 2014. In that month the amoebae were measured in higher concentrations at 10 m depth than at 50 m, concurring with earlier findings that in the early autumn *N. perurans* is more common in surface waters (Oldham et al. 2016). Although quite low, the abundances measured were comparable to those previously reported and these concentrations can induce AGD in Atlantic salmon. Only one sample was positive for *N. perurans* in 2015, at 50 m depth at site 3. Average temperature was highest in April 2014 (15.95 °C), however the temperature tolerance of the amoebae appears to be wide, ranging between 7 °C and 20 °C. Rainfall and salinity might be other important drivers of the distribution of *N. perurans* (Oldham et al. 2016), though neither of these parameters showed clear correlation with the amoebae in Storm Bay. Although *N. perurans* was found at the three sites examined in Storm Bay it is worth noting that the water column is not believed to be a significant reservoir for this AGD-forming amoeba (Oldham et al. 2016), and examination of the sediments at these sites is warranted.

Table 3.1 *Neoparamoeba perurans* detected in Storm Bay during 2014 and 2015. Temperature and salinity at the time and depth of sampling are also shown.

Date	Site	Sample depth m	<i>N. perurans</i> number L ⁻¹	Temperature °C	Salinity
09/04/2014	3	10	0.264	15.93	35.138
09/04/2014	3	10	0.383	15.93	35.138
09/04/2014	3	50	— ^a	15.61	35.081
09/04/2014	3	50	0.113	15.61	35.081
09/04/2014	5	10	—	16.39	34.979
09/04/2014	5	10	0.784	16.39	34.979
09/04/2014	6	10	1.062	15.89	35.107
09/04/2014	6	10	0.387	15.89	35.107
12/12/2014	3	10	—	14.16	35.179
12/12/2014	3	10	—	14.16	35.179
12/12/2014	3	50	0.392	13.37	35.187
12/12/2014	3	50	—	13.37	35.187
12/12/2014	5	10	0	15.01	34.758
12/12/2014	5	10	0	15.01	34.758
12/12/2014	6	10	0	14.67	35.065
12/12/2014	6	10	0	14.67	35.065
10/03/2015	3	10	—	nd ^c	nd
10/03/2015	3	10	—	nd	nd
10/03/2015	3	50	—	nd	nd
10/03/2015	3	50	<1 ^b	nd	nd
10/03/2015	5	10	—	nd	nd
10/03/2015	5	10	—	nd	nd
10/03/2015	6	10	—	nd	nd
10/03/2015	6	10	—	nd	nd
22/04/2015	3	10	—	14.85	35.265
22/04/2015	3	10	—	14.85	35.265
22/04/2015	3	50	—	14.91	35.283
22/04/2015	3	50	—	14.91	35.283
22/04/2015	5	10	—	14.55	34.718
22/04/2015	5	10	—	14.55	34.718
22/04/2015	6	10	—	15.32	35.286
22/04/2015	6	10	—	15.32	35.286

^aIndicates that no *N. perurans* were detected.

^bPositive but below the LOQ (limit of quantification).

^cnd: No data for available for salinity and temperature on this date.

3.5 Primary Production in Storm Bay

Andrew McMinn and Shiong Lee

3.5.1 Introduction

Primary productivity is a fundamental ecosystem process that influences all trophic levels. Chlorophyll biomass alone is not a proxy for marine primary productivity as the two are frequently decoupled and it is possible to have high biomass combined with low primary productivity and vice versa. Such decoupling may arise from factors such as changes in species composition, cellular physiology, carbon to chlorophyll ratios, photoinhibition and other factors (Chavez et al. 2011). Primary production measurements integrate the effects of irradiance, nutrient supply, species succession and temperature on phytoplankton and are therefore an important way of assessing ecosystem change.

However, primary productivity is highly variable on short spatial and temporal scales. On a daily basis it can be influenced by factors such as rapid changes in mixed layer depth, cloudiness and grazing pressure. On slightly longer time scales nutrient drawdown and replacement, passage of mesoscale eddies and species succession can also be influential (Chavez et al. 2011). Thus primary productivity measurements taken at the same location only a few days apart can be significantly different. Conventional discrete-bottle chlorophyll *a* and primary productivity measurements are time consuming to make, logistically difficult and expensive and therefore it is likely that in the future increasing use will be made of remote or automated systems. FRRF (Fast Repetition Rate Fluorometry) has been widely used to investigate marine photosynthesis and primary productivity (Suggett et al. 2001), where it can provide *in situ* measurement of the photosynthetic parameters that enable the calculation of gross primary production (Falkowski and Kolber 1995). Calibration of FRRF-based estimates with ¹⁴C-based measurements have robust relationships in several regions, including the North Atlantic (Suggett et al. 2001, Moore et al. 2003, Estevez-Blanco et al. 2006, Melrose et al. 2006), the Celtic Sea (Smyth et al. 2004), the Baltic Sea (Raateoja et al. 2004), the North Pacific (Corno et al. 2006) and the Southern Ocean (Cheah et al. 2011). However, the relationship is not consistent and the inconsistencies are thought to be linked to differences in how the two techniques estimate primary production. FRRF measurements are more closely correlated with gross oxygen evolution than with the assimilation of dissolved inorganic carbon because the oxygen evolving complex is close to Photosystem II (PSII) while carbon uptake occurs in the Calvin-Benson cycle, which is further down the electron transfer chain and associated with Photosystem I (PSI) (Suggett et al. 2001).

3.5.2 Materials and Methods

A FastOcean Fast Repetition Rate Fluorometer (Chelsea Technology Group, UK) was used to collect light, chlorophyll and gross primary production measurements. The instrument was deployed by ship-based winch and measurements were made every one second. FRRF fluorescence yields were measured using an inbuilt protocol that provided a flash sequence consisting of a series of 100 subsaturation flashlets (1.1 μ s flash duration and 2.8 μ s inter-flash period) and a series of 20 relaxation flashlets (1.1 μ s flash duration and 51.6 μ s inter flash period),

with the gain set in autoranging mode. Fluorescence transients obtained were manipulated in FastPro 8 software (Chelsea Technology Group). The absorption algorithm (Oxborough et al. 2012, Chelsea Technology Group 2012) was used to estimate the electron flow through Photosystem II (JV_{PSII} , electrons $m^{-3} s^{-1}$); gross primary production was calculated by multiplying this value by twelve to reflect that one atom of carbon is fixed for every one electron that flows through PSII. Chlorophyll concentration was estimated from the *in situ* fluorescent parameters. Data from every deployment, however, was calibrated against an extracted chlorophyll measurement from a depth of 10 m. Raw data were always within 90% of the final corrected data.

Maximum quantum yield (Fv/Fm) values, which are a measure of photophysiological stress, should be collected after a period of dark adaptation that is at least 30 minutes long. This is not practical in *in situ* deployments. Here, Fv/Fm values from depths of 10 m and 20 m are reported (Table 3.2). The light at these depths is considerably less than at the surface, i.e. mostly less than $100 \mu mol \text{ photons } m^{-2} s^{-1}$, and allows some comparison between times, depths and sites.

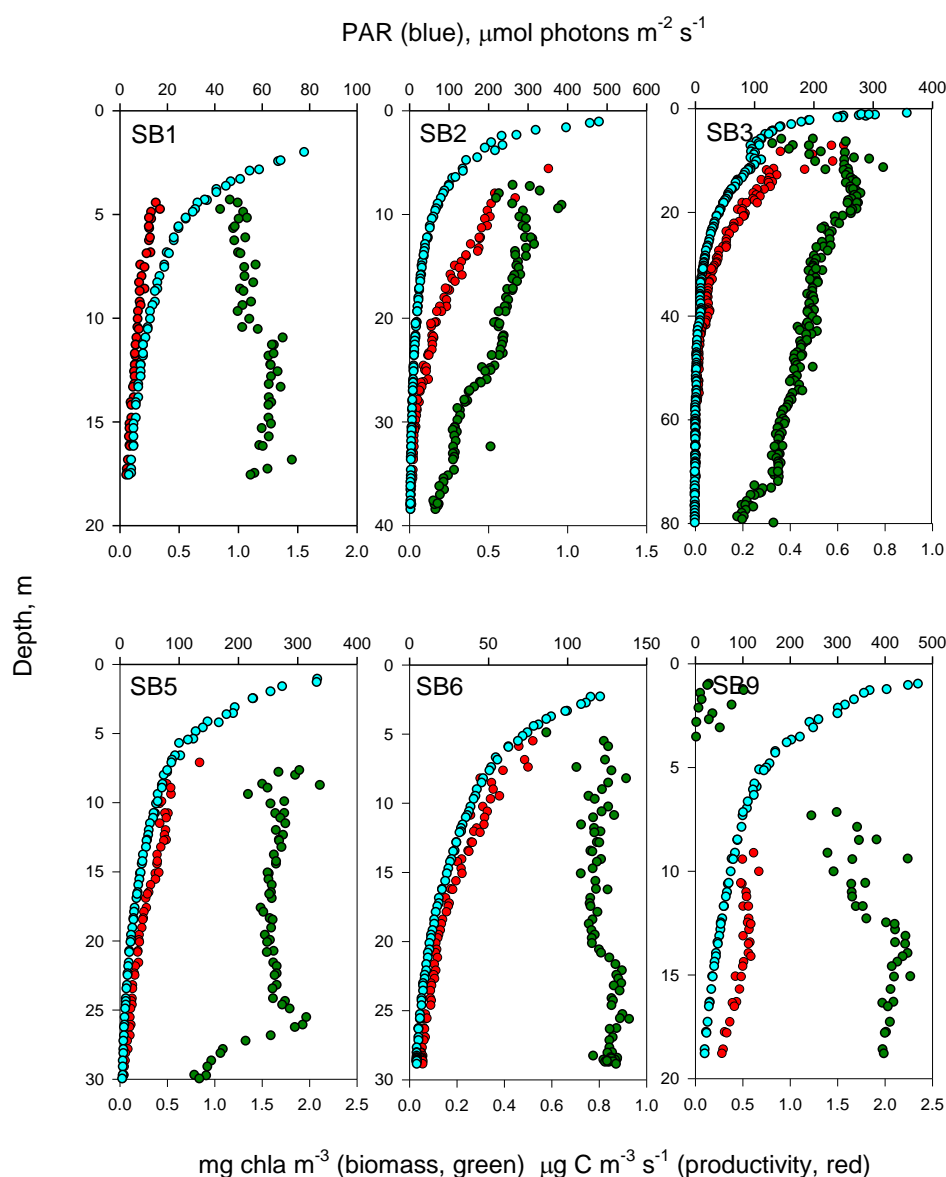


Figure 3.50 Light ($\mu mol \text{ photons } m^{-2} s^{-1}$), biomass ($mg \text{ Chla } m^{-3}$) and gross primary productivity ($\mu g \text{ C } m^{-3} s^{-1}$) at sites 1, 2, 3, 5, 6 and 9 in Storm Bay on January 27th 2015. Note that axes are not uniform in scale.

Table 3.2. Light (PAR, $\mu\text{mol photons m}^{-2} \text{ s}^{-1}$), Chlorophyll (Chl, mg chl a m^{-3}) and Fv/Fm (dimensionless) at sites 1, 2, 3, 5, 6 and 9, depths of 10 m and 20 m (or the greatest depth if less than 20 m) on the 15th January, 10th March and 22nd April 2015.

Site	Date	Depth	PAR	Chl	Fv/Fm
SB1	15/1/2016	10	12	1.03	0.499
SB1	15/1/2016	17.5	2	1.24	0.509
SB2	15/1/2016	10	62	0.469	0.473
SB2	15/1/2016	20	20	0.554	0.482
SB3	15/1/2016	10	104	0.508	0.409
SB3	15/1/2016	20	41	0.658	0.466
SB5	15/1/2016	10	62	1.59	0.478
SB5	15/1/2016	20	19	1.56	0.499
SB6	15/1/2016	10	39	0.841	0.491
SB6	15/1/2016	20	13	0.772	0.523
SB9	15/1/2016	10	70	1.65	0.479
SB9	15/1/2016	18.8	21	1.99	0.515
SB1	10/3/2016	10	24	0.589	0.485
SB1	10/3/2016	17.2	6	0.781	0.477
SB2	10/3/2016	10	262	0.46	0.377
SB2	10/3/2016	20	82	1.08	0.483
SB3	10/3/2016	10	113	0.215	0.374
SB3	10/3/2016	20	81	0.210	0.394
SB5	10/3/2016	10	183	0.529	0.405
SB5	10/3/2016	19.8	50	0.763	0.477
SB6	10/3/2016	10	77	0.950	0.488
SB6	10/3/2016	20	18	1.08	0.523
SB1	22/4/2016	10	8	1.47	0.485
SB2	22/4/2016	10	49	1.60	0.444
SB2	22/4/2016	20	19	0.893	0.504
SB3	22/4/2016	10	44	0.837	0.489
SB3	22/4/2016	10	20	1.12	0.493
SB5	22/4/2016	10	23	1.33	0.484
SB5	22/4/2016	20	4	1.24	0.509
SB9	22/4/2016	10	50	1.46	0.467
SB9	22/4/2016	20	6	1.24	0.497

3.5.3 Results and Discussion

January 2015

Details of light, chlorophyll concentration and gross primary production can be seen in **Error! Reference source not found.** Chlorophyll concentration was highest at Site 9 and lowest at Site 2. Biomass was evenly distributed with depth at Sites 1 and 6, but showed peaks at 15 m at site 3 and 25 m at sites 5 and 6. Values were comparable to summertime coastal areas elsewhere. Because productivity is a function of both light and biomass, it will usually be highest near the surface. Highest values, $> 0.5 \text{ mgC m}^{-3} \text{ s}^{-1}$ were found at sites 2, 3 and 6.

March 2015

Chlorophyll concentration was highest at site 5 ($\sim 1.5 \text{ mg chla m}^{-3}$, at 15 m) and lowest at site 3 (mostly less than $0.2 \text{ mg chla m}^{-3}$ at all depths; Figure 3.51). There were clear peaks in biomass at 30 m at site 2, 15 m at site 5 and 20 m at site 6. Gross primary production generally decreased with depth, although there was a clear peak, coinciding with the peak in chla, at 15 m at site 5. Values were greatest at site 5 ($> 1.0 \text{ mgC m}^{-3} \text{ s}^{-1}$) and lowest at site 3.

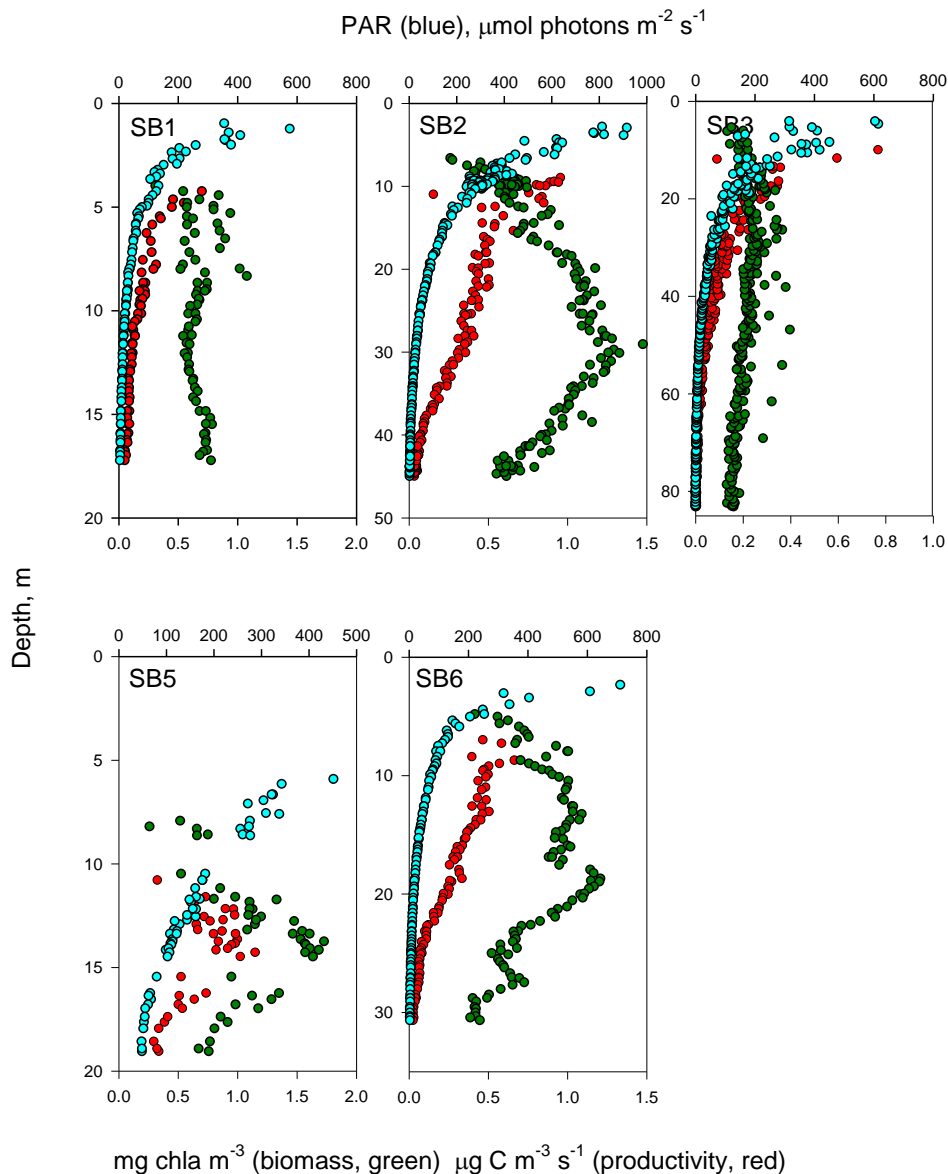


Figure 3.51. Light ($\mu\text{mol photons m}^{-2} \text{ s}^{-1}$), biomass (mg Chla m^{-3}) and gross primary productivity ($\mu\text{g C m}^{-3} \text{ s}^{-1}$) at sites 1, 2, 3, 5 and 6 in Storm Bay on March 10th 2015. Note that axes are not uniform in scale.

April 2015

Chlorophyll concentration was highest at site 6 (3-4 mg chla m⁻³ between 5 m and 10 m) and lowest at site 9 (< 1.5 mg chla m⁻³ above 10 m) (Figure 3.52) Gross primary production was highest at site 6 (1-2 mgC m⁻³ s⁻¹, between 5 m and 10 m) and lowest at site 3. Compared to the previous two months there was more structure in distribution of both biomass and productivity. At site 1 there was a clear biomass maximum at the bottom. Sites 2 and 9 both had clear peaks in biomass and productivity at 10 m. This also coincided with a local rise in irradiance levels, which was possibly caused by a bloom of highly reflective coccolithophores. Sites 2 and 6 also had clear increases in biomass and productivity in the top 10 m compared to greater depths. At site 9 there were increases in biomass and productivity below 10 m, while at site 3 there was a decline in biomass and productivity over the top 20 m, then were uniformly low below ~ 20 m.

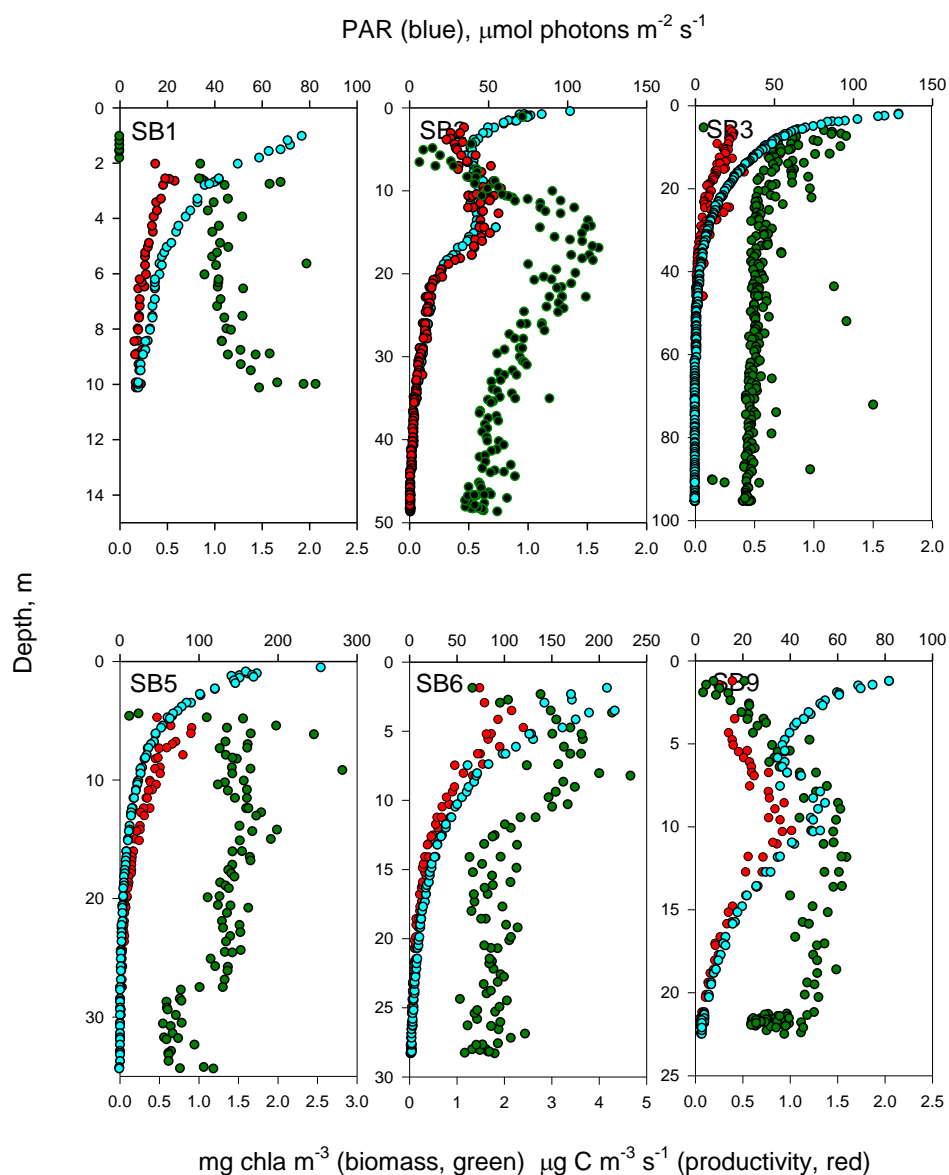


Figure 3.52. Light ($\mu\text{mol photons m}^{-2} \text{s}^{-1}$), biomass (mg Chla m^{-3}) and gross primary productivity ($\mu\text{g C m}^{-3} \text{s}^{-1}$) at sites 1, 2, 3, 5, 6 and 9 in Storm Bay on April 22nd 2015. Note that axes are not uniform in scale.

3.5.4 Maximum quantum yield (F_v/F_m)

Maximum quantum yield measurements are used widely to infer stress. Here values from 10 m and 20 m (or at the bottom if less than 20 m) are reported (Table 3.2). For these measurements to be reliable, however, the organisms need to undergo a period of dark adaptation, usually greater than 30 minutes. This is not possible in these in situ deployments. F_v/F_m was measured in the dark chamber of the instrument but dark adaptation time would have been only a few seconds and the recorded F_v/F_m value would still have been influenced by its prior light history. At depth, light values will approach zero. At 20 m in the deployments measured here, irradiances were mostly less than $100 \mu\text{mol photons m}^{-2} \text{s}^{-1}$ compared with surface values $> 1,500 \mu\text{mol photons m}^{-2} \text{s}^{-1}$. These values thus provide a qualitative way of comparing in situ stress between sites and months. F_v/F_m values (measured on a FRRF) > 0.45 are considered unstressed and well adapted. Values between 0.35 and 0.45 indicate some stress. Values < 0.35 indicate severe stress. In the data reported here prior light exposure will have caused a decrease in the values, compared to true F_v/F_m values.

3.6 Historical Comparison

From 1985 to 1989 CSIRO conducted weekly water quality measurements at site 2 at 10 m depth (Clementson et al. 1989, Harris et al. 1991). This was their 'master' site and we purposely chose to monitor this same site over a quarter century later. Direct comparisons between the two data sets, however, need to take into consideration that different equipment was used, and for some environmental variables, different methods as well. Additionally, we only sampled monthly and likely missed extreme highs and lows in values compared with weekly sampling by CSIRO.

As expected, temperature at 10 m at site 2 showed similar seasonal patterns in 2009-15 to almost three decades earlier (Figure 3.52 top). However, both summer maximum and winter minimum temperatures were generally higher in 2009-15 than 1985-89, suggesting an overall increase in temperatures in Storm Bay. Salinities were mostly within the range of 34.0– 35.0, except for higher recordings, up to almost 35.5, in autumn 1988 and 2010 (Figure 3.52 middle).

Chlorophyll *a* concentrations in 2009-15 were generally lower than those recorded in 1985–89, with most $< 1 \mu\text{g L}^{-1}$ (Figure 3.52 bottom). In the late 80's chlorophyll *a* values covered a broader range of 0-4 $\mu\text{g L}^{-1}$ and were more variable.

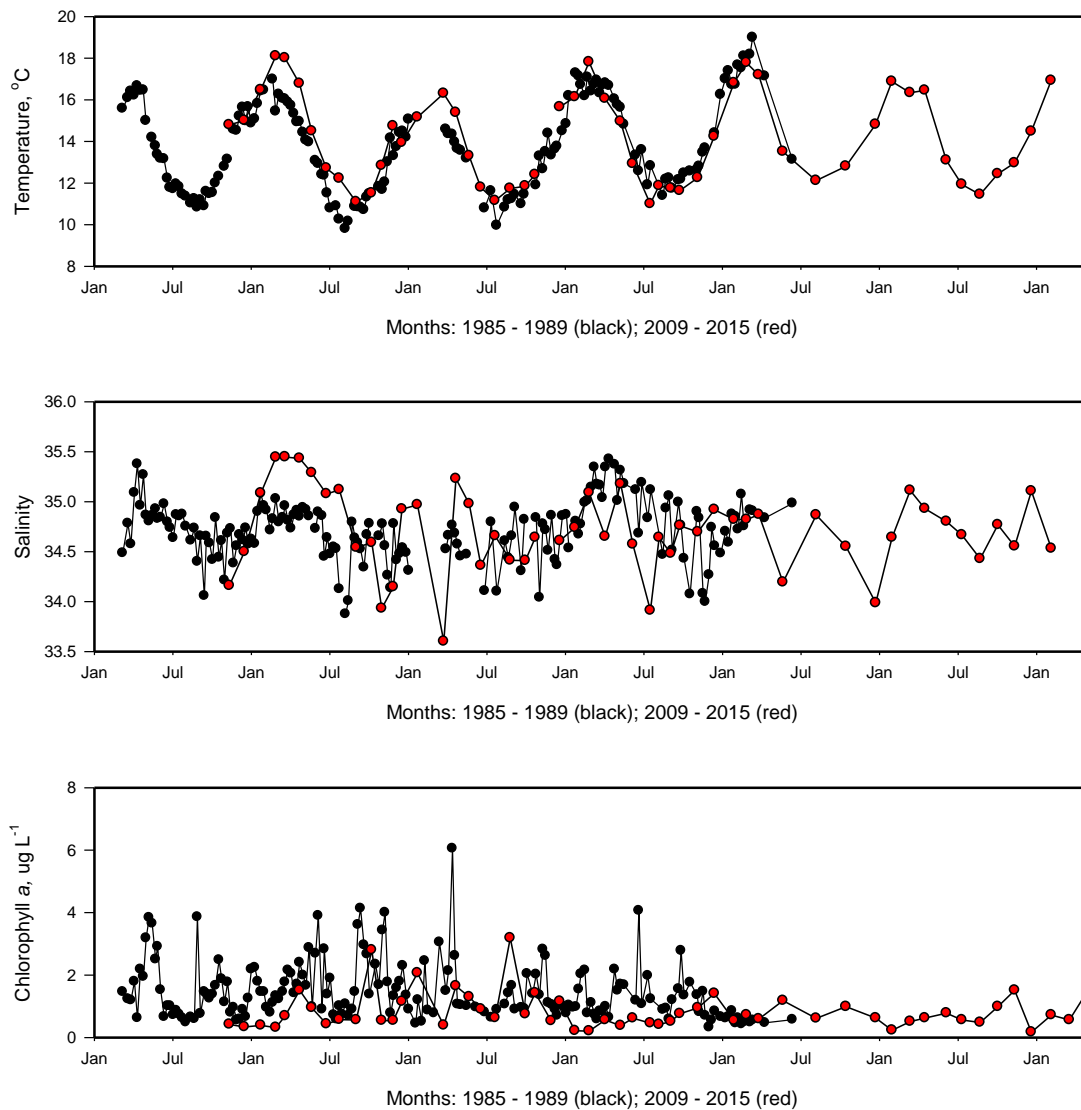


Figure 3.53 Comparison of temperature (top panel), salinity (middle panel) and chlorophyll concentration (bottom panel) at site 2, 10 m depth between the original CSIRO sampling period and the new study.

NO_x (nitrate plus nitrite) concentrations at 10 m depth at site 2 showed similar overall seasonal patterns in the two sampling periods, with higher nitrate concentrations over winter and much lower, often 0, values in summer (Figure 3.53 top). In 1985-79 higher winter values tended to last longer and extend into spring. There were also occasional peaks in summer and autumn, compared with recent sampling, especially in the summer of 1986/87.

The greatest difference in nutrients between the two samplings periods was for phosphate concentrations, which were consistently lower in the monthly samplings of 2009–15 than in the late 80s (Figure 3.53 middle). During 1985-89, phosphate concentrations were mostly within the 0.4-0.7 μM band, clearly decreased from 1985 to 1989, and did not show a consistent seasonal pattern. In 2009-15, however, phosphates mirrored the nitrate seasonal pattern with higher values in winter, approaching 0.4 μM , than other seasons.

Dissolved oxygen also tended to be in the lower range of values in 2009-15 compared with 1985-89 (Figure 3.53 bottom), although there were a couple of significantly lower recordings of around 7 mg L⁻¹ in the earlier time period.

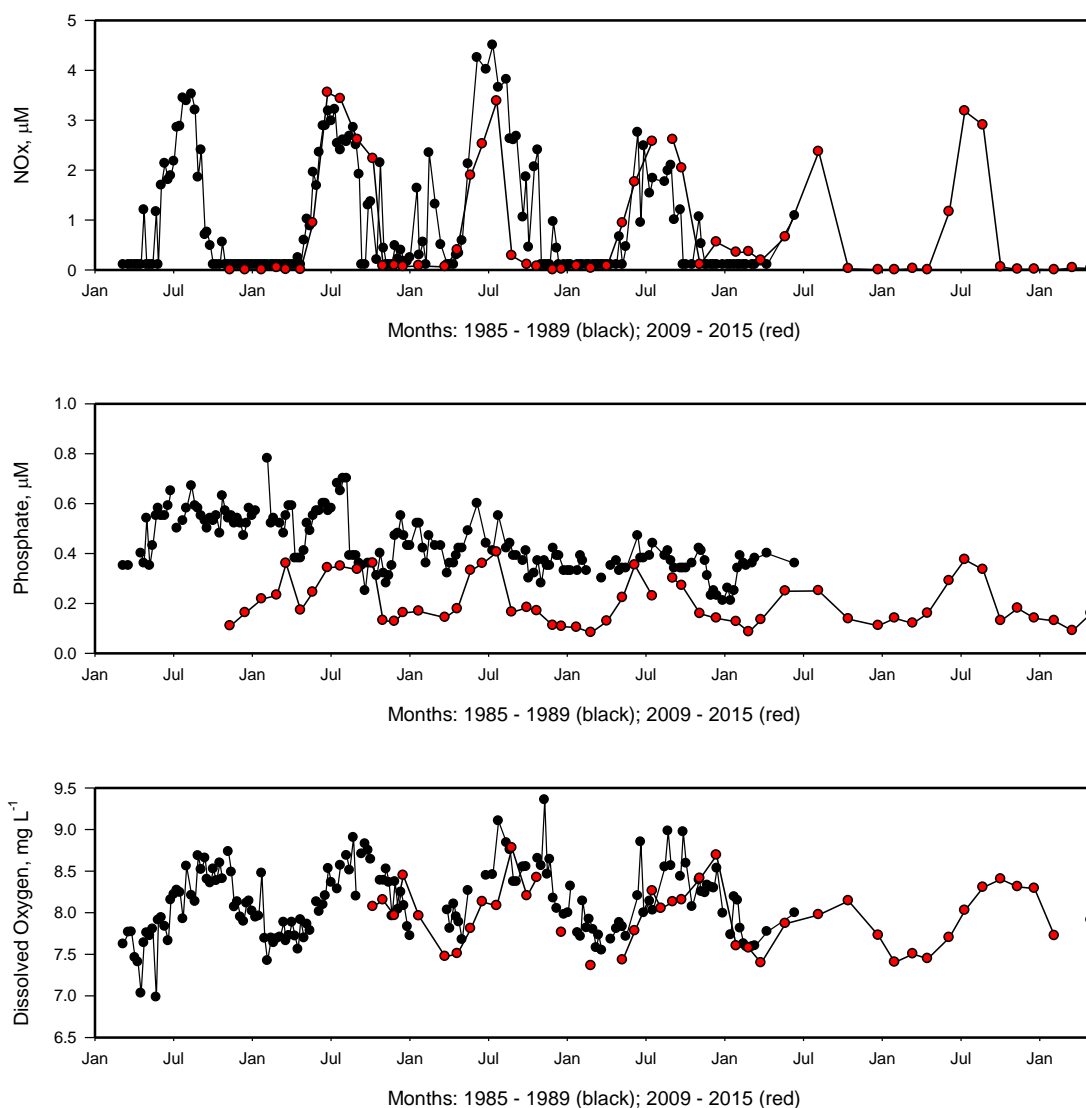


Figure 3.54 Comparison of nitrate + nitrite (top panel), phosphate (middle panel) and dissolved oxygen (bottom panel) at site 2, 10 m depth between the original CSIRO sampling period and the new study.

Analysis of five environmental variables from 1985-89 and 2009-2015 by PCA (Figure 3.54) accounted for almost 60% of the variation in the data. Phosphate was not included because of possible differences in analytical methods and equipment. Generally, the data from each of the time periods separated out in the PCA plot, with data from 1985-89 being associated with higher chlorophyll *a* and DO than in 2009-15. Much of the data from 1987 and to a lesser extent from 1986, were clearly separate from all the other years of data, and were linked to high nitrate levels. This was also a very strong El Niño period when westerly winds were stronger, driving nutrient-rich subantarctic waters into southeastern Tasmanian coastal waters (Clementson et al. 1989).

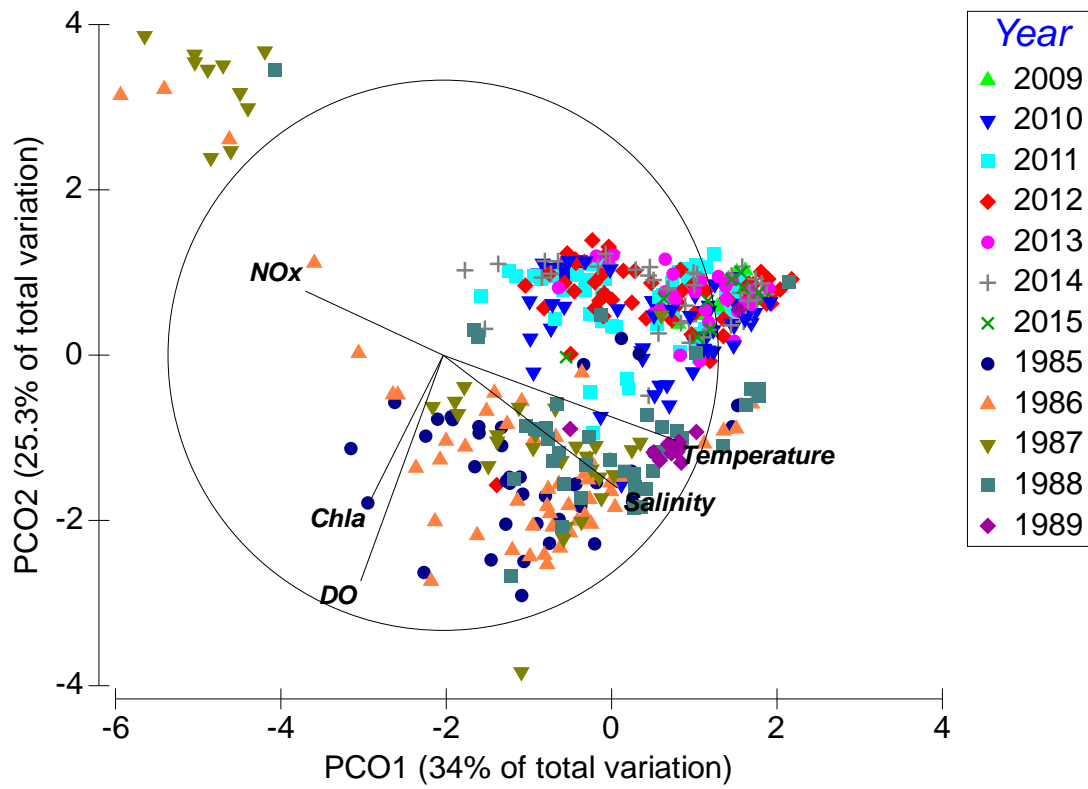


Figure 3.55 Plot showing principal components analysis for environmental data for the two periods of Storm Bay sampling, 1985 – 1989 and 2009 – 2015.

4. Discussion

4.1 Physical and chemical water quality in Storm Bay

The physical/ chemical water quality data collected in Storm Bay over five years highlight that this region is a complex mixing zone between the three major currents that influence Tasmanian coastal waters and the freshwater influx from the major drowned river valley systems of the Rivers Derwent and Huon. Freshwater flooding, which predominantly occurs in winter, spills out into Storm Bay and reduces surface water salinity at all sites, and even to 50 m depth at site 3 during major flooding (e.g. March 2011). On the other hand, when freshwater outflow is minimal, the occurrence of the Leeuwin Current (LC) in the bay can be observed in winter-spring in most years, using the physical characteristics of this current described by Ridgeway (2007) of warmer winter temperatures ($\sim 12\text{ }^{\circ}\text{C}$), high salinity (34.8-35.2) and high nitrate concentrations ($\sim 4\text{ }\mu\text{M}$). This current is dominant in winter when it flows down the west coast, curls around the southern tip of Tasmania and up the east coast.

Our results on the presence of the EAC in Storm Bay confirm previous observations that this current is highly variable (Ridgeway and Hill 2009, Buchanan et al. 2014). Previous evidence of the EAC penetrating as far south as Storm Bay is limited, although Clementson et al. (1989) observed higher salinity and temperature waters in Storm Bay in March/April 1985 and February/March 1988, which they considered to be characteristic of the EAC and confirmed by satellite imagery of sea surface temperatures. However, their temperature and salinity recordings were slightly lower than those subsequently documented by Ridgeway (2007) as being characteristic of EAC waters of temperatures $>18\text{ }^{\circ}\text{C}$ and salinity >35.6 . Using Ridgeway's 2007 description of EAC, we only recorded a clear EAC signal in Storm Bay in one of the six summer periods that we sampled, in early 2010. Nevertheless, the plankton periodically provided unequivocal evidence of the presence of EAC waters (see following discussion)

The highest concentrations of nitrate and phosphate in bottom waters in many months of the year were indicative of cooler, nutrient-rich subantarctic waters flowing across the shelf and upwelling in coastal waters. As discussed by Buchanan et al. (2014), few studies have shown the influence of subantarctic waters on southern Tasmanian coastal waters, although several lines of evidence support this being the case. They contend that the irregularity of the EAC's dominance in summer, at a time when the LC is much weaker, enables subantarctic waters to periodically penetrate into southern Tasmanian waters. This is supported by CONNIE2 modelling (see Methods 2.1), presence of subantarctic zooplankton species in southern Tasmanian coastal waters, and relatively high silicate and chlorophyll *a* values in summer (Buchanan et al. 2014).

Site 1 at the mouth of the Derwent and the entrance to Storm Bay displayed the characteristics of an estuarine-influenced inshore location, with the lowest surface salinities, especially in winter/spring, highest silicate concentrations and variable but generally high chlorophyll *a* values. Bottom water dissolved oxygen was also highest in most months at this site. The Derwent Estuary Program (DEP), which has been monitoring water quality in the Derwent estuary for over a decade, has a site B3 in the lower estuary that is in close proximity to our site 1 (Coughanowr

2015). They have recorded similar values for water quality at B3 as at site 1. However, the DEP observed an increase in chlorophyll *a* at site B3 over the ten years, but a general trend of declining nutrients in the lower estuary, and suggested that increasing water temperatures in marine waters may be a factor (Coughanowr 2015). Ammonia+ ammonium concentration at B3 showed a stronger trend towards highest values during the warmer months of the year than at our site 1; however, the actual concentrations are not directly comparable because of different analytical methods used.

The other inshore site, 9, at the entrance to Frederick Henry Bay, receives minimal freshwater influence and salinities were predominately marine during the five-year sampling period. It also had relatively high chlorophyll *a* concentrations.

A gradient in water quality from site 1 to site 3, moving from inshore to furthest out in Storm Bay, was evident in many water quality parameters, including a reduction in the variation in temperature and salinity, increase in median nitrate concentration and decline in chlorophyll *a* and silicate. However, ammonium concentrations in bottom water showed a clearer pattern of higher values in the warmer months of the year at sites 2 and 3, than at site 1. Ammonium values also often peaked in these deeper bottom waters. Profiles from a Slocum Glider deployed by IMOS in Storm Bay in September (IMOS, 2014) demonstrated the importance of horizontal mixing across the shelf. At depths akin to the sites sampled in this study, distinct horizontal and vertical variability in temperature, salinity and dissolved oxygen occurred. This complexity was intensified in inshore areas, which are more greatly affected by air-sea heat flux processes and rainfall events (Pearce et al. 2006).

Site 6 showed signs of oceanic influences, including relatively high nitrate concentration and low variation in salinity. Greater differences between surface and bottom water temperature, salinity and silicate concentrations at site 5, however, suggested a stronger freshwater influence, likely due to the freshwater from the River Derwent flowing along the eastern boundary of Storm Bay because of the Coriolis force and westerly winds.

Low nutrients, especially at the surface in summer and autumn, along with lowest dissolved oxygen concentrations in summer – autumn when the temperatures and biological activity are highest, suggest that a significant increase in nutrients, especially available N, from salmon aquaculture over this period could have a significant effect on the ecology of the system. On the other hand, these increased nutrients could potentially help mitigate the effect of increased penetration of nutrient-poor EAC waters in the region. This is a major factor in the demise of giant kelp (*Macrocystis pyrifera*) beds on the east coast of Tasmania (Johnson et al. 2011). The consistently higher ammonium concentration in bottom waters at site 6 from 2011 also requires further observation as this site is close to a salmon farm that has been in commercial production for around two years.

4.2 Historical comparison

When comparing results over a period of more than 25 years, the techniques may have changed and it is likely that analytical equipment used will be different, so the results may not be directly comparable. However, one of the co-investigators in the first project when we commenced sampling in Storm Bay in 2009, Lesley Clementson, conducted the nutrient analyses of the data at CSIRO Marine Labs in Hobart from 1985–89. The flow injection technique she used was relatively new at the time and is still used today. Although the nutrients were analysed in the same CSIRO laboratory in 2009-2015, the auto-analyser system that was used is a newer version of the analysers used in the 1980's.

The water quality results obtained by CSIRO at their master site 2 in 1985-89 were found by Clementson et al. (1989) and Harris et al. (1991) to be influenced by both large-scale oceanographic circulation and local wind stress. Clementson et al. (1989) considered that the master site 2 was representative of the seasonal cycle of events occurring in Storm Bay, based on an analysis of their results. According to Harris (1991), the location of south-eastern Tasmania between subtropical and subantarctic waters means that Tasmania is likely to experience significant interannual variability in climate, and the dominant water mass at the time will determine nutrient regimes in the bay,

The seasonal pattern of temperature was very similar in both reporting periods. However, the annual trends from 1985-89 described by Harris et al. (1991) are not so obvious in our data. They detected a 2.5 °C rise in sea surface temperature over their sampling period and an inverse relationship between temperature and nutrients as climatic conditions changed from El Niño to La Niña. In contrast, we recorded the highest maximum sea temperature over the 2009/2010 summer during El Niño conditions and the lowest over the 2010/2011 summer, during a strong La Niña event. Harris et al. (1991) also observed that winter nitrate concentrations were inversely related to the previous summer temperatures. This trend was also observed in our data in most years, but not in the summer 2009/10 temperatures and the following winter nitrate concentrations, when our maximum values for temperature and nitrate were recorded. However, we may have missed the extremes in temperature because we only sampled once per month.

Nevertheless, our results show an overall increase in summer maximum and winter minimum temperatures compared to a quarter century ago, which corresponds with water quality data collected systematically from the 1940's to the present at the nearby Maria Island, Tasmanian east coast long term Integrated Marine Observing System (IMOS) National Reference Station (NRS). Observations from this site show that coastal waters have become warmer and saltier, with mean trends of 2.28 °C and 0.34 psu increase per century over the 1944 to 2002 period. This has occurred due to increased influence of the EAC and associated wind patterns, and is partially due to ozone depletion and increases in atmospheric carbon dioxide (Ridgeway and Hill 2009, Johnson et al. 2011)

Salinity records in both periods showed a similar trend of seasonally higher values in late summer to early autumn when the influence of the EAC was likely to be greatest. The exceptions are during

heavy rainfall periods when freshwater floods from the Rivers Huon and Derwent influence salinity, such as in summer 2011, and possibly during summer-autumn 2013.

Nitrate plus nitrite concentrations showed similar seasonal trends over the two periods, except for lower values in spring and no periodic peaks over summer in the recent sampling. It is likely that the EAC that has been documented as extending further south along Tasmania's east coast in recent years (Buchanan et al. 2014) is restricting the inflow of cold nutrient-rich subantarctic waters into coastal waters off Tasmania's east coast, which in turn would reduce the level of production in the bay. However, this is clearly a complex system because during the strong La Nina period of 2010-2012, when the EAC would be expected to bring nutrient-poor water into the region, we recorded high nitrate concentrations, and the lowest under relatively neutral SOI conditions.

Phosphate results are particularly interesting because they were consistently lower in 2009-15 than in 1985-89. Unfortunately, phosphates were not measured at any long-term ocean monitoring sites in Australia during the 1980's, and at nearby Maria Island phosphates were not recorded from July 1962 to November 2003, so there are no long term records from other sites for comparison. Harris et al. (1991) suggested that the drop in phosphate concentrations by one half from 1985 to 1989 at site 2 was related to a reduction in westerly winds, which enabled warmer, nutrient poorer waters to penetrate into Storm Bay. They also found a clear inverse relationship between phosphate and temperature; phosphate concentrations declined as climatic conditions changed from El Niño to La Niña and temperatures increased. Conversely, at the nearby Maria Island NRS, Thompson et al. (2009) estimated an increase in phosphate concentration of $0.54 \mu\text{m century}^{-1}$. However, they do not mention that phosphate data were available from 1962 to 2003.

The obvious seasonal cyclic pattern of high phosphate concentrations over winter, similar to nitrate concentrations, that we observed in 2009-15, was not apparent in the 1985-89 data. In fact, we recorded the highest phosphate concentration during the strong La Niña period of 2010-2012. Thompson et al. (2009) also noted a significantly high correlation between average monthly surface nitrate and phosphate concentrations at Maria Island. There are no definitive explanations for the lower phosphate concentrations that we observed, and the lack of a seasonal pattern in the 1985-89 data raises questions. Although the analytical method was the same across the years, the different auto analysing equipment may have been an issue.

The consistently lower chlorophyll *a* results in 2009-15 than 1985-89 are also interesting. However, any comparison of chlorophyll *a* results must be conducted with caution because both the extraction and analytical techniques differed between the two sampling periods. Harris et al. (1991) considered that their data showed evidence of a seasonal pattern of variability as well as irregular peaks in phytoplankton biomass (using chlorophyll *a* as a proxy for biomass). Our chlorophyll *a* values peaked during the strong La Niña 2010-2012 period. Similarly, our dissolved oxygen concentrations were generally lower than those measured by CSIRO, although again sampling techniques differed between the two sampling periods.

4.3 Phytoplankton and Zooplankton in Storm Bay

Phytoplankton are key components of food webs, and a detailed understanding of floristic composition, succession and environmental triggers for blooms provides a framework for interpreting the response of zooplankton, and the fisheries they sustain. Additionally, knowledge of “baseline” conditions is critical for resource management and planning processes necessary for potential future aquaculture expansion. Plankton respond quickly to regional climate and oceanography, and community composition will change due to physiological coupling with temperature in particular (Hays et al. 2005). The timing of phytoplankton blooms or pulses that occur in response to seasonally driven nutrient, light and temperature cycles triggers annual reproduction in predator species, with a cascade of impacts possible when a mis-match or offset in events occur (Brander 2010). Southern Tasmania is characterised by winter minima in phytoplankton growth due to light limitation, despite the incursion of nutrient-rich Southern Ocean water.

Phytoplankton abundance and distribution in Storm Bay revealed complex patterns for the period 2009 – 2015. Notably, we did not always record distinct spring and/or autumn peaks in biomass during each of the five years. A previous study that combined in situ chlorophyll *a* measurements with satellite data in Storm Bay concluded that the phytoplankton biomass cycle was typical of southern hemisphere temperate waters where chlorophyll *a* peaks in September-October (Blondeau-Patissier et al. 2011), and this is in line with our expectations when we began this study. However, while there were general increases in biomass in spring, we did not always record clear peaks and there was considerable interannual fluctuation. In particular, we observed that chlorophyll *a* concentration tended to be higher overall in the first two years of the study, with highest concentrations observed in late 2010 to mid-2011, coinciding with the strong La Niña conditions experienced along the eastern seaboard from mid-2010 to mid-2011, while weaker blooms were associated with neutral or mild El Niño conditions (Bureau of Meteorology 2015). Clementson et al. (1989) also observed weak spring blooms in 1985 and 1987 in Storm Bay, which were years of reduced westerly wind intensity. A long term decline of ~8% per year in growth rate of the spring bloom near Maria Island has been calculated (Thompson et al. 2009), but we cannot presently conclude whether the change in chlorophyll *a* biomass prior to and following early 2012 was reflecting this long-term decline or whether it was more likely a function of prevailing weather conditions. Thompson et al. (2009) also reported increasing trends in sea surface temperatures and decreasing dissolved silicate concentrations at Maria Island, however our study did not indicate an overall decrease in silicate concentrations in Storm Bay during 2009 – 2015. In general we observed yearly replenishment of silicate, from both the Derwent and subantarctic waters, during the winter months, which was then drawn down in spring when diatoms became abundant.

Diatoms represented the majority of phytoplankton during winter, and this dominance continued into spring. Dinoflagellates rarely dominated the phytoplankton community, though they were present throughout the sampling period. Species capable of forming harmful blooms, such as *Gymnodinium catenatum*, were notable for occurring in occasional pulses and usually at several sites. Gymnodinioids typically comprise the dominant form of dinoflagellate taxa in coastal

eutrophic regions (Smayda & Reynolds, 2001), but it is not clear what lead to the pulses of *G. catenatum* in Storm Bay. The biological influence of the EAC was observed via the presence of the heterotrophic dinoflagellate *Noctiluca scintillans*. This species has been observed in Continuous Plankton Recorder samples at its most southerly global recording at 45°31'S 147°E, well below Tasmania, transported by an EAC warm-core eddy (McLeod et al. 2012). It should be noted that picoplankton (small plankton in the size range 0.2 – 2 µm) abundance was not quantified in this study. Picoplankton often represents a major percentage of primary production in most marine settings (Massana 2011) and Storm Bay is probably no exception.

Zooplankton form a link between primary producers and higher trophic levels within the food web. Zooplankton have been found to be influenced by both top down (from predators) and bottom up control (food availability) (Frederiksen et al. 2006, Fuchs and Franks 2010). The interactions within the food web are complex in that a change in zooplankton distribution or abundance will often result in a flow flow-on effect or in some cases a trophic cascade. It is therefore important to study zooplankton distribution, composition and abundance as changes may lead to commercial and ecological impacts.

The abundance and composition of zooplankton in Storm Bay fluctuated seasonally and annually. Zooplankton are known to have a patchy distribution in most marine environments, and are spread unevenly in the ocean (Blukacz et al. 2010). This patchiness was likely influenced by a combination of food availability, sea surface temperature and responses to other environmental conditions such as wind, nutrients and rainfall. For example, gelatinous species, such as salps and doliolids, tend to favour warmer, low productivity waters and their feeding mode (continuous filtration) means that they are capable of clearing large volumes of water. In Storm Bay the common salp species *Salpa fusiformis* and *Thalia democratica* were absent in years influenced by La Niña conditions; i.e. higher rainfall and warmer SST. Two genera of doliolids (gelatinous animals that are closely related to salps), *Doliolum* spp. and *Dolioletta* spp., dominated in waters with lower salinity and under different phytoplankton conditions: *Doliolum* spp. were favoured when diatoms and dinoflagellates were abundant, whereas *Dolioletta* spp. preferred high numbers of flagellates (Ahmad Ishak 2014).

As waters along the east coast of Tasmania warm, and the composition of the prey community changes, conditions might favour more salp blooms and this has important implications for energy transfer up the food chain. Salps are likely to be less palatable and offer lower food quality to higher consumers. If the species higher up in the food chain are commercially important, fluctuations in zooplankton can significantly alter fishery success (Pedersen et al. 2005). An example is in the Northern Hemisphere, where the Atlantic cod (*Gadus morhua*) in the North Sea have been overexploited since the 1960s; as well as being overfished, the productivity of the Atlantic cod is also influenced strongly by variations in the abundance and size of zooplankton. Beaugrand et al. (2003) found that low cod recruitment in the mid-1980s corresponded with a decrease in mean calanoid copepod size. The response of higher trophic levels to fluctuating zooplankton communities in Storm Bay is presently unknown, however given the likelihood of increased numbers of sardines in the region in coming years (J. Beard, unpublished observations)

understanding how changes at the base of the food web flow up to consumers and predators is of some importance.

In years when temperatures were warmer, a high number of EAC signature species, such as salps and the warm water copepod *Temora turbinata*, were observed in Storm Bay. During periods of cooler conditions, the zooplankton assemblage in Storm Bay was typical of a temperate coastal zooplankton community, being dominated by small copepods in the genera *Acartia* and *Paracalanus*. *Acartia tranteri* is a typical coastal species that often dominates zooplankton communities in coastal bays and estuaries (Kimmerer and McKinnon 1985). This species thrives in habitats where environmental conditions fluctuate because: (i) it can tolerate variable salinity levels (Kimmerer and McKinnon 1989), (ii) has the ability to use behavioural mechanisms such as vertical migration to avoid flushing from tides (Kimmerer and McKinnon 1987c), (iii) has a relatively fast growth and reproductive rate to account for those lost due to flushing (Kimmerer and McKinnon 1987a; Kimmerer and McKinnon 1987b), and (iv) can survive on a varied omnivorous diet, by eating their own nauplii, other copepods and microzooplankton (Landry 1983). *Paracalanus indicus* is the other small copepod that dominates temperate coastal waters, though it has been found to be less dominant in bays where *A. tranteri* is prevalent (Kimmerer and McKinnon 1985).

The presence of krill, *Nyctiphanes australis*, increases in Storm Bay when the EAC penetration into the bay is low. Reliance on *N. australis* as prey by many marine animals such as coastal fish and sea birds, as well as local fisheries, makes this species a critical species along the east coast of Tasmania (Bradford and Chapman 1988). We observed moderate abundances of *N. australis* in Storm Bay, though they reached high abundance in February 2013, which is notable as the species has not been shown to bloom in numbers since the 1980s (Johnson et al. 2011). The extension of warm, nutrient-depleted subtropical northern waters down the east coast of Tasmania has caused declines in *N. australis* populations in the past, as this species is unable to cope with those conditions; this has led to a decline in the population of jack mackerel *Trachurus declivis* (Young et al. 1993).

Further evidence of fluctuating EAC extension comes from examining the abundance of cladocerans, particularly *Evadne nordmanni*, *Podon intermedius* and *Penilia avirostris*. These three cladocerans were spatially and temporally variable in Storm Bay, however numbers were generally not 'blooming', except on a few occasions. Cladocerans are associated with warm saline waters (d'Elbée et al. 2014), such as those carried by the EAC, and are often found in high numbers when temperatures exceed 18 °C (Ramírez and Seijas 1985). Cladocerans generally reproduce parthenogenetically, by generating new individuals in brood pouches from unfertilised eggs, when conditions are warm and relatively saline (d'Elbée et al. 2014). When conditions are unfavourable, gametogenetic reproduction is favoured (Viñas et al. 2007). As brood pouches were not observed on the cladocerans we sampled, it is reasonable to suggest that the EAC was not prevalent enough to provide favourable conditions for parthenogenetic proliferation.

4.4 Detection of *Neoparamoeba perurans* in Storm Bay

Amoebic gill disease (AGD) has been a major health challenge for sea-cage Tasmanian salmon farming since commercial farming commenced in the mid 1980's. It has been estimated to increase costs of production of Atlantic salmon in Tasmania by 20% because of increased mortalities and treatment costs, and reduced growth rates (Kube et al. 2012). The parasitic amoeba, *Neoparamoeba perurans*, has only recently been identified as the causative agent for AGD in Tasmanian salmon (Crosbie et al. 2012) and little is known about the biology of this species (Oldham et al. 2016). A sensitive PCR assay for detecting *N. perurans* was developed in 2010 (Bridle et al. 2010) which has enabled studies of its distribution, including in Storm Bay as part of our current project.

Earlier surveys for *N. perurans* in Tasmania using PCR analysis found no evidence of *N. perurans* at unfarmed sites and at farm sites with no AGD infection (Bridle et al. 2010), whilst a structured study around nine commercial salmon cages at different depths and sampling times found that the amoeba were most prevalent in surface waters (Wright et al. 2015). *N. perurans* has subsequently been detected in low concentrations both at farmed and unfarmed sites (A. Bridle et al. unpublished, in Oldham et al. 2016).

In the current pilot survey for AGD-causing amoeba at sites closest to salmon farms in Storm Bay (Site 5 offshore from salmon farms in a sheltered bay at Nubeena and site 6 where trials for Atlantic salmon farming were underway) and at the furthest offshore site, *N. perurans* was detected in low concentrations in 25% of the samples analysed. They were most abundant in early autumn and in shallower water; however, there are insufficient data to make any clear correlations with environmental factors. Nevertheless, these low concentrations across three sites are considered to be sufficient to induce AGD in salmon when conditions are suitable. However, the water column is not thought to be a significant reservoir for the AGD causing amoeba (Oldham et al. 2016) and an examination of the sediments at selected sites in Storm Bay is recommended.

4.5 Assessment of the FRRF in Storm Bay

Fast repetition rate fluorometers (FRRF) are used to measure primary productivity and phytoplankton biomass in aquatic environments. FRRF can be used in a monitoring mode, where they can take surface measurements at a rate of more than once per second, or they can be deployed vertically to measure water column primary productivity. The main difference between the FRRF and ¹⁴C incubation methods is that FRRF measures carbon acquisition based on photosystem II, while ¹⁴C is based on photosystem I. Comparisons have shown that these two methods measure rates of primary productivity to within < 5% of each other (Oxborough et al. 2012). There are several advantages to using a FRRF over traditional ¹⁴C bottle incubations. The instrument takes measurements in real time, is not limited to measuring at only one or two depth strata, more rapid data acquisition, no need for long stays on site to undertake the incubations (up to 24 hours), no sample handling, safer operation and there is little in the way of post-processing. Disadvantages are that the instruments are expensive and require trained personnel to be onboard to undertake the deployment.

We deployed the FRRF during the last few sampling trips of our study, to determine its effectiveness as a monitoring tool for coastal waters. The light sensor measured photosynthetically active radiation (PAR), showing exponential decline from the surface waters down to ~ 20 m, then values close to zero below 20 m depth. This is somewhat shallower than the depth of 40 m quoted by Harris et al. (1987) as representing the euphotic zone in coastal Tasmanian waters. Chlorophyll *a*, as a proxy for phytoplankton biomass, was typical of other coastal sites including the Acteon Islands (Buchanan et al. 2014) and Maria Island (Kelly et al. 2015). Chlorophyll *a* concentration, as measured by the FRRF, did not reach the higher values reported in the monitoring program of the D'entrecasteaux Channel and Huon Estuary (Ross and Macleod 2013), suggesting that there were no point sources of nutrient enrichment near to our study sites in Storm Bay. Understanding photosynthesis of a system is fundamental to interpreting its health and functioning, as the rate of photosynthesis is a primary constraint on the availability of energy for the production of organic matter within aquatic ecosystems (Oxborough et al. 2012). There are few measures of primary productivity for Tasmanian coastal waters, probably a result of the difficulties associated with using the ¹⁴C method on a routine basis. Our results are consistent with those measured by Harris et al. (1987) using ¹⁴C bottle incubations, indicating moderate productivity in the euphotic zone of Storm Bay.

Output from the FRRF, specifically photosynthetic efficiency (Fv/Fm) is also used to measure stress resulting from environmental perturbation such as toxins, nutrient limitation, temperature changes and pH changes (Oxborough et al. 2012). The data we collected with the FRRF was indicative of healthy unstressed communities. The only significant deviation was from site 3 in March, when values < 0.4, indicated moderate stress. These low values coincided with low phytoplankton biomass and probably represented a senescent bloom (e.g. Franklin and Berges 2004). Deployment of a FRRF would produce regular measurements of stress in the Storm Bay system and various methods of active fluorometry, which could be routinely used by the scientific community and ecosystem managers as a non-intrusive technique for assessing the health of aquatic systems (Suggett et al. 2010).

5. Conclusion

The five-year study of baseline environmental conditions in Storm Bay revealed the water column to be a healthy productive system that supports considerable planktonic diversity. It is clear that Storm Bay is influenced by subantarctic and sub-tropical water masses, along with input from the River Derwent. Periodic incursions of EAC-extension water flows into Storm Bay, bring warmer, saltier water that is deficient in nutrients. In those instances biological signals of the EAC appear to be stronger than overtly physical signals. EAC-signature species such as salps, some copepods (e.g. *Temora turbinata*) and the dinoflagellate *Noctiluca scintillans* flow into the bay, where they can bloom in very large abundances. Blooms of these EAC-related species can affect the local temperate fauna, though the cooler-water fauna were seen to thrive again under suitable conditions. Thus, we can conclude the Storm Bay at present oscillates between sub-tropical and

temperate planktonic assemblages and there was no indication of a permanent shift to a more salp-based system.

Implications

The major implications of our project are:

Comprehensive baseline data on water quality and plankton composition and abundance that have been collected during this project are available before salmon farming commences in Storm Bay. This is crucial to future assessments of impacts of salmon farming on the Storm Bay ecosystem.

These data are very important to the development of a cost-effective monitoring program by the Tasmanian Government for salmon farm impacts in Storm Bay, including location of monitoring sites and establishing baseline water quality guidelines. This extensive environmental assessment prior to development should provide a greater level of assurance to the general public that any new salmon farming areas in Storm Bay are being managed sustainably.

Environmental Impact Assessments being prepared by the three salmon farming companies in Tasmania to support their applications to Government for new salmon growing areas in Storm Bay are based on actual environmental data collected in the proposed new growing areas over a significant five-year time period.

The data collected provide a valuable dataset to better understand the Storm Bay ecosystem for all uses of this important waterway at the entrance to the River Derwent, including commercial and recreational fishing. Improved knowledge of the influence of the three major oceanic currents on coastal waters, including the Storm Bay region, and associated effects on productivity is important to the local fishing industry as well as to aquaculture.

This longer term environmental dataset will be important to predictive modelling of effects of climate change and human activities in the region, including salmon farming. Modelling of the Storm Bay and broader south eastern Tasmanian ecosystem has been conducted by CSIRO, but this has been restricted by the limited availability of data. Using the data collected in this project, more comprehensive and reliable predictive modelling can occur in this designated climate change hotspot region.

Further development

As discussed in Implications, the results from this project are already being used by industry and Government. Further recommendations include continued monitoring of at least the six sites assessed in this project as salmon farming progresses in the region. They also include refining predictive models of the effects of salmon farming, with the data collected being very valuable for model calibration. These models would provide a stronger background for effective management, including setting carrying capacity limits and monitoring requirements.

New and rapidly developing technology for remote data collection, storage and transmission should also be investigated. This includes in situ continuously monitoring environmental systems for temperature, salinity, fluorescence (chlorophyll *a*), turbidity and dissolved oxygen, with results telemetered to onshore computers. Techniques to continuously measure nitrate and phosphate concentrations in ocean observing systems have also been developed in recent years, and would provide a better understanding of nutrient dynamics than the monthly sampling conducted in the present study. For example, Wild-Allen et al (2014) trialled new techniques for continuous monitoring of nutrient concentrations in Storm Bay and observed intrusion and mixing of higher nutrient offshore waters with shelf waters with finer temporal resolution than is achievable by monthly sampling. However, any such sensor systems would need to be able to withstand the extreme weather conditions that can be experienced in Storm Bay.

Extension and Adoption

The water quality data – Secchi depth, chlorophyll a surface and bottom, nutrients: nitrate, nitrite, ammonium, phosphate and silicate, temperature, salinity and dissolved oxygen at the surface, 10 m depth and the bottom were provided to The Tasmanian Salmon Growers Association in August 2016 at the request of the three salmon growing companies, Tassal, Huon Aquaculture and Petuna. A summary of the Methods and Results and 12 graphs of the data were also provided. These three companies were eager to obtain the data as quickly as possible because they wanted to include the data in Environmental Impact Assessments that they were preparing to support their applications to Government for new lease areas in Storm Bay.

The data and graphs were also provided to the Marine Farming Branch in DPIPWE in September 2016 at their request because they are developing environmental monitoring programs for the proposed salmon farms in Storm Bay. These data provide a comprehensive baseline of environmental conditions before salmon farming commenced in Storm Bay. The EISs and the government required monitoring program have not been made available to the public yet.

The information on phytoplankton, zooplankton, gill amoeba surveys and primary product in Storm Bay will be provided to the salmon farming industry and the Tasmanian Government in this final FRDC report and in the papers that are currently being prepared for publication in international journals.

Glossary

El Niño an irregularly occurring and complex series of climatic changes affecting the equatorial Pacific region and beyond every few years, characterized by the appearance of unusually warm, nutrient-poor water off northern Peru and Ecuador, typically in late December. The effects of El Niño include reversal of wind patterns across the Pacific, drought in Australasia, and unseasonal heavy rain in South America.

La Niña is the positive phase of the El Niño Southern Oscillation and is associated with cooler than average sea surface temperatures in the central and eastern tropical Pacific Ocean.

Photosystem I (PS I, or plastocyanin: ferredoxin oxidoreductase) is the second photosystem in the photosynthetic light reactions of algae, plants, and some bacteria. Photosystem I is named because it was discovered before photosystem II.

Photosystem II (PS II, or water-plastoquinone oxidoreductase) is the first protein complex in the light-dependent reactions of oxygenic photosynthesis. It is located in the thylakoid membrane of plants, algae, and cyanobacteria.

Southern Oscillation Index (SOI) gives an indication of the development and intensity of El Niño or La Niña events in the Pacific Ocean. The SOI is calculated using the pressure differences between Tahiti and Darwin.

Project materials developed

Presentations

Crawford C, Swadling K, Frusher S (2012) Productivity and Water Quality Changes in Coastal Waters in Southeastern Tasmania, a Climate Change 'Hotspot'. 50th ECSA Conference: Today's science for tomorrow's Management. Venice, Italy.

Crawford C, Swadling K, Frusher S (2012) Productivity and Water Quality Changes in Coastal Waters in Southeastern Tasmania, a Climate Change 'Hotspot'. 49th Australian Marine Science Annual Conference, Hobart, Australia.

Beard J, Crawford C, Eriksen R, Kelly P, Swadling K (2015) Zooplankton as indicators of changing dominance of water masses in Storm Bay, Tasmania: comparing the 1970s to now. 52nd Australian Marine Science Annual Conference, Geelong, Australia.

Crawford C and Swadling K (2016) Changing environmental conditions in SE Tasmanian inshore waters and flow on effects to marine industries. Cruising Yacht Club of Tasmania seminar series.

Student projects

Ahmad Ishak, N.H. (2014) The bloom dynamics and trophic ecology of salps and doliolids in Storm Bay, Tasmania. University of Tasmania unpublished PhD thesis, 193 pp.

Picone, K. (2011) The community structure and production of the euphausiid *Nyctiphanes australis* in Storm Bay, south-east Tasmania, and its change over 30 years. Directed study project, University of Tasmania.

Scientific papers

Ahmad Ishak, N. H., Clementson, L.A., Eriksen, R.S., van den Enden, R.L., Williams, G.D. and Swadling, K.M. (2017) Gut contents and isotopic profiles of *Thalia democratica* and *Salpa fusiformis*. *Marine Biology* 164: 144

Baird ME, Ralph PJ, Rizwi F, Wild-Allen K, Steven ADL (2013) A dynamic model of the cellular carbon to chlorophyll ratio applied to a batch culture and a continental shelf ecosystem. *Limnology and Oceanography* 58: 125-1226.

Blondeau-Patissier D, Dekker AG, Schroeder T, Brando VE (2011) Phytoplankton dynamics in shelf waters around Australia. Report prepared for the Australian Government Department of Sustainability, Environment, Water, Population and Communities on behalf of the State of the Environment 2011 Committee. Canberra: DSEWPaC, 34 pp.

Clarke, L., Beard, J., Swadling, K. and Deagle, B. Effect of marker choice and thermal cycling protocol on zooplankton DNA metabarcoding studies. *Ecology and Evolution* 7: 873-883.

Davies, C.H., Coughlan, A., Hallegraef, G., Ajani, P., Armbrecht, L., Atkins, N., Bonham, P., Brett, S., Brinkman, R., Burford, M., Clementson, L., Coad, P., Coman, F., Davies, D., Dela-Cruz, J., Devlin, M., Edgar, S., Eriksen, R., Furnas, M., Hassler, C., Hill, D., Holmes, M., Ingleton, T., Jameson, I., Leterme, S.C., Lønborg, C., Mclaughlin, J., McEnnulty, F., McKinnon, A.D., Miller, M., Murray, S., Nayar, S., Patten, R., Pritchard, T., Proctor, R., Purcell- Meyerink, D., Raes, E., Rissik, D., Ruszczyk, J., Slotwinski, A., Swadling, K.M., Tattersall, K., Thompson, P., Thomson, P., Tonks, M., Trull, T.W., Uribe-Palomino, J., Waite, A.M., Yauwenas, R., Zammit, A. and Richardson, A.J. (2016). A database of marine phytoplankton abundance, biomass and species composition in Australian waters. *Scientific Data* 3: 160043ase

Industry update

Crawford C, and Swadling K. (2016) Storm Bay Water Quality, Report to Petuna, August 2016, 17pp. (plus 24pp Appendices)

Appendices

Appendix 1: List of researchers and project staff (boat skippers, technicians, consultants)

Principal Investigators: Dr Christine Crawford and Dr Kerrie Swadling

IMAS researchers and technical staff: Dr Ruth Eriksen, Jason Beard, Lisette Robertson, Andrew Pender

IMAS students: Jake Wallis, Kate Picone, Nurul Huda Ahmad Ishak, Danielle Mitchell, Samantha Castle, Eldene O'Shea, Mary Clarke

Volunteer field staff, in particular Andreas Seger and Shi Hong Lee

Boat skippers and crew: skipper, Pieter van der Woude, of 'Odalisque', and first mate Dave Denisen; skippers, Phil Pyke and Scott Palmer, of 'ICON'

Appendix 2: Intellectual Property

There are no intellectual property issues associated with this project.

Appendix 3: References

- Ahmad Ishak, N. H. A. 2014. The bloom dynamics and trophic ecology of salps and doliolids in Storm Bay, Tasmania. Doctor of Philosophy Thesis, Institute for Marine and Antarctic Science, Hobart, Tasmania.
- ANZECC (2000) Australian and New Zealand Guidelines for fresh and marine water quality. National Water Quality Management Strategy Paper N0. 4, Australian and New Zealand Environment and Conservation Council.
- Baines PG, Edwards RJ, Fandry CB (1983) Observations of a new baroclinic current along the western continental slopes of Bass Strait. *Australian Journal of Marine and Freshwater Research* 34: 155-157.
- Beaugrand G, Brander KM, Lindley JA, Souissi S, Reid PC (2003) Plankton effect on cod recruitment in the North Sea. *Nature* 426:661-664.
- Blondeau-Patissier D, Dekker AG, Schroeder T, Brando VE (2011) Phytoplankton dynamics in shelf waters around Australia. Report prepared for the Australian Government Department of Sustainability, Environment, Water, Population and Communities on behalf of the State of the Environment 2011 Committee. Canberra: DSEWPaC, 34 pp.
- Blukacz EA, Sprules WG, Shuter BJ, Richards JP (2010) Evaluating the effect of wind-driven patchiness on trophic interactions between zooplankton and phytoplankton. *Limnology and Oceanography* 55: 1590-1600.
- Bowie AR, Griffiths FB, Dehairs F, Trull TW (2011) Oceanography of the subantarctic and Polar Frontal Zones south of Australia during summer: Setting of the SAZ-Sense study. *Deep-Sea Research II* 58: 2059-2070.
- Bradford JM, Chapman B (1988) *Nyctiphanes australis* (Euphausiacea) and an upwelling plume in western Cook Strait, New Zealand. *New Zealand Journal of Marine & Freshwater Research* 22: 237-247.
- Brander K (2010) Impacts of climate changes on fisheries. *Journal of Marine Systems* 79: 389-402.
- Bray JR, Curtis JT (1957) An ordination of the upland forest communities of southern Wisconsin. *Ecological Monographs* 27: 325-349.
- Bridle A, Crosbie P, Cadoret K, and Nowak B. (2010) Rapid detection and quantification of *Neoparamoeba perurans* in the marine environment. *Aquaculture*, 309: 56–61
- Buchanan PJ, Swadling KM, Eriksen RS, Wild-Allen, K (2014) New evidence links changing shelf phytoplankton communities to boundary currents in Southeast Tasmania. *Reviews in Fish Biology and Fisheries* 24: 427-442.
- Bureau of Meteorology (2012) Record-breaking La Nina events. Published by the Bureau of Meteorology, Melbourne, July 2012, 25 pp.

Burgess S, Roberts S, Shanton A, Chen C, Smith H, Gorman J (1993) Environmental quality of the lower Huon River catchment. Centre for Environmental Studies, University of Tasmania, Unpublished report.

Chavez FP, Messie M, Pennington JT (2011) Marine primary production in relation to climate variability and change. *Annual Review of Marine Science* 3: 227-260.

Cheah W, McMinn A, Griffiths B, Westwood KJ, Webb J, Molina E, Wright SW, van den Enden R (2011) Assessing Sub-Antarctic Zone primary productivity from fast repetition rate fluorometry. *Deep Sea Research II: Topical Studies in Oceanography* 58: 2179-2188.

Chelsea Technologies Group (2012) <http://www.chelsea.co.uk/allproduct/marine/fluorometers/fast-ocean-system/fastocean-apd-profiling-system>.

Clementson LA, Harris GP, Griffiths FB, Rimmer DW (1989) Seasonal and inter-annual variability in chemical and biology parameters in Storm Bay, Tasmania. I. physics, chemistry and the biomass of components of the food chain. *Australian Journal of Marine and Freshwater Research* 40: 25-38.

Clementson LA, Parslow JS, Turnbull AR, Bonham PI (2004) Properties of light absorption in a highly coloured estuarine system in south-east Australia which is prone to blooms of the toxic dinoflagellate *Gymnodinium catenatum*. *Estuarine, Coastal and Shelf Science* 60: 101-112.

Clementson LA, Blackburn SI, Berry KM, Bonham PI (2008) Temporal and spatial variability in phytoplankton community composition in the mouth of the Huon River Estuary. *Appendix in: Volkman, J.K. et al. (eds) A whole-of-ecosystem assessment of environmental issues for salmonid aquaculture. Final report to Aquafin CRC Project 4.2(2) and Fisheries Research and Development Corporation. Project number 2004/074.*

Condie SA, Hepburn M, Mansbridge J (2012) Modelling and visualisation of connectivity for the Great Barrier Reef. In: Proceedings of the 12th international coral reef symposium, Cairns, Australia, 9-13 July 2012.

CONNIE (2012) CSIRO Connectivity interface. Available at: <http://www.csiro.au/connie2/>

Corno G, Letelier RM, Abbott MR, Karl DM (2006) Assessing primary production variability in the North Pacific subtropical gyre: A comparison of fast repetition rate fluorometry and ¹⁴C measurements. *Journal of Phycology* 42: 51-60.

Coughanowr C, Whitehead S, Whitehead J, Einoder L, Taylor U, Weeding B (2015) State of the Derwent estuary: a review of environmental data from 2009 to 2014. Derwent Estuary Program.

Cresswell GR (2000) Currents of the continental shelf and upper slope of Tasmania. *Proceedings of the Royal Society of Tasmania* 133: 23-30.

Crosbie P, Bridle A, Cadoret K, Nowak B (2012) In vitro cultured *Neoparamoeba perurans* causes amoebic gill disease in Atlantic salmon and fulfils Koch's postulates. *International Journal of Parasitology* 42: 511-515.

CSIRO Huon Estuary Study Team (2000) Huon Estuary Study – environmental research for integrated catchment management and aquaculture. CSIRO Division of Marine Research. Marine Laboratories, Hobart.

Estevez-Blanco P, Cermeno P, Espineira M, Fernandez E (2006) Phytoplankton photosynthetic efficiency and primary production rates estimated from fast repetition rate fluorometry at coastal embayments affected by upwelling (Rias Baixas, NW of Spain). *Journal of Plankton Research* 28: 1153–1165.

Falkowski PG, Kolber Z (1995) Variations in chlorophyll fluorescence yields in phytoplankton in the world oceans. *Australian Journal of Plant Physiology* 22: 341-355.

Franklin DJ, Berges JA (2004) Mortality in cultures of the dinoflagellate *Amphidinium carterae* during culture senescence and darkness. *Proceedings of the Royal Society of London, Series B* 271: 2099-2107.

Frederiksen M, Edwards M, Richardson AJ, Halliday NC, Wanless S (2006) From plankton to top predators: bottom-up control of a marine food web across four trophic levels. *Journal of Animal Ecology* 75: 1259–1268.

Fuchs HL, Franks PJS (2010) Plankton community properties determined by nutrients and size-selective feeding. *Marine Ecology Progress Series* 413: 1-15.

Hallegraeff GM, Bolch CJS, Huisman JM, De Salas MF (2010), Planktonic dinoflagellates, *Algae of Australia: Phytoplankton of Temperate Coastal Waters* 145–212.

Harris GP, Nilsson C, Clementson L, Thomas D (1987) The water masses of the east coast of Tasmania: seasonal and inter-annual variability and the influence on phytoplankton biomass and productivity. *Australian Journal of Marine and Freshwater Research* 38: 569-590.

Harris GP, Davies P, Nunez M, Meyers G (1988) Interannual variability in climate and fisheries in Tasmania. *Nature* 333: 754-757.

Harris GP, Griffiths FB, Clementson LA, Lyne V, Van der Doe H (1991) Seasonal and interannual variability in physical processes, nutrient cycling and the structure of the food chain in Tasmanian shelf waters. *Journal of Plankton Research* 13: 109-131.

Hassler CS, Djajadikarta JR, Doblin MA, Everett JD, Thompson PA (2011) Characterisation of water masses and phytoplankton nutrient limitation in the East Australian Current separation zone during spring 2008. *Deep-Sea Research II* 58: 664-677.

Hays GC, Richardson AJ, Robinson C (2005) Climate changes and marine plankton. *Trends in Ecology and Evolution* 20: 337-344.

Herzfeld M (2008) Connectivity in Storm Bay. Report to CSIRO.

Hill KL, Rintoul SR, Coleman R, Ridgway KR (2008) Wind forced low frequency variability of the East Australian Current. *Geophysical Research Letters* 35: L08602

Hillebrand H, Durselen CD, Kirschtel D, Pollinger U, Zohary T (1999) Biovolume calculation for pelagic and benthic microalgae. *Journal of Phycology* 35: 403-424.

Integrated Marine Observing System (IMOS) (2015) Sea Surface Temperature maps. Available at: <http://oceancurrent.imos.org.au/sst.php>. Accessed 20 October 2016.

Johnson CR, Banks SC, Barrett NS, Cazassus F, Dunstan PK, Edgar GJ, Frusher SD, Gardner C, Haddon M, Helidoniotis F, Hill KL, Holbrook NJ, Hosie GW, Last PR, Ling SD, Melbourne-Thomas J, Miller K, Pecl G, Richardson AJ, Ridgway KR, Rintoul SR, Ritz DA, Ross DJ, Sanderson JC, Shepherd SA, Slotwinski A, Swadling KM, Nyan Taw (2011) Climate change cascades: shifts in oceanography, species' ranges and subtidal marine community dynamics in eastern Tasmania. *Journal of Experimental Marine Biology and Ecology* 400:17-32.

Kelly P, Clementson L, Lyne V (2015) Decadal and seasonal changes in temperature, salinity, nitrate and chlorophyll in inshore and offshore waters along southeast Australia. *Journal of Geophysical Research: Oceans* 120: 4226-4244.

Kimmerer WJ, McKinnon AD (1985) A comparative study of the zooplankton in two adjacent embayments, Port Phillip and Westernport Bays, Australia. *Estuarine, Coastal and Shelf Science* 21: 145-159.

Kimmerer WJ, McKinnon AD (1987a) Growth, mortality, and secondary production of the copepod *Acartia tranteri* in Westernport Bay, Australia. *Limnology & Oceanography* 32: 14-28.

Kimmerer WJ, McKinnon AD (1987b) Zooplankton in a marine bay. I. Horizontal distributions used to estimate net population growth rates. *Marine Ecology Progress Series* 41: 43-52.

Kimmerer WJ, McKinnon AD (1987c) Zooplankton in a marine bay. II. Vertical migration to maintain horizontal distributions. *Marine Ecology Progress Series* 41: 53-60.

Kimmerer WJ, McKinnon AD (1989) Zooplankton in a marine bay. III. Evidence for influence of vertebrate predation on distributions of two common copepods. *Marine Ecology Progress Series* 53: 21-35.

Kube PD, Taylo RS, and Elliott NG. (2012) Genetic variation in parasite resistance of Atlantic salmon to amoebic gill disease over multiple infections. *Aquaculture*, 364:165–172.

Landry M (1983) The development of marine calanoid copepods with comment on the isochronal rule. *Limnology and oceanography* 28: 614-624.

Massana R (2011) Eukaryotic picoplankton in surface oceans. *Annual review of microbiology* 65: 91-110.

McLeod DJ, Hallegraeff GM, Hosie GW, Richardson AJ (2012) Climate-driven range expansion of the red-tide dinoflagellates *Noctiluca scintillans* into the Southern Ocean. *Journal of Plankton Research* 34: 332-337.

Moore CM, Suggett D, Holligan PM, Sharples J, Abraham ER, Lucas MI, Rippeth TP, Fisher NR, Simpson JH, Hydes DJ (2003) Physical controls on phytoplankton physiology and production at a

- shelf sea front: a fast repetition-rate fluorometer based field study. *Marine Ecology Progress Series* 259: 29–45.
- Newell BS (1961) Hydrology of south-east Australian waters: Bass Strait and New South Wales tuna fishing area. CSIRO Division of Fisheries and Oceanography Technical Paper 10: 22 pp.
- Oldham T, Rodger H, Nowak BF (2016) Incidence and distribution of amoebic gill disease (AGD) – An epidemiological review. *Aquaculture* 457: 35-42.
- Oke PR, England MH (2004) Oceanic response to changes in the latitude of the Southern Hemisphere subpolar westerly winds. *Journal of Climate* 17: 1040-1054.
- Oxborough K, Moore CM, Suggett DJ, Lawson T, Chan HG, Geider RJ (2012) Direct estimation of functional PSII reaction center concentration and PSII electron flux on a volume basis: a new approach to the analysis of Fast Repetition Rate fluorometry (FRRf) data. *Limnology and Oceanography Methods* 10: 142-154.
- Parsons TR, Maita Y, Lalli CM (1984) *A Manual of Chemical and Biological Methods for Seawater Analysis*. Pergamon Press, New York, 173 pp.
- Pearce A (1981) Temperature-salinity relationships in the Tasman Sea. Division of Fisheries and Oceanography report 135, CSIRO.
- Pedersen SA, Ribergaard MH, Simonsen CS (2005) Micro- and mesozooplankton in Southwest Greenland waters in relation to environmental factors. *Journal of Marine Systems* 56: 85–112.
- Quinn GP, Keough MJ (2002) *Experimental Design and Data Analysis for Biologists*. Cambridge University Press, Cambridge, pp. 537.
- Raateoja M, Seppala J, Kuosa H (2004) Bio-optical modelling of primary production in the SW Finnish coastal zone, Baltic Sea: fast repetition rate fluorometry in Case2 waters. *Marine Ecology Progress Series* 267: 9–26.
- Ramírez FC Seijas P (1985) New data on the ecological distribution of cladocerans and first local observations on reproduction of *Evadne nordmanni* and *Podon intermedius* (Crustacea, Cladocera) in Argentine sea waters. *Physis, Seccion A* 43: 131-143.
- Ridgway KR (2007) Seasonal circulation around Tasmania: an interface between eastern and western boundary dynamics. *Journal of Geophysical Research* 112: C10016, doi:10.1029/2006JC003898.
- Ridgway KR (2007b) Long-term trend and decadal variability of the southward penetration of the East Australian Current. *Geophysical Research Letters* 34: 1-5.
- Ridgway K, Hill K (2009) The East Australian Current. In: Poloczanska ES, Hobday AJ, Richardson AJ (eds). *A marine climate change impacts and adaptation report card for Australia 2009*, NCCARF Publication 05/09, ISBN 978-1-921609-03-9.

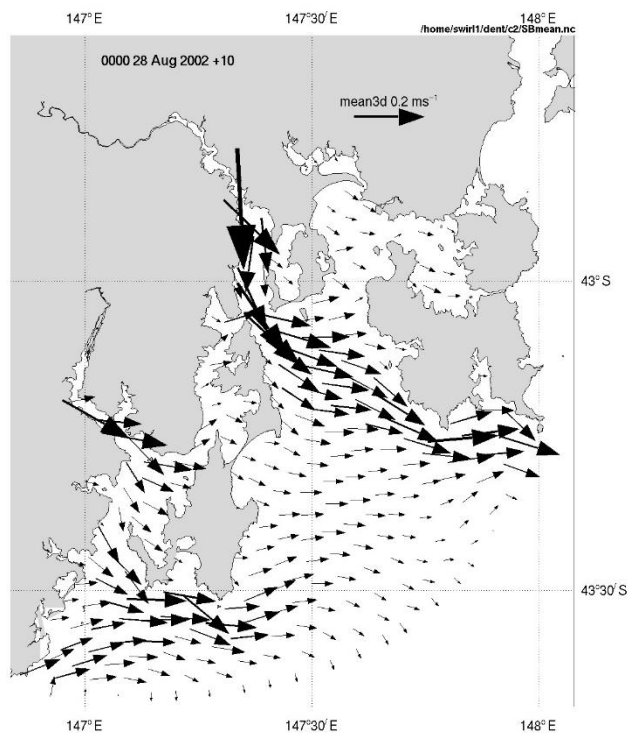
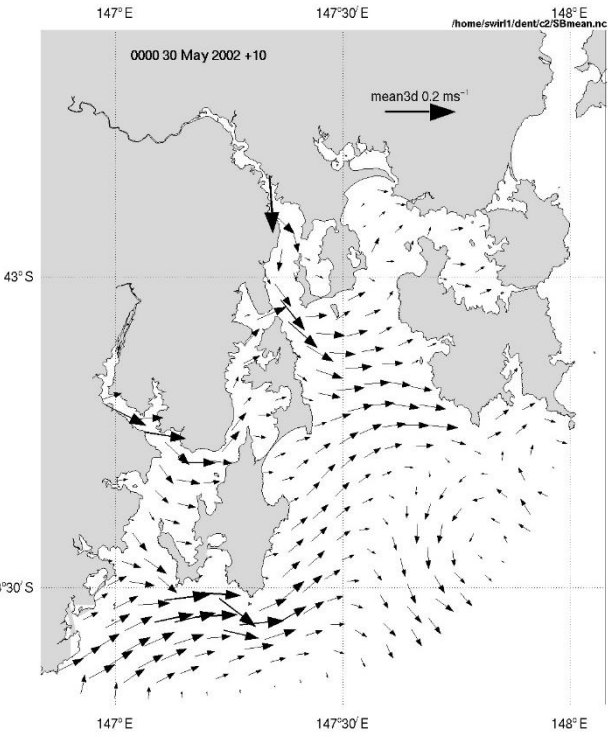
- Rizwi F, MacDonald L, Wild-Allen K, Jones E (2010) Autonomous profiling glider observations in Storm Bay OCEANS 2010 IEEE-Sydney, 1-3.
- Ross DJ, Macleod CK (2013) Evaluation of Broadscale Environmental Monitoring Program (BEMP) data from 2009-2012. IMAS Technical Report 140 pp.
- Smayda TJ, Reynolds CS (2001) Community assembly in marine phytoplankton: Application of recent models to harmful dinoflagellate blooms. *Journal of Plankton Research* 23: 447-461.
- Smyth TJ, Pemberton KL, Aiken J, Geider RJ (2004) A methodology to determine primary production and phytoplankton photosynthetic parameters from Fast Repetition Rate Fluorometry. *Journal of Plankton Research* 26: 1337-1359.
- Suggett D, Kraay G, Holligan P, Davey M, Aiken J, Geider R (2001) Assessment of photosynthesis in a spring cyanobacterial bloom by use of a fast repetition rate fluorometer. *Limnology and Oceanography* 46: 802-810.
- Suggett DJ, Prasil O, Borowitzka MA (2010) Chlorophyll a fluorescence in aquatic sciences: methods and applications. Springer, *Developments in Applied Phycology*, Volume 4, 323 pp.
- Thompson PA, Baird ME, Ingleton T, Doblin MA (2009) Long-term changes in temperate Australian coastal waters: implications for phytoplankton. *Marine Ecology Progress Series* 394: 1-19.
- Viñas MD, Ramírez FC, Santos BA, Marrari M (2007) Spatial and temporal distribution patterns of Cladocera in the Argentine Sea. *Hydrobiologia* 594: 59-68.
- Wild-Allen K, Rayner M (2014) Continuous nutrient observations capture fine-scale estuarine variability simulated by a 3D biogeochemical model. *Marine Chemistry* 167: 135-149.
- Wright DW, Nowak B, Oppedal F, Bridle A, Dempster T (2015) Depth distribution of the amoebic gill disease agent, *Neoparamoeba perurans*, in salmon sea-cages. *Aquaculture Environment Interactions* 7: 67-74.
- Wu L, Cai W, Zhang L, Nakamura H, Timmermann A, Joyce T, McPhaden MJ, Alexander M, Qiu B, Visbeck M (2012) Enhance warming over the global subtropical western boundary currents. *Nature Climate Change* 2: 161-166.
- Young JW, Jordan AR, Bobbi C, Johannes RE, Haskard K, Pullen G (1993) Seasonal and interannual variability in krill (*Nyctiphanes australis*) stocks and their relationship to the fishery for jack mackerel (*Trachurus declivis*) off eastern Tasmania, Australia. *Marine Biology* 116: 9-18.
- Young ND, Dykova I, Snekvik K, Nowak BF, Morrison RN (2008) *Neoparamoeba perurans* is a cosmopolitan aetiological agent of amoebic gill disease. *Dis. Aquatic Organisms* 78: 217-223.

Appendix 4

Figure 2.1. Surface residual flow (from Herzfeld 2008)

(a) Autumn

(b) Winter



(c) Spring

(d) Summer

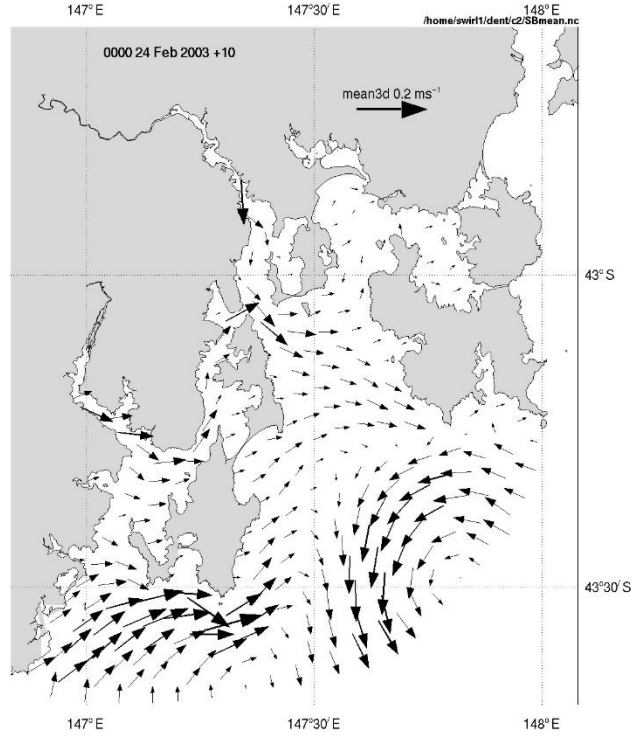
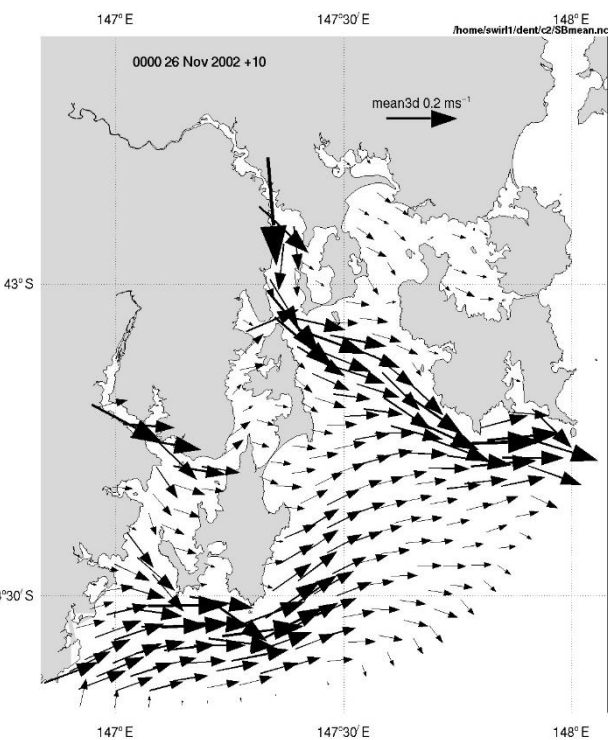
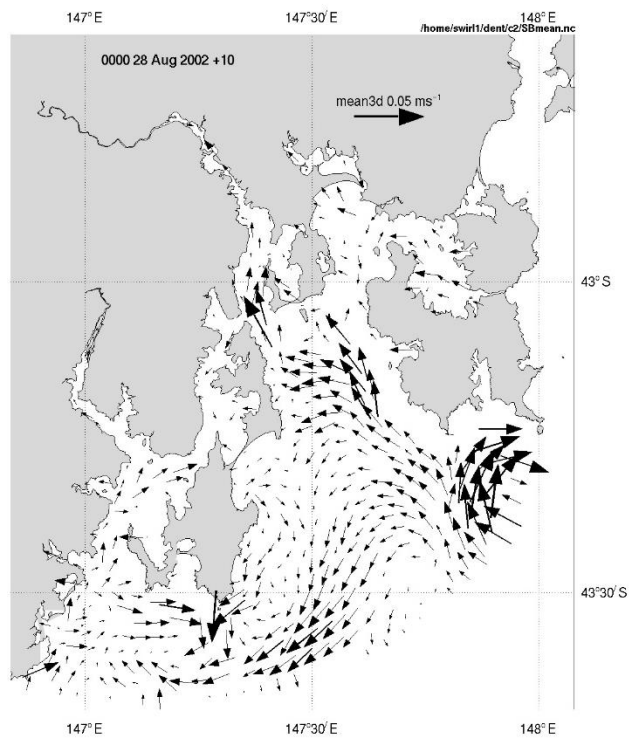
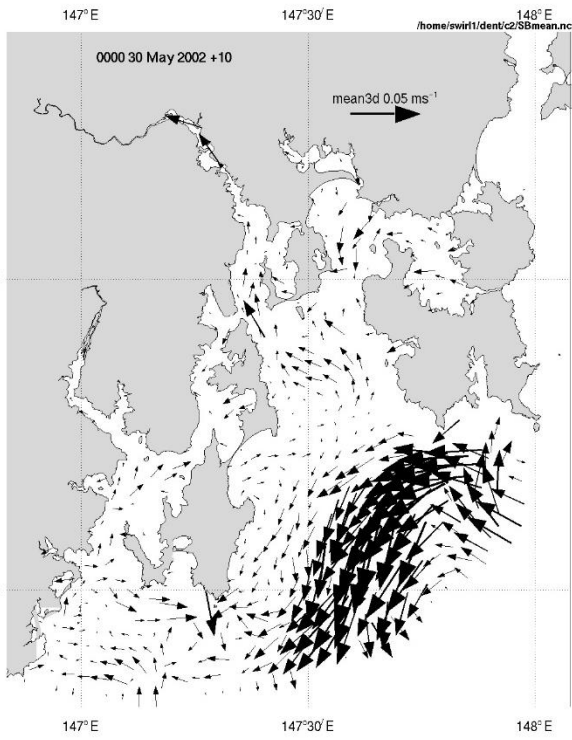


Figure 2.2. Bottom residual flow (from Herzfeld 2008)

(a) Autumn

(b) Winter



(c) Spring

(d) Summer

